Managing Highly Distorted Corneas

A John Kanellopoulos MD

The corneal surface is the principal refracting element of the eye; the air-to-tear film interface is responsible for the majority of refraction of light entering the eye.[1] Any change to this surface dramatically changes the refraction, which is what is accomplished in refractive surgery. Likewise, any irregularity in this surface dramatically affects the quality of vision. This may be the problem in eyes with decentered and/or small optical zone ablations; in these cases the cornea acts like a multifocal lens and causes uneven distribution of light. As a consequence, patients experience loss of BSCVA and contrast sensitivity and haloes and starbursts around objects. These symptoms are especially annoying during scotopic and/or mesopic conditions, when the pupil dilates and exposes more of the irregular cornea. [1,3,4,6,10-14]

Methods and Results

We have previously presented and published our experience in utilizing wavefront[1] as well as topography-guided[2]excimer ablations in order to treat highly irregular corneas such as eccentric previous ablations, keratoconus and post LASIK ectasias. To correct these irregularities, surgeons have gone to "customized" forms of ablation, which include wavefront-guided ablations as well as techniques of topography-guided treatment.[3-9]

We have been working with the topography-guided platform by Wavelight (Erlangen, Germany) over the last four years. This proprietary software utilizes topographic data from the linked topography device (Topolyzer-Wavelight, Erlagen, Germany). It by default permits the consideration of eight topographies (of predetermined threshold accuracy), averages the data, and enables the surgeon to adjust desired postoperative cornea asphericity, to include, or not, tilt correction, and to adjust sphere, cylinder, axis, and treatment zone.

The mechanism of topography-guided ablation is the fitting of an ideal cornea shape (usually a sphere) under the present topography map with the ablation of tissue in between. The advantages of topography-guided treatments over wavefront-guided treatments include the following:

1. It can be used in highly irregular corneas that are beyond the limits of wavefront measuring devices.
2. It can be used in cases that have media opacity such as in eyes with corneal scars, since its measurements are based solely on the surface.
3. Since it is based on the corneal surface, it is theoretically possible to factor in the asphericity (Q value) and maintain the natural aspheric shape of the cornea.

Recent studies have demonstrated that there is a shift in the pupillary center between normal (photopic) and dark-adapted (mesopic, scotopic state). Therefore topography-guided treatments would hold greater accuracy on delivery to the cornea since they are captured with the photopic pupil, the same as in the treatment. The major disadvantage of topography-guided ablation is that ignores the rest of the refractive media since it concentrates mainly on the corneal contour. This may induce some refractive "surprises" previously encountered when utilizing this technique. One example of this would be in the treatment to widen the optical zone of previously myopic patients. The treatment would require the laser to flatten a broader area of the cornea and therefore ablate tissue peripherally; this ablation pattern will resemble a hyperopic treatment and thus will cause some amount of

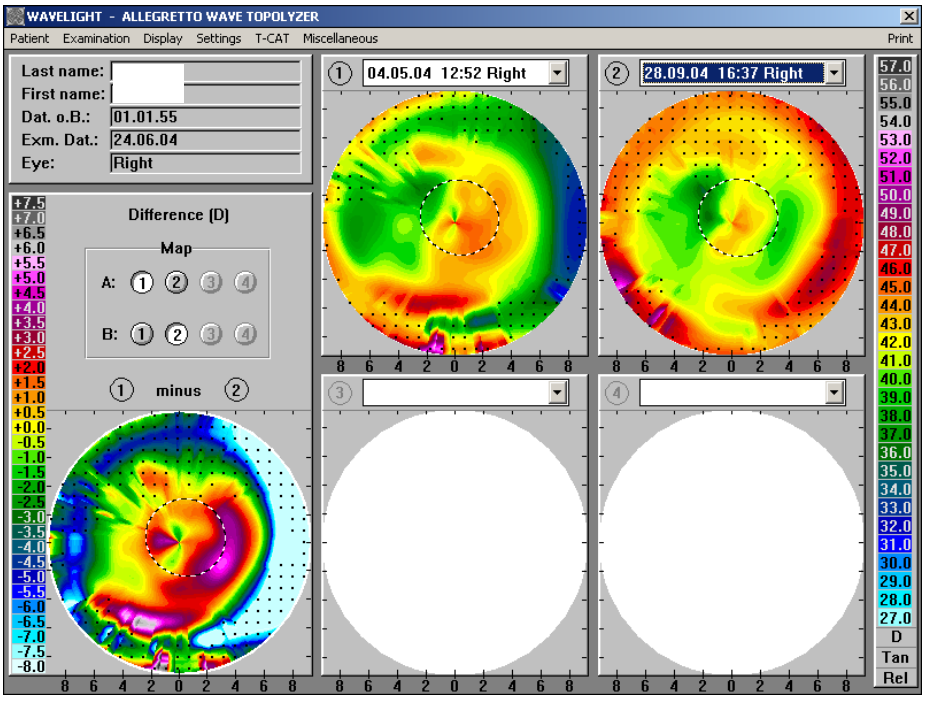

Figure 1. This is the pre– and post– LASIK topography (1 and 2, respectively) of an irregular cornea having topography-guided LASIK with the TCAT Wavelight platform. The cornea irregularity was caused by an old contact lens-related bacterial ulcer. The difference map ("1 minus 2") demonstrates the highly irregular flattening achived by the topography-guided treatment.

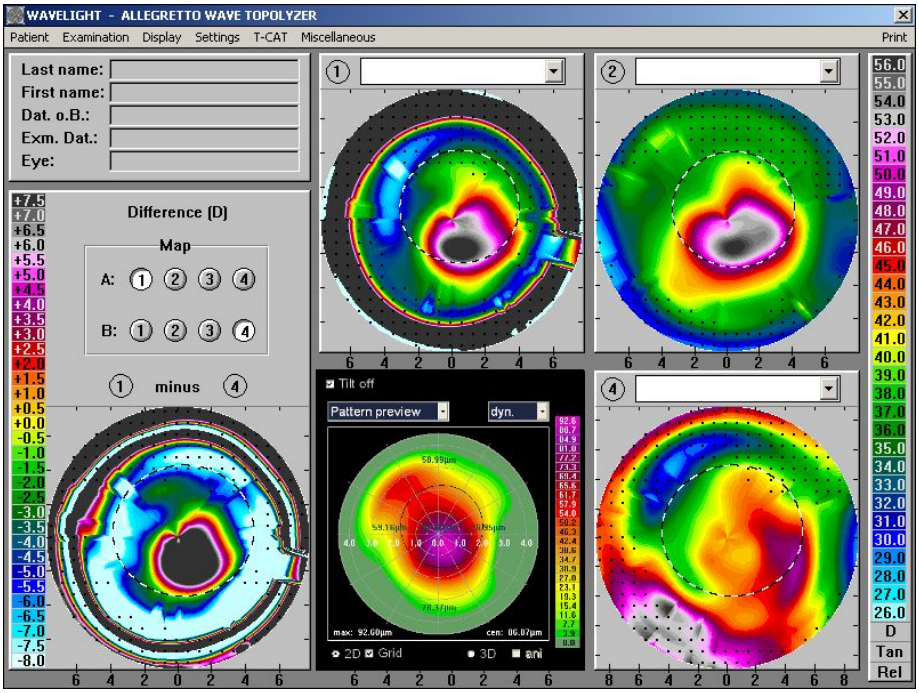

Figure 2. This display of topographies depicts the following: (1) The cornea topography of this case when first seen by the authors with central cornea ectasia and midperiphery flattening as an effect of the Intacs that were present. At this point BSCVA was 20/200. (2) The cornea topography here is two months after the removal of Intacs and one month after UVA collagen crosslinking. The central steepening is still present and the effect of the Intacs removal is appreciated compared to the previous image, mostly at the midperiphery, that appears steeper now. At this point BSCVA was 20/200. (3) The lower row image in the center is an estimated cornea topographic ablation pattern as a laser treatment plan of the topography-guided procedure that took place in the case. It is notable that this ablation pattern is highly irregular with a "deeper" ablation plan just inferior and right to the center, that matches through the central cornea irregularity in the previous topographies. (4) The cornea topography here is six months after topography-guided PRK. The central cornea appears more regular and much flatter. At this point BSCVA and UCVA is 20/20. (5) The lower row image on the left is a comparison map. This map depicts the difference of subtracting the cornea topography 4 (final result) from the cornea topography 1 (original state of this complication when encountered by us). The difference resembles impressively the topography-guided ablation pattern (next image to the right), demonstrating effectively the specificity of this treatment in reducing the pathogenic cornea irregularity, which we theorize contributed to the drastic improvement of BSCVA.

myopic shift. Some of these patients may later require an enchancement procedure with a "standard" treatment to correct for the remaining spherical refractive error. We made adjustments to the refractive targets (ie, putting in a myopic postop target) to our later cases to compensate for this shift in refraction.

The Q value was targeted to the ideal endpoint of –0.46 in all cases, which is believed to be an ideal cornea asphericity for an average human eye using a Navarro eye model. A common flaw in the theoretical calculation of the ablation profile is its basis on a static-shape subtraction model, in which the postoperative cornea shape is determined only by the difference between the preoperative shape and the ablation profile. However, other factors may be responsible for explaining the discrepancy between the clinical findings and the theoretical predictions in cornea asphericity (ie, biological effects of healing and the variations of the applied fluence at the cornea). Epithelial hyperplasia is a more predominant factor after PRK, while flap-induced changes, together with indirect biomechanical shifts of the cornea, are present in LASIK eyes. This could explain the refractive inaccuracy, as well as the asphericity adjustments imprecision, of the topography-guided treatments, despite a notable improvement in the cornea surface regularity.

We have previously reported utilizing topography-guided treatments in keratectasias. [13-15] Both post-LASIK ectasias and keratoconus have been successfully treated with a topo-guided PRK following stabilization with collagen crosslinking (CCL). The first scale of this treatment was employed in order to stabilize the cornea ectasia, as reported in previous laboratory and clinical studies. The use of the riboflavin solution over the de-epithelialized cornea was employed in order to, first, protect the crystalline lens and possibly the retina from UVA radiance and, secondly, to enchance UVA absorption in the anterior stroma and facilitate the crosslinking process as described previously.[10,11] We employed the subsequent topo-guided PRK procedure in order to visually rehabilitate the irregular corneas. The visual rehabilitation had been very rewarding in a relatively moderate postop follow-up of one year. Representative corneal topographies are shown in Figure 2.One can appreciate the difference map between pre– and post-UVA CCL (2C) as well as the difference map between pre– and post-topography guided treatments (2F) and, finally, the actual ablation profile that was used for the treatment (Figure 2D: "treatment plan"). It is quite interesting to appreciate the qualitative changes on the cornea surface. Both in the treatment plan D as well as the difference map F there is strong evidence of "deeper" ablation over the steep cone area. Another important factor is the attempt in 1D and actual effect in 2F of a mid-peripheral "steepening" effect of the diametrically opposite cornea to the cone center. This is achieved by flattening the outer of the mid-cornea that is planned to be "steepened."

Therefore, normalization of the cornea is achieved by both flattening the cone apex and steepening its diametrical opposite, preserving significant tissue thickness reduction that a similar wavefront-guided treatment would require.

We employed topography-guided PRK on the crosslinked cornea in that case in order to obtain better visual rehabilitation. This customized approach can in my opinion address the extreme corneal irregularity that these cases may have and enchance visual rehabilitation, leads us to believe that this combined approach may have a wider application in the near future.

Conclusions

All this work has complemented our customized approach to refractive surgery and addresses the most irregular corneas that a regular or wavefront-guided ablation cannot treat.

The limitation of refractive outcome in regard to sphere can be refined by incorporating axial length measurements in the topography images. More studies and continuous treatments algorithm evolution may enchance our treatment armamentarium as refractive surgeons.

References

1. Kanellopoulos AJ, Pe LH. Wavefront-guided enchancements using the Wavelight excimer laser in symptomatic eyes previously treated with LASIK. *J Refract Surg.* 2006; 22:345-349.
2. Kanellopoulos AJ, Topography-guided custom re-treatments in 27 symptomatic eyes. *Refract Surg.* 2005; 21:S513-S518.
3. Campell C. Corneal topography in corneal ablations. In: Mcrae SM, Krueger RR, Applegate RA, eds. *Customized Corneal Ablation: The Quest for Supervision.* Thorofare, NJ: SLACK, Inc.; 2001:229-236.
4. Applegate RA ,Himatel G, Thibos LN. Visual performance assessment. Mcrae SM, Krueger RR, Applegate RA, eds. *Customized Corneal Ablation: The Quest for Supervision.* Thorofare, NJ: SLACK, Inc.; 2001: 81-92
5. Knorz MC, Jendritza B. Topographically-guided laser in situ keratomileusis to treat corneal irregularities. *Ophthalmology* 2000; 107(6):1138-1143.
6. Kanjani N, Jacob S, Agarwal A, et al. Wavefront-and topography-guided ablation in myopic eyes using Zyoptix. *J Cataract Refractive Surg.* 2004; 30(2):398-402.
7. Alio JL, Belda JI, Osman AA, Shalaby AM. Topography-guided laser in situ keratomileusis (TOPOLINK) to correct irregular astigmatism after *previous* refractive surgery. *J Refract Surg.* 2003; 19(5):516-527.
8. Seiler T, Dastjerdi MH. Customized corneal ablation [review]. *Curr Opin Ophthalmol.* 2002; 13(4):256-260.
9. Gatinel D, Malet J, Hoang-Xuan T, Azar D. Analysis of customized corneal ablations: theoretical limitations of increasing negative asphericity. *Invest Ophthalmol Vis Sci.* 2002; 43:941-948.
10. Spoerl E, Huhle M, Seiler T. Induction of cross-links in corneal tissue. *Exp Eye Res.* 1998; 66:97-103
11. Wollensak G, Spoerl E, Seiler T. Riboflavin/ultraviolet-A–induced collagen crosslinking for the treatment of keratoconus. *Am J Ophthalmol.* 2003; 135:620-627.
12. Kanellopoulos AJ, Pe LH, Perry HD, Donnenfeld ED. Modified intracorneal ring segment implantations (INTACS) for the management of moderate to advanced keratoconus: efficacy and complications. *Cornea* 2006; 25(1):29-33.
13. Kanellopoulos AJ. Post-LASIK ectasia. *Ophthalmology.* 2007; 114(6): 1230.
14. Hafezi F, Mrochen M, Jankov M, Hopeler T. Wiltfang R, Kanel -lopoulos AJ, Seiler T. Corneal collagen crosslinking with riboflavin/UVA for the treatment of induced keratectasia after laser in situ keratomileusis. Submitted.
15. Kanellopoulos AJ, Binder PS. Collagen cross-linking (CCL) with ultraviolet A light (UVA) and riboflavin in keratoconus, followed by customized topography-guided PRK. A case report of a temporizing alternative to penetrating keratoplasty. *J Cornea.* In press

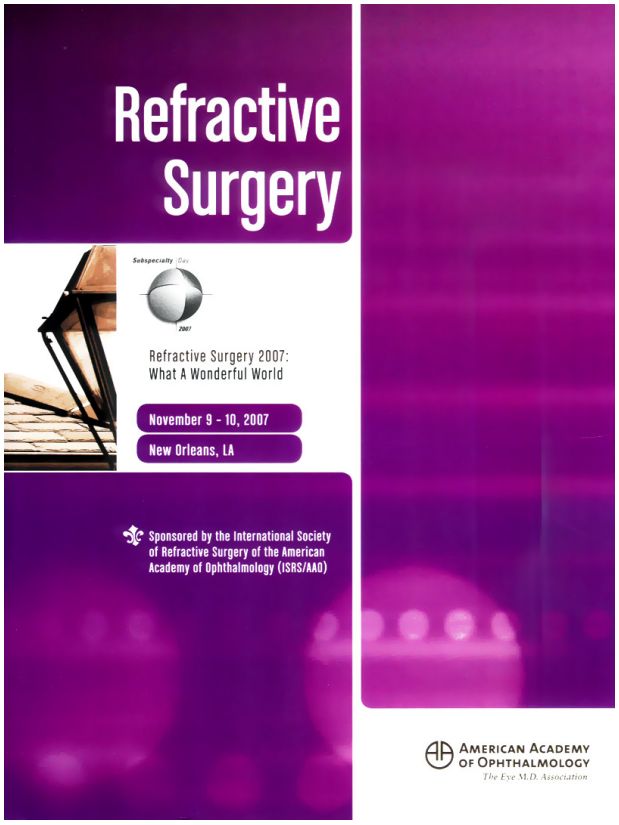

This is the content of the keynote lecture presented by Dr. Kanellopoulos by invitation at the annual Subspecialty Refractive Surgery meeting organized by the ***International Society of Refractive Surgery and American Academy of Ophthalmology*** in New Orleans, LA, USA on Friday November 9th, 2007.

Management of Corneal Ectasia After LASIK With Combined, Same-day, Topography-guided Partial Transepithelial PRK and Collagen Cross-linking: The Athens Protocol

Anastasios John Kanellopoulos, MD; Perry S. Binder, MS, MD

ABSTRACT

PURPOSE: To evaluate a series of patients with corneal ectasia after LASIK that underwent the Athens Protocol: combined topography-guided photorefractive keratectomy (PRK) to reduce or eliminate induced myopia and astigmatism followed by sequential, same-day ultraviolet A (UVA) corneal collagen cross-linking (CXL).

METHODS: Thirty-two consecutive corneal ectasia cases underwent transepithelial PRK (WaveLight ALLEGRETTO) immediately followed by CXL (3 mW/cm^2) for 30 minutes using 0.1% topical riboflavin sodium phosphate. Uncorrected distance visual acuity (UDVA), corrected distance visual acuity (CDVA), manifest refraction spherical equivalent, keratometry, central ultrasonic pachymetry, corneal tomography (Oculus Pentacam), and endothelial cell counts were analyzed. Mean follow-up was 27 months (range: 6 to 59 months).

RESULTS: Twenty-seven of 32 eyes had an improvement in UDVA and CDVA of 20/45 or better (2.25 logMAR) at last follow-up. Four eyes showed some topographic improvement but no improvement in CDVA. One of the treated eyes required a subsequent penetrating keratoplasty. Corneal haze grade 2 was present in 2 eyes.

CONCLUSIONS: Combined, same-day, topography-guided PRK and CXL appeared to offer tomographic stability, even after long-term follow-up. Only 2 of 32 eyes had corneal ectasia progression after the intervention. Seventeen of 32 eyes appeared to have improvement in UDVA and CDVA with follow-up >1.5 years. This technique may offer an alternative in the management of iatrogenic corneal ectasia. [*J Refract Surg*. 2011;27(5):323-331.]

doi:10.3928/1081597X-20101105-01

Progressive, asymmetrical corneal steepening associated with an increase in myopic and astigmatic refractive errors, combined with midperipheral and/or peripheral corneal thinning, represents a constellation of findings in ectatic corneal disorders, such as keratoconus and pellucid marginal degeneration. Asymmetry in presentation and unpredictability of progression associated with a myriad of abnormal topographic findings describe these entities. Similar findings following LASIK have been described as corneal ectasia.[1-3] Analysis of different series of eyes developing corneal ectasia after LASIK has suggested that certain preoperative and/or operative features may be associated with this adverse outcome of LASIK or photorefractive keratectomy (PRK).[4] The fact that corneal ectasia can occur in the absence of these features, or that it does not occur despite the presence of these features,[5] has confounded our understanding of this entity. Nevertheless, corneal ectasia after LASIK is a visually disabling complication with an ultimate surgical treatment of penetrating keratoplasty when spectacles or contact lenses can no longer provide patients with the quality of vision to permit activities of daily living.

Over the past 10 years, the use of topical riboflavin combined with ultraviolet A (UVA) irradiation to increase collagen cross-linking (CXL) has demonstrated the potential for retarding or eliminating the progression of keratoconus and corneal ectasia after LASIK. The application of CXL in corneal ectasia after LASIK has been reported previously.[6] Once

From LaserVision.gr Institute, Athens, Greece (Kanellopoulos); New York University Medical College (Kanellopoulos) and Manhattan Eye, Ear and Throat Hospital (Kanellopoulos), New York, New York; and Gavin Herbert Eye Institute Department of Ophthalmology, University of California, Irvine, California (Binder).

The authors have no financial interest in the materials presented herein.

Presented as a paper at the American Society of Cataract and Refractive Surgery annual meeting; April 9-14, 2010; Boston, Massachusetts.

Correspondence: A. John Kanellopoulos, MD, LaserVision.gr Institute, 17 Tsocha St, Athens, 11521 Greece. Tel: 30 210 7472777; Fax: 30 210 7472789; E-mail: ajkmd@mac.com

Received: April 20, 2010; Accepted: October 13, 2010

Posted online: November 5, 2010

the progression has stabilized, it is possible to treat the surface of the eye with customized PRK to normalize the corneal surface by reducing irregular astigmatism and potentially reducing the refractive error as well as providing improved visual outcomes in addition to stabilizing the disease process.[7,8] We have subsequently introduced the combined, same-day use of these two intervention modalities in the management of keratoconus.[9-11]

We present a series of patients with corneal ectasia after LASIK who have undergone combined, same-day, topography-guided PRK and subsequent UVA collagen CXL to achieve stabilization of corneal ectasia and enhance visual rehabilitation.

PATIENTS AND METHODS

Patient Selection

Patients entered into this study were seen by one of the authors (A.J.K.) in his private practice, either through individual patient referral, referral from other eye care practitioners, or were his own patients. Once a diagnosis of corneal ectasia after LASIK was confirmed (see below), patients were presented with the options of contact lens fitting, intracorneal ring segment implantation, or, in advanced cases, penetrating keratoplasty. If these modalities did not serve the needs of the patient, he/she was then presented with the option of undergoing topography-guided PRK and UVA collagen CXL as a possible technique to prolong or prevent the need for penetrating keratoplasty. Patients provided verbal and written consent prior to undergoing the combined topography-guided PRK/CXL procedure.

A diagnosis of corneal ectasia was made when patients developed progressive corneal steepening associated with an increasing myopic and/or astigmatic refractive error 2 or more months after LASIK surgery. These findings were combined with increasing inferior corneal steepening and thinning based on videokeratography and ultrasound pachymetry. Preoperative LASIK clinical data and topography were requested from the referring physician or primary LASIK surgeon for analysis. Progression of the myopic refractive error with or without progression of the manifest astigmatism, decreasing uncorrected distance visual acuity (UDVA), loss of corrected distance visual acuity (CDVA), progressive inferior corneal steepening on topography, and/or decreasing inferior corneal thickness were findings in all cases.

Clinical Examination

Each patient underwent manifest refraction as well as measurement of UDVA and CDVA, which was recorded in a 20-foot lane using high-contrast Snellen visual acuity testing. Cycloplegic refractions were performed using 1% tropicamide solution (Alcon Laboratories Inc, Ft Worth, Texas). Slit-lamp microscopy confirmed the presence of a LASIK flap. Keratometry readings were obtained by videokeratography (Topolyzer; WaveLight AG, Erlangen, Germany) and/or manual keratometry (model 71-21-35; Bausch & Lomb, Rochester, New York). Pachymetry was performed using at least one of the following devices/instruments: Pentacam (Oculus Optikgeräte GmbH, Wetzlar, Germany), Orbscan II (Bausch & Lomb), or EchoScan US-1800 (NIDEK Co Ltd, Gamagori, Japan). Specular microscopy was performed using the Konan specular microscope (Konan Medical, Boston, Massachusetts). Topography was performed using the Orbscan II or Pentacam.

Surgical Technique—The Athens Protocol

We have reported this technique in the management of keratoconus.[9-11]

Step 1. The (Partial, Spherically Corrected) Topography-guided Transepithelial PRK Technique. We devised this technique based on the proprietary WaveLight customized platform. As noted above, we previously described the use of the topography-guided platform with this device to normalize irregular corneas as well as corneal ectasia.

This customized excimer laser treatment is guided by topographic images and is different from wavefront-guided treatments. It received CE mark for clinical use in the European Union in 2003; however, it has yet to receive US Food and Drug Administration approval.

This proprietary software utilizes topographic data from the linked topography device (Topolyzer). By default, it permits the consideration of eight topographies (of predetermined threshold accuracy), averages the data and enables the surgeon to adjust the desired postoperative cornea asphericity (chosen as zero in all cases), provides the option of including tilt correction (no tilt was chosen in all cases), as well as the adjustment of sphere, cylinder, axis, and treatment zone (optical zone of 5.5 mm was chosen in all cases). The image of the planned surgery is generated by the laser software.

We used topography-guided PRK to normalize the cornea by reducing irregular astigmatism while treating part of the refractive error. To remove the minimum possible tissue, we decreased the effective optical zone diameter to 5.5 mm in all cases (compared to our usual treatment diameter of at least 6.5 mm in routine PRK and LASIK). We also planned ~70% treatment of cylinder and sphere (up to 70%) so as not to exceed 50 µm in planned stromal removal. We chose the value of 50 µm as the maximum ablation depth effected, based

on our experience of treating irregular corneas with this platform.[7-10]

Following the placement of an aspirating lid speculum (Rumex, St Petersburg, Florida), a 6.5-mm, 50-µm phototherapeutic keratectomy (PTK) was performed to remove the corneal epithelium. Partial topography-guided PRK laser treatment was applied. A cellulose sponge soaked in mitomycin C (MMC) 0.02% solution was applied over the ablated tissue for 20 seconds followed by irrigation with 10 mL of chilled balanced salt solution.

Step 2. Collagen CXL Procedure. For the next 10 minutes, the proprietary 0.1% riboflavin sodium phosphate ophthalmic solution (Priavision, Menlo Park, California) was applied topically every 2 minutes. The solution appeared to "soak" into the corneal stroma rapidly, as it was centrally devoid of Bowman layer. Following the initial riboflavin administration, 4 diodes emitting UVA light of mean 370-nm wavelength (range: 365 to 375 nm) and 3 mW/cm^2 radiance at 2.5 cm were projected onto the surface of the cornea for 30 minutes (Keracure prototype device, Priavision). The Keracure device, which has a built-in beeper, alerts clinicians every 2 minutes during the 30-minute treatment to install the riboflavin solution in a timely fashion. A bandage contact lens was placed on the cornea at the completion of the combined procedures.

Postoperatively, topical ofloxacin (Ocuflox 0.3%; Allergan Inc, Irvine, California) was used four times a day for the first 10 days and prednisolone acetate 1% (Pred Forte, Allergan Inc) was used four times a day for 60 days. Protection from all natural light with sunglasses was encouraged, with administration of oral 1000 mg vitamin C daily for 60 days postoperative. The bandage contact lens was removed at or around day 5 following complete re-epithelialization.

Evaluation

The following evaluations were completed before and after both treatments: age, sex, UDVA, CDVA, refraction, keratometry, tomography, pachymetry, endothelial cell count, corneal haze on a scale of 0 to 4 (0=clear cornea, 1=mild haze, 2=moderate haze, 3=severe haze, and 4=reticular haze [obstructing iris anatomy]), and corneal ectasia stability as defined by stability in mean keratometry and tomography.

CASE REPORTS

Case 1

A 39-year-old man had undergone LASIK in May 2004 at another institution. At that time, according to patient history, UDVA was counting fingers in both eyes. Manifest refraction was −6.50 −0.50 × 020 (20/20) in the right eye and −6.00 −0.50 × 165 (20/20) in the left eye. Preoperative keratometry and corneal thickness readings were not available. No surgical data were available. The patient achieved UDVA of 20/20 in each eye, and reportedly plano refraction in both. In October 2005, he complained of progressively decreasing vision in both eyes. At that time, UDVA was 20/50 in the right eye and 20/40 in the left eye and he was told that "astigmatism was developing."

The patient presented in March 2006, 26 months after LASIK, with a manifest refraction of +2.25 −1.75 × 090 (20/20) in the right eye and −1.25 −0.75 × 010 (20/20) in the left eye. Uncorrected distance visual acuity was 20/40 in the right eye and 20/30 in the left eye. Keratometry was 38.75@90/35.62@180 in the right eye and 40.65@05/39.55@95 in the left eye. Central corneal thickness (measured with Pentacam and ultrasound) was 495 µm in the right eye and 505 µm in the left eye, respectively. A diagnosis of bilateral corneal ectasia was made.

Because of the decrease in UDVA and the presence of corneal ectasia, the patient was informed of the risks, benefits, and alternatives of the combined topography-guided PRK/CXL technique. This procedure was performed on both eyes in January 2007, 32 months after LASIK. Based on the clinical manifest refraction of right (+2.25 −1.75 × 90 [20/20]) and left (−1.25 −0.50 × 005 [20/20]) eyes, the attempted correction was reduced to +1.75 −1.50 × 90 and −0.75 −0.50 × 005 for the right and left eyes, respectively. (The goal in the treatment was modified to anticipate the possible long-term flattening effect that CXL may have on these corneas.)

In February 2010, 37 months after topography-guided PRK/CXL, UDVA improved to 20/40 in the right eye and 20/20 in the left eye with a manifest refraction of −0.75 (20/20) in the right eye and +0.25 −0.25 × 95 (20/20) in the left eye. Keratometry was 37.50@85/36.62@175 in the right eye and 37.75@79/37.87@169 in the left eye. Ultrasound pachymetry was 440 µm and 414 µm in the right and left eyes, respectively. Figure 1 demonstrates the pre- and postoperative topographies of the right eye as well as the difference map after treatment with the Athens Protocol.

Case 2

A 33-year-old woman reportedly had a manifest refraction of −4.00 −2.50 × 90 (20/20) in the right eye and −1.50 −2.00 × 100 (20/20) in the left eye. No other preoperative data were available. The patient had a history of eye rubbing.

Sometime in 2002, the patient underwent bilateral

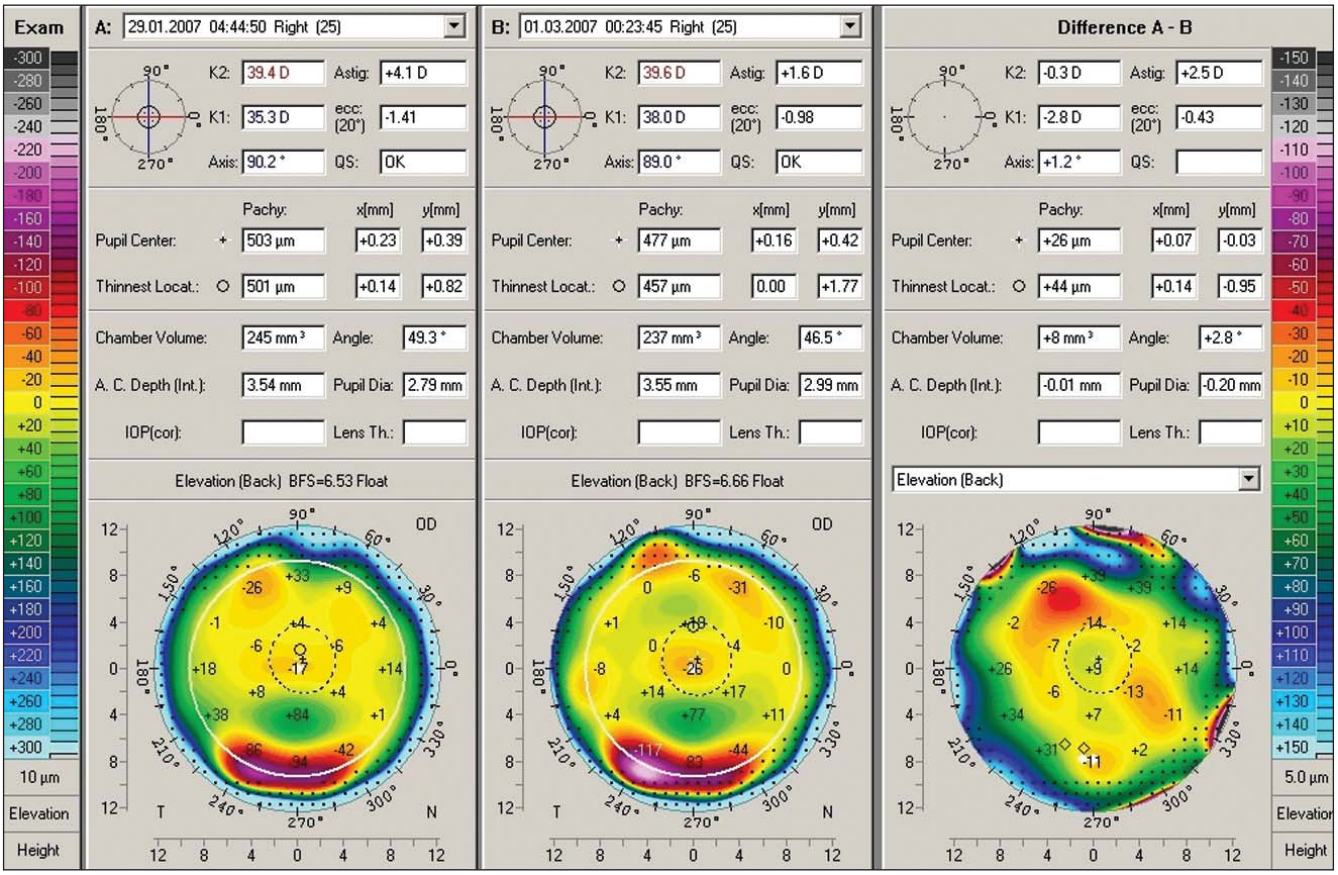

Figure 1. *Case 1.* Clinical course of the right eye. Topography on the left shows marked central inferior corneal steepening consistent with corneal ectasia. The center image shows the final topography 2 years after initial LASIK, which is flatter and normalized. The image on the right demonstrates the comparison between preoperative and postoperative.

LASIK (the exact date is unknown and the surgical data were unavailable). Initially, the patient recovered excellent UDVA, but in December 2005, approximately 3 years postoperatively, she presented with slowly decreasing vision in both eyes. At that time, UDVA was 20/800 in each eye. Manifest refraction was −10.50 −6.00 × 105 (20/40) in the right eye and −7.75 −2.50 × 110 (20/30) in the left eye. Central corneal thickness measured by ultrasound was 395 µm in the right eye and 410 µm in the left eye. Keratometry was 52.87@103/46.12@13 in the right eye and 47.12@111/45.00@021 in the left eye. Corneal topography revealed bilateral corneal ectasia after LASIK, which was more pronounced in the right eye.

On December 19, 2005, >3 years after LASIK, the patient underwent topography-guided PRK/CXL in the right eye only, with no treatment in the left eye. At this time, manifest refraction was −10.50 −6.00 × 105 (20/30) in the right eye and −7.75 −4.50 × 130 (20/40) in the left eye. In June 2007, 18 months after topography-guided PRK/CXL, UDVA was 20/800 in each eye. Manifest refraction in the treated right eye had worsened to −12.00 −2.50 × 100 (20/40). Keratometry was 48.00@29/47.30@119 in the right eye and 47.87@20/46.20@110 in the left eye, and ultrasound pachymetry was 424 µm in the right eye and 388 µm in the left eye. Corneal topography revealed flattening in the difference map in the right eye (Fig 2). The patient was unhappy with this result and is currently uncomfortable with her anisometropia. She decided not to proceed with treatment in the fellow eye because she was unconvinced she had benefited from the topography-guided PRK/CXL procedure. She is currently wearing rigid gas permeable contact lenses in both eyes.

CASE 3

A 26-year-old male helicopter pilot underwent LASIK in both eyes in June 2004. No operative data were available. The only data available from the initial LASIK procedure was that he had "about" −3.00 diopters (D) of myopia in both eyes prior to LASIK. Uncorrected distance visual acuity during the initial 2 years after LASIK was "good" but then deteriorated in his right eye. He was subsequently diagnosed with corneal

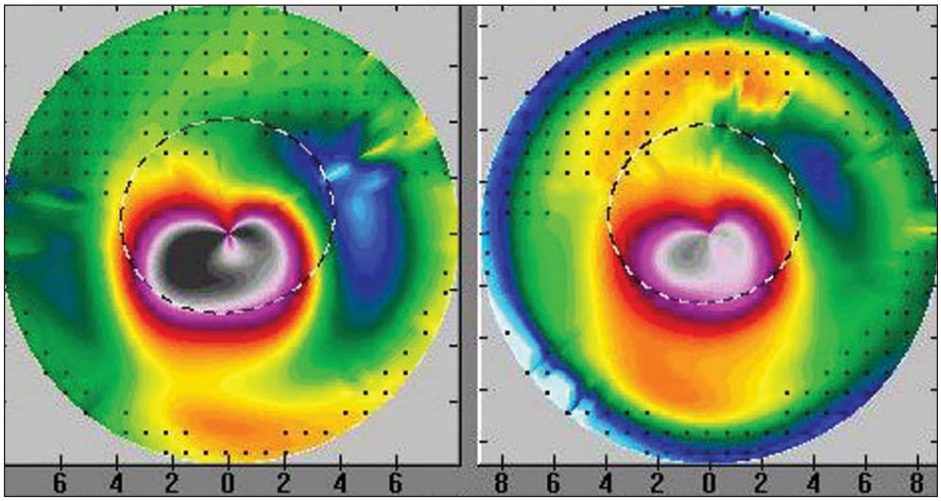

Figure 2. *Case 2.* Topography on the left shows marked inferior steepening before topography-guided PRK/CXL treatment. The topography on the right shows the same cornea 18 months after topography-guided PRK/CXL with marked flattening of the corneal ectasia and normalization of the cornea.

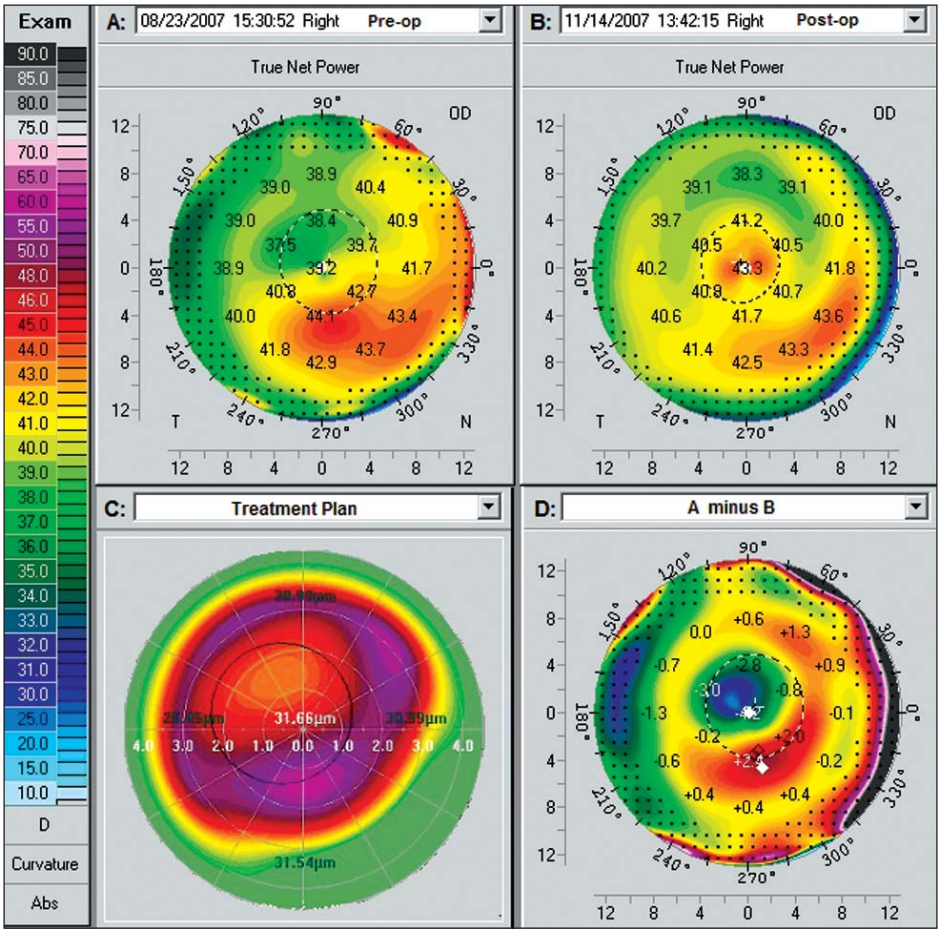

Figure 3. *Case 3.* Clinical course of the right eye. **A)** Topography 3 years after LASIK demonstrates irregular astigmatism and marked inferior corneal steepening. Uncorrected distance visual acuity was 20/40 and corrected distance visual acuity was 20/20 with refraction of +1.50 −2.00 × 65. **B)** Topography 3 months after topography-guided PRK/CXL procedure demonstrates a flatter and normalized cornea. Uncorrected distance visual acuity was 20/15. **C)** Topographic reproduction of the topography-guided PRK treatment plan with the WaveLight platform. This platform plans to remove tissue in an irregular fashion to normalize the corneal ectasia seen in Figure 3A. **D)** Comparison map, derived from subtracting image B from A, represents the topographic difference in this case 3 months after the combined treatment. The paracentral flattening is self-explanatory, as the PRK and CXL have flattened the cone apex. The superior nasal arcuate flattening represents the actual part-hyperopic correction, which the topography-guided treatment has achieved, to accomplish steepening in the area central to this arc. Thus, the topography-guided treatment has normalized the ectatic cornea by flattening the cone apex and at the same time by "steepening" the remainder of the central cornea.

ectasia and was offered Intacs (Addition Technology Inc, Des Plaines, Illinois) or a corneal transplant.

He presented to our institution in September 2007, 3 years after LASIK. Uncorrected distance visual acuity was 20/40 in the right eye and 20/15 in the left eye. Manifest refraction was +1.50 −2.00 × 65 (20/20) in the right eye and plano (20/15) in the left eye. Keratometry was 41.62@65/43.62@155 in the right eye and 41.75/42.12@10 in the left eye. Central ultrasound pachymetry was 476 µm in the right eye and 490 µm in the left eye.

On September 13, 2007, 39 months after LASIK,

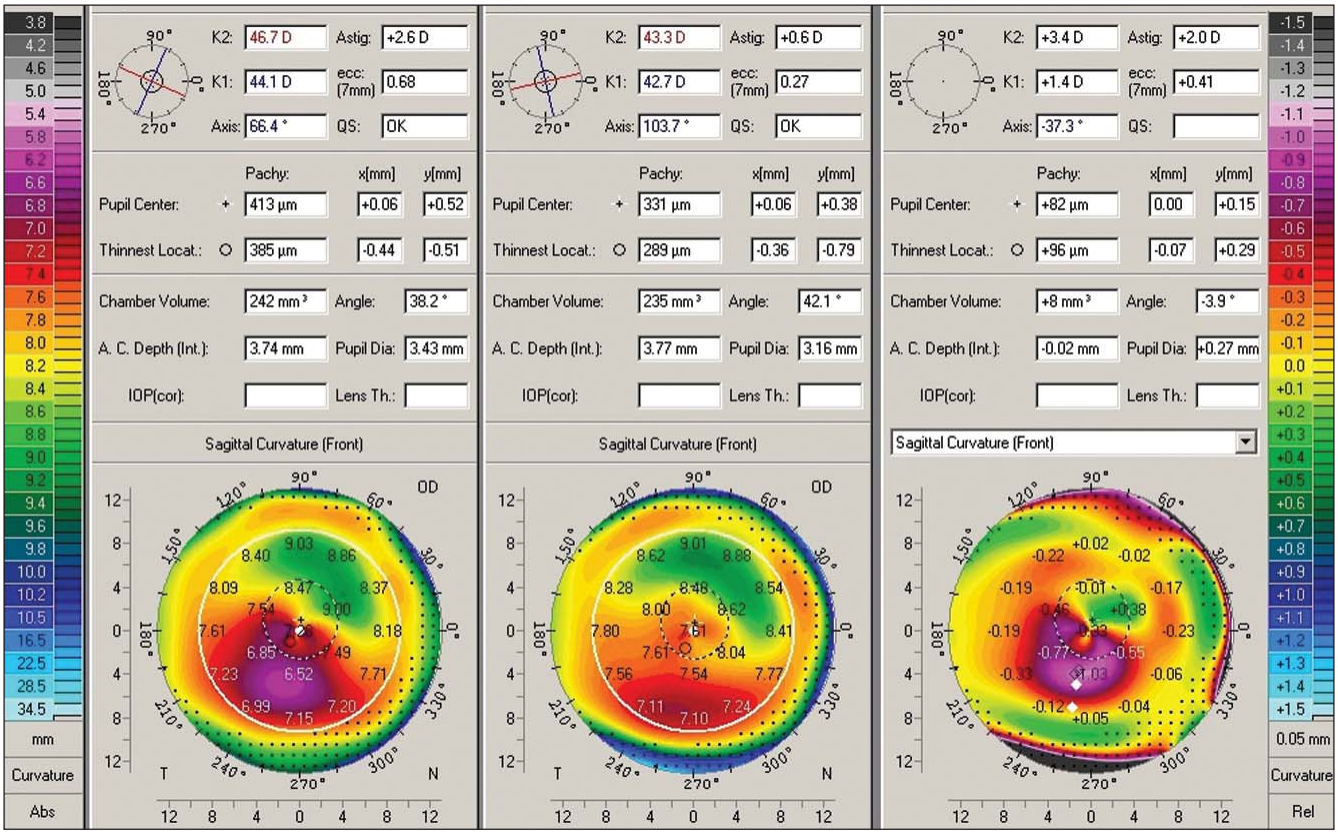

Figure 4. *Case 4.* Pentacam comparison of the right eye. The left column shows the data and topography before topography-guided PRK/CXL. The center column shows the postoperative data and topography. The right column shows the difference (pre- minus postoperative).

combined topography-guided PRK and immediate CXL was performed in the right eye for +0.50 −1.50 × 60. The planned laser resection was 35 µm. Prior to treatment, manifest refraction was +1.50 −2.00 × 65; we reduced the attempted sphere and cylinder, anticipating a subsequent flattening effect of the sequential CXL procedure. Within 6 months, UDVA improved to 20/25 and 24 months later in September 2009, UDVA improved to 20/15 and the manifest refraction improved to plano −0.25 × 05 (20/10). Keratometry in the right eye was 43.00@97/43.25@07 and ultrasound pachymetry was 441 µm. The difference maps (Pentacam) before topography-guided PRK/CXL and 2 years postoperative are shown in Figure 3. At 3-year follow-up, UDVA remains at 20/10.

As a result of the improvement and stability in visual function, this patient has joined the United States Air Force as a fighter pilot and is currently serving in active duty.

CASE 4

A 32-year-old woman underwent LASIK in both eyes in December 2006 for a refractive error of −3.75 D in the right eye and −4.00 D in the left eye. No other data were available in regard to the surgery. Her vision was good for 2 years and then started to deteriorate. The treating surgeon made the diagnosis of corneal ectasia after LASIK in December 2008.

The patient presented to our institution in January 2009. Uncorrected distance visual acuity was 20/100 in the right eye and $20/20^{-2}$ in the left eye. Corrected distance visual acuity was 20/30 with manifest refraction of −3.25 −3.25 × 45 in the right eye and 20/15 with +0.50 −1.25 × 100 in the left eye. Keratometry was 46.70@156/44.10@66 and 39.75@155/41.75@65 in the right and left eyes, respectively. Pachymetry readings were 419 µm and 460 µm in the right and left eyes, respectively. The diagnosis of corneal ectasia after LASIK was confirmed by Pentacam in the right eye (Fig 4, left image). The patient was contact lens–intolerant and opted to undergo topography-guided PRK/CXL despite the informed consent that the estimated residual corneal thickness would be 360 µm. This procedure was performed in February 2009 in the right eye.

The planned correction was −2.50 −2.50 × 45 after 6-mm diameter, 50-µm depth PTK. After ablation, 0.02% MMC in a moistened weck-cell sponge was used on the stroma for 20 seconds. In January 2010

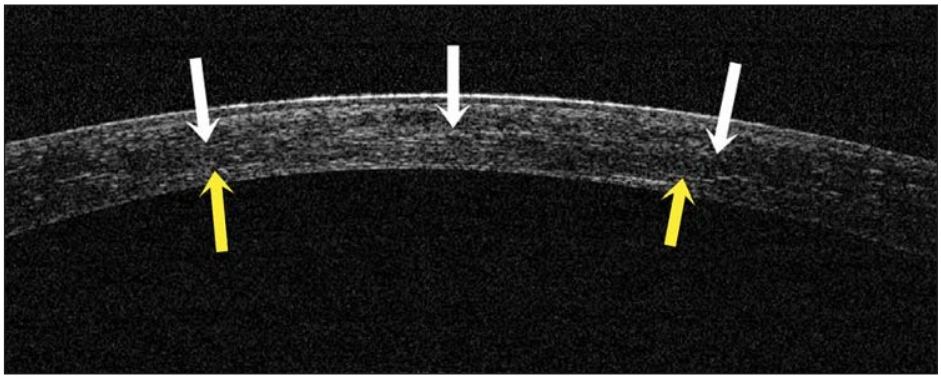

Figure 5. *Case 4.* Optical coherence tomography of the central cornea in the right eye 11 months after topography-guided PRK/CXL. The hyper-reflectivity of the anterior 2/3 of the cornea suggests (as reported previously[10]) the CXL effect (yellow arrows). The hyper-reflective demarcation in the middle of the cornea (white arrows) suggests a thick LASIK flap calculated to >200 μm.

(11 months following treatment), UDVA was 20/30, and CDVA was 20/20^{-1} with manifest refraction of −0.50 −0.75 × 141. Keratometry was 43.30 and 42.70@103. Central corneal thickness was 330 μm. The pre- and postoperative difference map is shown in Figure 4. Endothelial cell count was unchanged at 20 months (2600 cells/mm^2 from 2650 cells/mm^2 prior to application of the Athen's protocol).

Optical coherence tomography (OCT) of the central cornea in the right eye at 11 months postoperative shows hyper-reflectivity of the anterior 2/3 of the cornea (Fig 5) demonstrating the CXL effect, which we reported previously when applying similar treatment in cases of keratoconus.[10,11] The hyper-reflective demarcation in the middle of the cornea in this case suggests a thick LASIK flap calculated to >200 μm by corneal OCT prior to application of the Athen's protocol.

Summary of All Cases

A total of 32 eyes in 22 patients with corneal ectasia occurring 1 to 4 years after LASIK were treated. Preoperative LASIK data were not available in most cases. In the 5 patients who had available data, no irregularity on topography or tomography was noted and no other factor of the LASIK procedure was evaluated to be high risk (eg, thick flap, residual stromal bed <250 μm). All patients had documented progression of inferior steepening in topography and/or tomography maps. Patient age ranged from 23 to 66 years (mean: 32 years) with gender divided (women:men=11:11). The mean measurements representing values after corneal ectasia were confirmed and preoperative to our technique were as follows. Mean sphere was −7.50 D and mean preoperative astigmatism was −2.40 D in the 32 eyes. Mean preoperative to the original LASIK central corneal thickness was ⩾525 μm in 25 of 32 eyes. The original LASIK laser resection data were unavailable in 27 eyes, and flap thickness was assumed or calculated using corneal OCT (Optovue, Fremont, California). The mean residual stromal thickness was 285 μm (range: 210 to 355 μm). Of all 32 ectasia cases, 15 were thought to have resulted from thicker than planned flaps (mean residual stromal bed 230 μm), 10 showed signs of corneal irregularity on preoperative LASIK topography, and 7 had no recognizable risk factor for the development of corneal ectasia.

All topography-guided PRK procedures were planned to reduce corneal thickness by a maximum of 50 μm, despite the existing refractive error, to avoid exacerbation of the ectasia. Most patients (19 patients, 25 eyes) complained of significant pain the first postoperative night whereas others reported minimal discomfort. Mean follow-up after the procedure was 27 months.

Uncorrected distance visual acuity improved in 27 eyes, was unchanged in 4 eyes, and worsened in 1 eye; it was 20/30 or better (+0.18 logMAR) in 11 of 32 eyes and 20/60 or worse (+0.47 logMAR) in 2 eyes. Corrected distance visual acuity was 20/40 or better (+0.30 logMAR) in 27 of 32 eyes and 20/25 or better (+0.10 logMAR) in 14 eyes.

Mean refractive error decreased by more than 2.50 D in 27 of 32 eyes, appeared to increase by 0.75 D in 3 eyes, and remained stable in 2 eyes. Mean final spherical equivalent refraction was −1.75 D, indicating the reduction of cornea irregularity was the target and not emmetropia.

DISCUSSION

Topography-guided PRK flattens some of the cone apex (in a fashion similar to an eccentric partial myopic PRK) but simultaneously flattens an arcuate, broader area of the cornea away from the cone, usually in the superior nasal periphery; this ablation pattern (see Fig 3C) resembles part of a hyperopic treatment and thus will cause some amount of steepening or elevation adjacent to the cone, effectively normalizing the cornea. We have introduced this concept as an effective tissue-saving ablation pattern in highly irregular corneas such as ectasia in keratoconus.[12] It is this core concept in the topography-guided PRK treatment that makes it, in our opinion, more therapeutic than refractive. We have reported[7-10] that in theory, the new "flatter" and

less irregular corneal shape may perform better biomechanically in eyes with corneal ectasia. Specifically, as the corneal apex becomes a flatter and "broader" cone (see Figs 3A and 3B), this may redistribute the biomechanical strain from the eye's intraocular pressure and other external factors (eg, eye rubbing, blinking, etc). This effect may be further enhanced with additional collagen CXL strengthening.

Same-day simultaneous topography-guided PRK and CXL has several advantages: 1) the combination reduces the patient's time away from work, 2) performing both procedures at the same time with topography-guided PRK appears to minimize the potential superficial stromal scarring resulting from topography-guided PRK (unpublished observations, December 2005), and 3) when topography-guided PRK is performed following the CXL procedure, some of the cross-linked anterior cornea is removed, minimizing the potential benefit of CXL (unpublished observations, December 2005). We believe it may be counterintuitive to remove the cross-linked tissue with topography-guided PRK at a later time, as we are potentially removing a beneficial layer of the stiffer, cross-linked cornea, which helps maintain the normalized corneal shape. Lastly, 4) by removing the Bowman layer with topography-guided PRK, this may facilitate riboflavin solution penetration in the corneal stroma and less "shielding" of UVA light in its passage through the cornea, resulting in more effective CXL.

Although a patient with corneal ectasia can have an improved visual result with the addition of the topography-guided PRK, completely removing significant refractive errors was not our goal. We have placed an arbitrary "ceiling" of 50 µm to the amount of tissue that we safely removed centrally, anticipating that further thinning might destabilize the cornea's biomechanical integrity, even following the "stiffening" effect of CXL.

It should be noted that the proprietary riboflavin solution used was a slightly hypotonic (340 mOsm) formulation, resulting in slight "swelling" of the cornea intraoperatively (during CXL). This restored the corneal thickness to approximately 400 µm during CXL to protect the corneal endothelium; we did not encounter any corneal endothelial decompensation in any of the eyes studied herein despite treating cases with corneal thickness less than the theoretical limit of 400 µm[13] prior to CXL (case 4).

In addition, the laser treatment was applied with caution, as the refractive effect of CXL (corneal flattening) had to be anticipated. For this reason, we elected to always attempt a significant undercorrection of both sphere and cylinder by at least 30%. At a later time, we hope to more accurately determine the new ablation rate of CXL stroma.

Simultaneous topography-guided PRK and CXL appears to be effective in the rehabilitation of corneal ectasia after LASIK. The reality of the efficacy of this treatment has been the reduction of penetrating keratoplasty cases performed for the indication of keratoconus and corneal ectasia after LASIK in our practice over the past 4 years. The same-day, simultaneous topography-guided PRK and CXL procedure was easy to perform, but in some cases, the central epithelial surface took up to 1 month to regularize and become lucent. It took from 1 to 4 weeks for us to detect stable changes in keratometry and topography, which seemed to match the visual and refractive changes.

The main goal for all refractive surgeons is to try to eliminate or at least significantly reduce the number of eyes developing corneal ectasia after PRK and LASIK. In some eyes, a preexisting condition that may lead to corneal ectasia with either PRK or LASIK may not be able to be detected, but by eliminating eyes with abnormal preoperative topography and leaving corneas with the maximum clinically acceptable residual stromal thickness, we will be able to reduce the number of eyes that develop corneal ectasia.

Our findings suggest potentially promising results with same-day, simultaneous topography-guided PRK and collagen CXL as a therapeutic intervention in highly irregular corneas with progressive corneal ectasia after LASIK. We have reported herein effective CXL treatment in cases with minimal corneal thickness $<$350 µm. Our study demonstrates that we now have another means of improving the visual and refractive results of a devastating complication while avoiding or delaying penetrating keratoplasty.

AUTHOR CONTRIBUTIONS

Study concept and design (A.J.K.); data collection (A.J.K., P.S.B.); analysis and interpretation of data (A.J.K., P.S.B.); drafting of the manuscript (A.J.K., P.S.B.); critical revision of the manuscript (A.J.K., P.S.B.); administrative, technical, or material support (A.J.K., P.S.B.); supervision (A.J.K.)

REFERENCES

1. Binder PS. Ectasia after laser in situ keratomileusis. *J Cataract Refract Surg*. 2003;29(12):2419-2429.
2. Randleman JB, Russell B, Ward MA, Thompson KP, Stulting RD. Risk factors and prognosis for corneal ectasia after LASIK. *Ophthalmology*. 2003;110(2):267-275.
3. Tabbara K, Kotb A. Risk factors for corneal ectasia after LASIK. *Ophthalmology*. 2006;113(9):1618-1622.
4. Klein SR, Epstein RJ, Randleman JB, Stulting RD. Corneal ectasia after laser in situ keratomileusis in patients without apparent preoperative risk factors. *Cornea*. 2006;25(4):388-403.
5. Binder PS. Analysis of ectasia after laser in situ keratomileusis: risk factors. *J Cataract Refract Surg*. 2007;33(9):1530-1538.

6. Hafezi F, Kanellopoulos J, Wiltfang R, Seiler T. Corneal collagen crosslinking with riboflavin and ultraviolet A to treat induced keratectasia after laser in situ keratomileusis. *J Cataract Refract Surg.* 2007;33(12):2035-2040.
7. Kanellopoulos AJ. Post LASIK ectasia. *Ophthalmology.* 2007;114(6):1230.
8. Kanellopoulos A, Binder PS. Collagen cross-linking (CCL) with sequential topography-guided PRK: a temporizing alternative for keratoconus to penetrating keratoplasty. *Cornea.* 2007;26(7):891-895.
9. Ewald M, Kanellopoulos J. Limited topography-guided surface ablation (TGSA) followed by stabilization with collagen cross-linking with UV irradiation and riboflavin (UVACXL) for keratoconus (KC). *Invest Ophthalmol Vis Sci.* 2008;49:E-Abstract 4338.
10. Kanellopoulos AJ. Comparison of sequential vs same day simultaneous collagen cross-linking and topography-guided PRK for treatment of keratoconus. *J Refract Surg.* 2009;25(9):S812-S818.
11. Krueger RR, Kanellopoulos AJ. Stability of simultaneous topography-guided photorefractive keratectomy and riboflavin/UVA cross-linking for progressive keratoconus: case reports. *J Refract Surg.* 2010;26(10):S827-S832.
12. Kanellopoulos AJ. Managing highly distorted corneas with topography-guided treatment. In: *ISRS/AAO 2007 Subspecialty Day/Refractive Surgery Syllabus. Section II: Ablation Strategies.* San Francisco, CA: American Academy of Ophthalmology; 2007:13-15.
13. Spoerl E, Mrochen M, Sliney D, Trokel S, Seiler T. Safety of UVA-riboflavin cross-linking of the cornea. *Cornea.* 2007;26(4):385-389.

Keratoconus Management: Long-Term Stability of Topography-Guided Normalization Combined With High-Fluence CXL Stabilization (The Athens Protocol)

Anastasios John Kanellopoulos, MD; George Asimellis, PhD

ABSTRACT

PURPOSE: To investigate refractive, topometric, pachymetric, and visual rehabilitation changes induced by anterior surface normalization for keratoconus by partial topography-guided excimer laser ablation in conjunction with accelerated, high-fluence cross-linking.

METHODS: Two hundred thirty-one keratoconic cases subjected to the Athens Protocol procedure were studied for visual acuity, keratometry, pachymetry, and anterior surface irregularity indices up to 3 years postoperatively by Scheimpflug imaging (Oculus Optikgeräte GmbH, Wetzlar, Germany).

RESULTS: Mean visual acuity changes at 3 years postoperatively were +0.38 ± 0.31 (range: -0.34 to +1.10) for uncorrected distance visual acuity and +0.20 ± 0.21 (range: -0.32 to +0.90) for corrected distance visual acuity. Mean K1 (flat meridian) keratometric values were 46.56 ± 3.83 diopters (D) (range: 39.75 to 58.30 D) preoperatively, 44.44 ± 3.97 D (range: 36.10 to 55.50 D) 1 month postoperatively, and 43.22 ± 3.80 D (range: 36.00 to 53.70 D) up to 3 years postoperatively. The average Index of Surface Variance was 98.48 ± 43.47 (range: 17 to 208) preoperatively and 76.80 ± 38.41 (range: 7 to 190) up to 3 years postoperatively. The average Index of Height Decentration was 0.091 ± 0.053 μm (range: 0.006 to 0.275 μm) preoperatively and 0.057 ± 0.040 μm (range: 0.001 to 0.208 μm) up to 3 years postoperatively. Mean thinnest corneal thickness was 451.91 ± 40.02 μm (range: 297 to 547 μm) preoperatively, 353.95 ± 53.90 μm (range: 196 to 480 μm) 1 month postoperatively, and 370.52 ± 58.21 μm (range: 218 to 500 μm) up to 3 years postoperatively.

CONCLUSIONS: The Athens Protocol to arrest keratectasia progression and improve corneal regularity demonstrates safe and effective results as a keratoconus management option. Progressive potential for long-term flattening validates using caution in the surface normalization to avoid overcorrection.

[*J Refract Surg.* 2014;30(2):88-92.]

Keratoconus is a degenerative bilateral, noninflammatory disorder characterized by ectasia, thinning, and irregular corneal topography.[1] The disorder usually has onset at puberty and often progresses until the third decade of life, may manifest asymmetrically in the two eyes of the same patient, and can present with unpredictable visual acuity, particularly in relation to corneal irregularities.[2] One of the acceptable options[3] for progressive keratoconus management is corneal collagen cross-linking (CXL) with riboflavin and ultraviolet-A.[4]

To further improve the topographic and refractive outcomes, CXL can be combined with customized anterior surface normalization.[5-7] Our team has developed a procedure[8,9] we have termed the Athens Protocol,[10] involving sequentially excimer laser epithelial debridement (50 μm), partial topography-guided excimer laser stromal ablation, and high-fluence ultraviolet-A irradiation (10 mW/cm^2), accelerated (10', or minutes) CXL. Early results[11] and anterior segment optical coherence tomography quantitative findings[12] are indicative of the long-term stability of the procedure.

Detailed studies on postoperative visual rehabilitation and anterior surface topographic changes by such combined CXL procedures are rare,[13-16] particularly those reporting results longer than 1 year. This study aims to investigate safety and efficacy of the Athens Protocol procedure by analysis of long-term (3-year) refractive, topographic, pachymetric, and visual rehabilitation changes on clinical keratoconus management with the Athens Protocol in a large number of cases.

PATIENTS AND METHODS

This clinical study received approval by the Ethics Committee of our Institution and adhered to the tenets of the Declaration

From Laservision.gr Eye Institute, Athens, Greece (AJK, GA); and New York University School of Medicine, New York, New York (AJK).

Submitted: April 6, 2013; Accepted: August 21, 2013; Posted online: January 31, 2014

Dr. Kanellopoulos is a consultant for Alcon/WaveLight. The remaining author has no financial or proprietary interest in the materials presented herein.

Correspondence: Anastasios John Kanellopoulos, MD, 17 Tsocha str. Athens, Greece Postal Code 11521. E-mail: ajk@brilliantvision.com

doi:10.3928/1081597X-20140120-03

TABLE 1
Visual Acuity Data (N = 231 Eyes)[a]

Value	Preop	Postoperative					
		1 Month	3 Months	6 Months	12 Months	24 Months	36 Months
UDVA							
Average	0.18	0.42	0.49	0.55	0.57	0.59	0.59
SD (±)	±0.20	±0.27	±0.29	±0.29	±0.28	±0.28	±0.28
Gain/loss	n/a	+0.23	+0.30	+0.36	+0.36	+0.39	+0.38
CDVA							
Average	0.62	0.69	0.76	0.80	0.81	0.82	0.82
SD (±)	±0.23	±0.22	±0.20	±0.20	±0.19	±0.19	±0.19
Gain/loss	n/a	+0.07	+0.14	+0.18	+0.18	+0.19	+0.20

preop = preoperative; UDVA = uncorrected distance visual acuity; SD = standard deviation; n/a = not applicable; CDVA = corrected distance visual acuity
[a]Expressed as the difference of postoperative minus preoperative values (gain/loss). Units are decimal.

of Helsinki. Written informed consent was obtained from each participant at the time of the intervention or the first clinical visit.

Patient Inclusion Criteria

Two hundred thirty-one consecutive keratoconic cases subjected to the Athens Protocol procedure between 2008 and 2010 were investigated. All procedures were performed by the same surgeon (AJK) using the Alcon/WaveLight 400 Hz Eye-Q[17] or the EX500 excimer lasers.[18] Inclusion criteria were clinical diagnosis of progressive keratoconus, minimum age of 17 years, and corneal thickness of at least 300 µm. All participants completed an uneventful Athens Protocol procedure and all 231 eyes were observed for up to 3 years. Exclusion criteria were systemic disease, previous eye surgery, chemical injury or delayed epithelial healing, and pregnancy or lactation (female patients).

Measurements and Analysis

Postoperative evaluation included uncorrected distance visual acuity (UDVA), manifest refraction, corrected distance visual acuity (CDVA) with this refraction, and slit-lamp biomicroscopy for clinical signs of CXL.[12] For the quantitative assessment of the induced corneal changes, postoperative evaluation was performed by a Pentacam Scheimpflug imaging device (Oculyzer II, WavLight AG, Erlangen, Germany)[19] and processed via Examination Software (Version 1.17r47). Specific anterior surface irregularity indices provided by the Scheimpflug imaging analysis were evaluated in addition to keratometric and pachymetric values. These indices are employed in grading and classification based on the Amsler and Krumeich criteria.[20,21] These are the Index of Surface Variance, an expression of anterior surface curvature irregularity, and the Index of Height Decentration, calculated with Fourier analysis of corneal height (expressed in microns) to quantify the degree of cone decentration.[22] Index of Surface Variance and Index of Height Decentration were computed for the 8-mm diameter zone.

Descriptive and comparative statistics, analysis of variance, and linear regression were performed by Minitab version 16.2.3 (MiniTab Ltd., Coventry, UK) and Origin Lab version 9 (OriginLab Corp., Northampton, MA). Paired analysis *P* values less than .05 were considered statistically significant. Visual acuity is reported decimally and keratometry in diopters (D). Results are reported as mean ± standard deviation and range as minimum to maximum.

RESULTS

The 231 eyes enrolled belonged to 84 female and 147 male participants. Mean participant age at the time of the operation was 30.1 ± 7.5 years (range: 17 to 57 years). All eyes were followed up to the 3-year follow-up.

Visual Acuity Changes

Table 1 presents preoperative and postoperative UDVA and CDVA. UDVA increased by +0.38 ± 0.31 (range: -0.34 to +1.10) and CDVA by +0.20 ± 0.21 (range: -0.32 to +0.90). **Figure 1** illustrates, in the form of box plots, visual acuity gained or lost 3 years postoperatively. These graphs (the 95% median confidence range box) indicate that 95% of the cases had at least +0.1 increase in UDVA and 95% had positive change in CDVA.

Keratometric and Anterior Surface Indices Progression

Anterior keratometry continued to flatten over the 3-year follow-up (**Figure 2**). Descriptive statistics for anterior keratometry, preoperatively and postoperatively, are presented in **Table A** (available in the online version of this article).

The values for the Index of Surface Variance and the Index of Height Decentration continued to

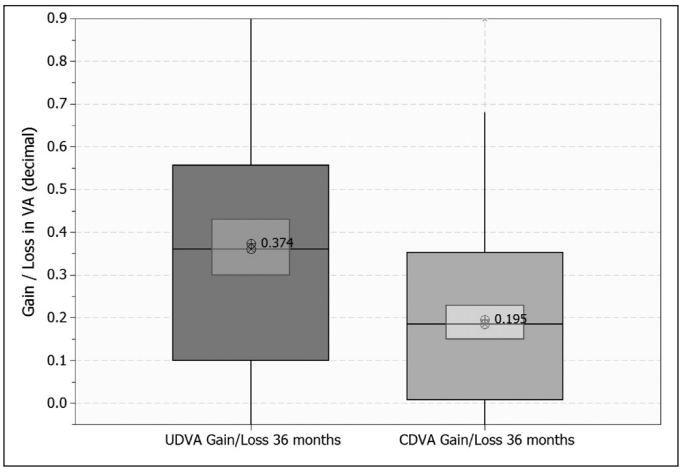

Figure 1. Change (gain/loss) in visual acuity, expressed as the difference of postoperative minus preoperative values (expressed decimally), showing median level (indicated by (+), average symbol (x), 95% median confidence range box (red borderline boxes), and interquartile intervals range box (black borderline boxes).

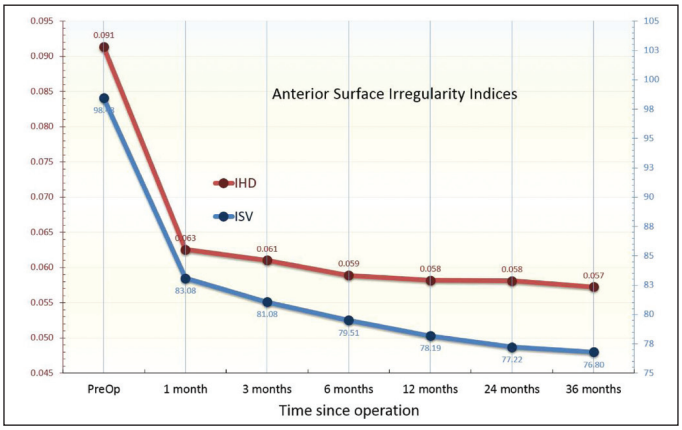

Figure 3. Anterior surface topometric indices Index of Surface Variance (no units) and Index of Height Decentration (units μm) as measured by the Scheimpflug imaging device (Oculyzer II, WavLight AG, Erlangen, Germany) preoperatively, 1 month postoperatively, and up to 36 months postoperatively.

decrease over time (**Figure 3**, **Table B**, available in the online version of this article).

Pachymetric Progression

The thinnest corneal decreased as a result of excimer laser ablation but then stabilized over time without additional thinning (**Table 2**).

DISCUSSION

Many reports describe the effects of CXL with or without same-session excimer laser ablation corneal normalization.[3] There is general consensus that the intervention strengthens the cornea, helps arrest the ectasia progression, and improves corneal keratometric values, refraction, and visual acuity.

The key question is the long-term stability of these induced changes. For example, is the cornea 'inactive' after the intervention and, if not, is there steepening or flattening and/or thickening or thinning? These issues are even more applicable in the case of the Athens Protocol, due to the partial corneal surface ablation. Ablating a thin, ectatic cornea may sound unorthodox. However, the goal of the topography-guided ablation is to normalize the anterior cornea and thus help improve visual rehabilitation to a step beyond that a simple CXL would provide.

Figure 2. Anterior keratometry (K1 flat and K2 steep) as measured by the Scheimpflug device (Oculyzer II, WavLight AG, Erlangen, Germany) preoperatively up to 3 years postoperatively. All units in keratometric diopters (D).

This study aims to address some of the above issues. The large sample and follow-up time permit sensitive analysis with confident conclusion of postoperative efficacy. We monitored visual acuity changes and for the quantitative assessment we chose to standardize on one Scheimpflug screening device and to focus on key parameters of visual acuity, keratometry, pachymetry, and anterior surface indices.[23] All of these parameters reflect changes induced by the procedure and describe postoperative progression. However, variations in the two anterior surface indices (Index of Surface Variance and Index of Height Decentration) may provide a more valid analysis than keratometry and visual function.[24] Our results indicate that the apparent disadvantage of thinning the cornea is balanced by a documented long-term rehabilitating improvement and synergy from the CXL component.

Visual Acuity Changes

Based on our results, the Athens Protocol appears to result in postoperative improvement in both UDVA and CDVA. Average gain/loss in visual acuity was consistently positive, starting from the first postoperative month, with gradual and continuous improvement toward the 3-year visit. These visual rehabilitation improvements appear to be superior to those reported in cases of simple CXL treatment.[25]

However, it is noted that the visual acuity presented with large variations. The standard deviation of UDVA

TABLE 2
Thinnest Corneal Thickness Measured by the Scheimpflug Device (N = 231 Eyes) (μm)

		Postoperative					
Value	**Preoperative**	**1 Month**	**3 Months**	**6 Months**	**12 Months**	**24 Months**	**36 Months**
Average	451.91	353.95	356.67	364.92	367.15	370.52	370.52
SD	±40.02	±53.90	±56.41	±53.64	±55.70	±57.84	±58.21
Maximum	547	480	501	501	490	500	500
Minimum	297	196	179	220	216	218	218

SD = standard deviation

was ±0.20 preoperatively and ±0.28 postoperatively. Likewise, the standard deviation of CDVA was ±0.23 preoperatively and ±0.20 postoperatively.

We theorize that the reason for visual acuity in keratoconic cases having such large fluctuations (and often being unexpectedly good) can be attributed to a 'multifocal' and 'soft' (ie, adaptable) cornea, in addition to advanced neural processing in the individual visual system. However, these 'advantages' are essentially negated with CXL treatment, which stiffens the cornea. Over time, possibly due to further topography improvement and adaptation to the partially normalized cornea, a noteworthy improvement in visual acuity is observed.

Keratometric and Anterior Surface Indices Progression

After the 1-month visit, keratometric values are reduced. This progressive potential for long-term flattening has been clinically observed in many cases over at least 10 years. Peer-reviewed reports on this matter have been rare and only recent.[26,27]

The two anterior surface indices, Index of Surface Variance and Index of Height Decentration, also demonstrated postoperative improvement. A smaller value is indication of corneal normalization (lower Index of Surface Variance, less irregular surface, lower Index of Height Decentration, cone less steep and more central). These changes are therefore suggestive of corneal topography improvement, in agreement with other smaller sample studies.[13] Such changes in Index of Surface Variance and Index of Height Decentration have been reported only recently.[28]

The initial more 'drastic' change of the Index of Height Decentration can be justified by the chief objective of surface normalization, cone centering,[6] which is noted even by the first month. The subsequent surface normalization, as also indicated by keratometric flattening, suggests further anterior surface improvement.

Pachymetric Progression

As expected by the fact that Athens Protocol includes a partial stromal excimer ablation, there is reduction of postoperative corneal thickness, manifested by the thinnest corneal thickness. What seemed to be a 'surprising' result is that the cornea appears to rebound, by gradually thickening, up to 3 years postoperatively. Postoperative corneal thickening after the 1-month 'lowest thickness baseline' has also been discussed recently.[29,30] In another report,[31] the lowest thinnest corneal thickness was noted at the 3-month interval. In that study of 82 eyes treated only with CXL, the average cornea thickened by +24 μm after 1 year compared to the 3-month baseline. In our study of 212 eyes treated with the Athens Protocol procedure, the cornea thickening rate after the baseline first postoperative month was approximately half (+12 μm over the first year), in agreement with a recent publication.[29]

Therefore, it is possible that stromal changes initiated by the CXL procedure are not just effective in halting ectasia, but are prompting corneal surface flattening and thickening, which appears to be longer lasting than anticipated.

We note, however, that CXL alone results not just in corneal reshaping, but also in stromal density and refractive index, both possibly influencing the reported thickness by the Scheimpflug device. Therefore, true corneal thickness differences may not be accurately explored by Scheimpflug imaging due to the principle of operation (densitometry), which has been our clinical experience with abnormal density corneas (ie, corneal scars or arcus senilis corneas). Further studies of corneal thickness chances by modalities, such as anterior segment optical coherence tomography, which currently also measure epithelial thickness,[32] may be warranted. In addition, corneal biomechanical analysis and corneal volume studies may be necessary to further validate such findings.

Our study indicates a significant improvement in all parameters studied. The changes induced by the procedure indicate a consistent trend toward improved visual rehabilitation, corneal flattening (validating ectasia arrest), and anterior surface improvement. The Athens Protocol procedure demonstrates impressive refractive, keratometric, and topometric results. Progressive potential for long-term flattening documented

in this study suggests employment of caution in the surface normalization process to avoid overcorrection.

AUTHOR CONTRIBUTIONS

Study concept and design (AJK, GA); data collection (AJK, GA); analysis and interpretation of data (AJK, GA); drafting of the manuscript (GA); critical revision of the manuscript (AJK, GA); statistical expertise (GA); administrative, technical, or material support (AJK); supervision (AJK)

REFERENCES

1. Gordon-Shaag A, Millodot M, Shneor E. The epidemiology and etiology of keratoconus. *Int J Keratoco Ectatic Corneal Dis*. 2012;1:7-15.
2. Katsoulos C, Karageorgiadis L, Mousafeiropoulos T, Vasileiou N, Asimellis G. Customized hydrogel contact lenses for keratoconus incorporating correction for vertical coma aberration. *Ophthalmic Physiol Opt*. 2009;29:321-329.
3. Chan E, Snibson GR. Current status of corneal collagen cross-linking for keratoconus: a review. *Clin Exp Optom*. 2013;96:155-164.
4. Kanellopoulos AJ. Collagen cross-linking in early keratoconus with riboflavin in a femtosecond laser-created pocket: initial clinical results. *J Refract Surg*. 2009;25:1034-1037.
5. Kanellopoulos AJ, Binder PS. Collagen cross-linking (CCL) with sequential topography-guided PRK: a temporizing alternative for keratoconus to penetrating keratoplasty. *Cornea*. 2007;26:891-895.
6. Kanellopoulos AJ. Comparison of sequential vs same-day simultaneous collagen cross-linking and topography-guided PRK for treatment of keratoconus. *J Refract Surg*. 2009;25:S812-S818.
7. Labiris G, Giarmoukakis A, Sideroudi H, Gkika M, Fanariotis M, Kozobolis V. Impact of keratoconus, cross-linking and cross-linking combined with photorefractive keratectomy on self-reported quality of life. *Cornea*. 2012;31:734-739.
8. Kanellopoulos AJ, Binder PS. Management of corneal ectasia after LASIK with combined, same-day, topography-guided partial transepithelial PRK and collagen cross-linking: the athens protocol. *J Refract Surg*. 2011;27:323-331.
9. Ewald M, Kanellopoulos J. Limited topography-guided surface ablation (TGSA) followed by stabilization with collagen crosslinking with UV irradiation and ribofl avin (UVACXL) for keratoconus (KC). *Invest Ophthalmol Vis Sci*. 2008;49:E-Abstract 4338.
10. Kanellopoulos AJ. Long term results of a prospective randomized bilateral eye comparison trial of higher fluence, shorter duration ultraviolet A radiation, and riboflavin collagen cross linking for progressive keratoconus. *Clin Ophthalmol*. 2012;6:97-101.
11. Krueger RR, Kanellopoulos AJ. Stability of simultaneous topography-guided photorefractive keratectomy and riboflavin/UVA cross-linking for progressive keratoconus: case reports. *J Refract Surg*. 2010;26:S827-S832.
12. Kanellopoulos AJ, Asimellis G. Introduction of quantitative and qualitative cornea optical coherence tomography findings, induced by collagen cross-linking for keratoconus; a novel effect measurement benchmark. *Clin Ophthalmol*. 2013;7:329-335.
13. Greenstein SA, Fry KL, Hersh PS. Corneal topography indices after corneal collagen crosslinking for keratoconus and corneal ectasia: one-year results. *J Cataract Refract Surg*. 2011;37:1282-1290.
14. Guedj M, Saad A, Audureau E, Gatinel D. Photorefractive keratectomy in patients with suspected keratoconus: five-year follow-up. *J Cataract Refract Surg*. 2013;39:66-73.
15. Alessio G, L'abbate M, Sborgia C, La Tegola MG. Photorefractive keratectomy followed by cross-linking versus cross-linking alone for management of progressive keratoconus: two-year follow-up. *Am J Ophthalmol*. 2013;155:54-65.
16. Hersh PS, Greenstein SA, Fry KL. Corneal collagen crosslinking for keratoconus and corneal ectasia: one-year results. *J Cataract Refract Surg*. 2011;37:149-160.
17. Kanellopoulos AJ. Topography-guided hyperopic and hyperopic astigmatism femtosecond laser-assisted LASIK: long-term experience with the 400 Hz eye-Q excimer platform. *Clin Ophthalmol*. 2012;6:895-901.
18. Kanellopoulos AJ, Asimellis G. Long-term bladeless LASIK outcomes with the FS200 femtosecond and EX500 Excimer Laser workstation: the Refractive Suite. *Clin Ophthalmol*. 2013;7:261-269.
19. Kanellopoulos AJ, Asimellis G. Correlation between central corneal thickness, anterior chamber depth, and corneal keratometry as measured by Oculyzer II and WaveLight OB820 in preoperative cataract surgery patients. *J Refract Surg*. 2012;28:895-900.
20. Krumeich JH, Daniel J, Knülle A. Live-epikeratophakia for keratoconus. *J Cataract Refract Surg*. 1998;24:456-463.
21. Faria-Correia F, Ramos IC, Lopes BT, et al. Topometric and tomographic indices for the diagnosis of keratoconus. *Int J Kerat Ectatic Dis*. 2012;1:100-106.
22. Kanellopoulos AJ, Asimellis G. Revisiting keratoconus diagnosis and progression classification based on evaluation of corneal asymmetry indices, derived from Scheimpflug imaging in keratoconic and suspect cases. *Clin Ophthalmol*. 2013;7:1539-1548.
23. Markakis GA, Roberts CJ, Harris JW, Lembach RG. Comparison of topographic technologies in anterior surface mapping of keratoconus using two display algorithms and six corneal topography devices. *Int J Kerat Ectatic Dis*. 2012;1:153-157.
24. Ambrósio R Jr, Caiado AL, Guerra FP, et al. Novel pachymetric parameters based on corneal tomography for diagnosing keratoconus. *J Refract Surg*. 2011;27:753-758.
25. Legare ME, Iovieno A, Yeung SN, et al. Corneal collagen crosslinking using riboflavin and ultraviolet A for the treatment of mild to moderate keratoconus: 2-year follow-up. *Can J Ophthalmol*. 2013;48:63-68.
26. Vinciguerra P, Albè E, Trazza S, et al. Refractive, topographic, tomographic, and aberrometric analysis of keratoconic eyes undergoing corneal cross-linking. *Ophthalmology*. 2009;116:369-378.
27. Raiskup-Wolf F, Hoyer A, Spoerl E, Pillunat LE. Collagen crosslinking with riboflavin and ultraviolet-A light in keratoconus: longterm results. *J Cataract Refract Surg*. 2008;34:796-801.
28. Kanellopoulos AJ, Asimellis G. Comparison of Placido disc and Scheimpflug image-derived topography-guided excimer laser surface normalization combined with higher influence CXL: The Athens Protocol, in progressive keratoconus cases. *Clin Ophthalmol*. 2013;7:1539-1548.
29. Mencucci R, Paladini I, Virgili G, Giacomelli G, Menchini U. Corneal thickness measurements using time-domain anterior segment OCT, ultrasound, and Scheimpflug tomographer pachymetry before and after corneal cross-linking for keratoconus. *J Refract Surg*. 2012;28:562-566.
30. O'Brart DP, Kwong TQ, Patel P, McDonald RJ, O'Brart NA. Long-term follow-up of riboflavin/ultraviolet A (370 nm) corneal collagen cross-linking to halt the progression of keratoconus. *Br J Ophthalmol*. 2013;97:433-437.
31. Greenstein SA, Shah VP, Fry KL, Hersh PS. Corneal thickness changes after corneal collagen crosslinking for keratoconus and corneal ectasia: one-year results. *J Cataract Refract Surg*. 2011;37:691-700.
32. Kanellopoulos AJ, Asimellis G. Anterior segment optical coherence tomography: assisted topographic corneal epithelial thickness distribution imaging of a keratoconus patient. *Case Rep Ophthalmol*. 2013;4:74-78.

TABLE A

Anterior Keratometry (K) Measured by the Scheimpflug Device (N = 231 Eyes)[a]

		Postoperative					
Value	**Preop**	**1 Month**	**3 Months**	**6 Months**	**12 Months**	**24 Months**	**36 Months**
K1 (flat)							
Average	46.56	44.44	43.99	43.73	43.54	43.35	43.22
SD	±3.83	±3.97	±3.86	±3.76	±3.73	±3.74	±3.80
Maximum	58.30	55.50	53.75	53.70	53.70	53.70	53.70
Minimum	39.75	36.10	36.10	36.10	36.10	36.10	36.00
K2 (steep)							
Average	50.71	47.61	47.03	46.84	46.63	46.44	46.30
SD	±5.14	±5.15	±4.99	±4.92	±4.91	±4.88	±4.91
Maximum	66.62	62.75	61.25	60.25	60.00	60.00	60.00
Minimum	42.60	38.00	37.90	37.90	37.90	37.90	37.20

preop = preoperative; SD = standard deviation
[a]All units in keratometric diopters (D).

TABLE B

Anterior Surface Topometric Indices and Postoperative Progression (N = 231 Eyes)

		Postoperative					
Value	**Preoperative**	**1 Month**	**3 Months**	**6 Months**	**12 Months**	**24 Months**	**36 Months**
Index of Surface Variance							
Average	98.48	83.08	81.08	79.51	78.19	77.22	76.80
SD	±43.47	±38.73	±38.13	±37.79	±38.04	±38.28	±38.41
Maximum	208	190	190	190	190	190	190
Minimum	17	18	17	16	15	14	7
Index of Height Decentration (μm)							
Average	0.091	0.063	0.061	0.059	0.058	0.058	0.057
SD	±0.053	±0.041	±0.040	±0.040	±0.040	±0.040	±0.040
Maximum	0.275	0.208	0.208	0.208	0.208	0.208	0.208
Minimum	0.006	0.001	0.001	0.001	0.001	0.001	0.001

SD = standard deviation

Corneal Refractive Power and Symmetry Changes Following Normalization of Ectasias Treated With Partial Topography-Guided PTK Combined With Higher-Fluence CXL (The Athens Protocol)

Anastasios John Kanellopoulos, MD; George Asimellis, PhD

ABSTRACT

PURPOSE: To investigate preoperative and postoperative anterior and posterior keratometry and simulated corneal astigmatism in keratoconic eyes treated with collagen cross-linking combined with anterior surface normalization by partial topography-guided excimer ablation (the Athens Protocol).

METHODS: Anterior and posterior corneal keratometry were measured by Scheimpflug imaging for 267 untreated keratoconic eyes. Following treatment, they were assessed 1 year postoperatively.

RESULTS: Before treatment, average anterior keratometric value was 47.06 ± 6.02 diopters (D) for flat and 51.24 ± 6.75 D for steep. The posterior keratometric values were -6.70 ± 0.99 D (flat) and -7.67 ± 1.15 D (steep). Anterior astigmatism was on average with-the-rule (-1.97 ± 6.21 D), whereas posterior astigmatism was against-the-rule (+0.53 ± 1.02 D). The posterior and anterior astigmatism were highly correlated (r^2 = 0.839). After treatment, anterior keratometric values were 43.97 ± 5.81 D (flat) and 46.55 ± 6.82 D (steep). Posterior keratometric values were -6.58 ± 1.05 D (flat) and -7.69 ± 1.22 D (steep). Anterior astigmatism was on average with-the-rule (-1.56 ± 3.80 D), whereas posterior astigmatism was against-the-rule (+0.45 ± 1.29 D). The statistically significant ($P < .05$) keratometric changes indicated anterior surface flattening -3.09 ± 2.67 D (flat) and -4.19 ± 2.96 D (steep). The posterior keratometric changes were not statistically significant ($P > .05$).

CONCLUSIONS: Before treatment, there was a strong correlation between posterior and anterior corneal astigmatism. After treatment, statistically significant anterior keratometric values flattened. The posterior surface keratometric values did not demonstrate statistically significant postoperative change: there was minimal posterior change, despite the significant anterior surface normalization.

[*J Refract Surg.* 2014;30(5):342-346.]

Keratoconus assessment employs indicators such as keratometric values, inferior-superior index, skew percentage, astigmatism, and the KISA% index.[1] Acceptable quantitative keratometric criteria include central corneal refractive power larger than 47.2 diopters (D), inferior-superior dioptric asymmetry larger than 1.2 D, and simulated astigmatism, expressed as the difference between steep and flat keratometric values greater than 1.5 D.[2] The steep and flat meridian keratometric values correspond to the smaller and larger anterior corneal curvature radius, respectively.

Corneal cross-linking (CXL) is an in vivo intrastromal photo-oxidative technique with riboflavin and ultraviolet-A light aiming to address the advancing corneal ectasia and, consequently, the keratoconus progression. With CXL, additional covalent bonding between stromal collagen can be achieved, which stabilizes the collagen framework structure.[3] The remodeling effects of CXL on the cornea can be described by the reduction of mean anterior surface keratometric values.[4] Few studies have been published on the quantitative link between anterior and posterior keratometric values in keratoconic eyes or particularly on the postoperative effects of CXL on either corneal surface.

This study aims to investigate the distribution of and relationship between anterior and posterior corneal keratometric values and simulated anterior and posterior astigmatism on a large group of clinically diagnosed, untreated keratoconic eyes, and the 1-year postoperative effects on both anterior and posterior keratometric values and astigmatism induced by a combined procedure known as the Athens Protocol,[5,6] which intends to arrest the keratoconus progression and normalize the anterior corneal surface.

From Laservision.gr Eye Institute, Athens, Greece (AJK, GA); and New York University School of Medicine, New York, New York (AJK).

Submitted: July 22, 2013; Accepted: January 16, 2014; Posted online: May 2, 2014

The authors have no financial or proprietary interest in the materials presented herein.

Correspondence: Anastasios John Kanellopoulos, MD, Laservision.gr Eye Institute, 17 Tsocha str, Athens 11521, Greece. E-mail: ajk@brilliantvision.com

doi:10.3928/1081597X-20140416-03

PATIENTS AND METHODS

This study was performed in patients visiting our clinical practice and which received approval by the ethics committee of our institution and adhered to the tenets of the Declaration of Helsinki. Informed written consent was obtained from all patients at the time of the first clinical visit.

Inclusion Criteria and Surgical Technique

The study group consisted of 267 eyes. Patients' ages at the time of the screening ranged from 19 to 57 years. Each patient received a complete ocular examination, including subjective refraction, visual acuity, and slit-lamp biomicroscopy for clinical signs of keratoconus. Inclusion criteria included definite findings consistent with keratoconus, described by the Collaborative Longitudinal Evaluation of Keratoconus group.[7] Exclusion criteria included systemic disease, previous corneal surgery, history of chemical injury or delayed epithelial healing, and pregnancy or lactation (female patients) during the study.

The same cases received treatment with the Athens Protocol,[8] which involved excimer laser epithelial debridement (50 µm), partial (maximum ablation 80 µm) topography-guided excimer laser stromal ablation, and high-fluence ultraviolet-A irradiation (10 mW/cm^2), accelerated (10') CXL performed with the Avedro KXL System (Avedro, Inc., Waltham, MA). The Athens Protocol treatments employed the Oculyzer II (WaveLight AG, Erlagen, Germany)[9,10] for corneal topography imaging. The Oculyzer II is a high-resolution Pentacam Scheimpflug imaging rotating camera (Oculus Optikgeräte GmbH, Wetzlar, Germany) incorporated by a proprietary network in the WaveLight Refractive Suite (WaveLight AG)[11] to provide corneal elevation data to the excimer laser, namely the EX500 (Alcon Laboratories, Fort Worth, TX).

For a patient to be considered for the Athens Protocol procedure, the criteria included clinical diagnosis of progressive keratoconus, minimum age of 18 years, and 300-µm minimum corneal thickness. Further details of the Athens Protocol procedure have been published.[12,13] All patients were observed at 1 week and 1, 3, 6, and 12 months postoperatively, and on an annual basis thereafter. The corneal data reported in this study after treatment comprised measurements obtained at the 12-month postoperative visit.

Imaging, Measurement, and Analysis

The Scheimpflug camera (Oculyzer II) was regularly calibrated according to manufacturer recommendations. The measurements were obtained and processed via the Examination Software (Version 1.17r47; WaveLight AG). The default settings and 25 images per single acquisition were implemented. Keratometric and simulated astigmatism data were obtained with the best fit toric ellipsoid reference surface.

Linear regression analysis was performed to seek possible correlations. Descriptive and comparative statistics and analysis of variance were performed with statistics tools provided by Minitab version 16.2.3. (MiniTab Ltd., Coventry, UK) and Origin Lab version 9 (OriginLab Corp, Northampton, MA). A *P* value less than .05 was considered statistically significant.

RESULTS

The sample consisted of 267 eyes (82 female and 185 male). There was preponderance toward male gender, consistent with our clinical experience in male-to-female incidence in keratoconic patients[14] and keratoconus incidence studies.[15] Of the 267 eyes, 140 were right eyes and 127 were left eyes. The average age for all patients at the time of the procedure was 30.80 ± 7.25 years (range: 19 to 57 years). The average preoperative corrected distance visual acuity was 20/32, ranging from 20/200 to 20/20 (0.628 ± 0.241). One year postoperatively, average corrected distance visual acuity was 20/25, ranging from 20/100 to 20/16 (0.762 ± 0.225).

Anterior and Posterior Keratometry and Corneal Astigmatism Before Treatment

Average, standard deviation, and maximum and minimum anterior and posterior central corneal surface keratometric values before and after treatment with the Athens Protocol are reported in **Table 1**.

The astigmatism sign is dependent on the flat meridian horizontal or vertical orientation: the sign is considered positive if the flat meridian orientation is between +45° and +135°, which is called "against-the-rule," whereas it is considered negative if between -45° and +45°, which is called "with-the-rule."

After treatment, the resulting anterior astigmatism was on average with-the-rule, whereas the posterior astigmatism was against-the-rule (**Figure 1**). Paired analysis of the differences regarding astigmatism change indicated a *P* value of .067 for the anterior surface and .358 for the posterior surface.

Keratometric Changes and Analysis

Figure 1 illustrates the correlation between posterior versus anterior astigmatism in the form of scatter and fitted line plots with 95% confidence intervals and 95% prediction intervals before and after treatment. Before treatment, the coefficient of determination (r^2) was 0.839 with a *P* value less than .001. After

TABLE 1
Anterior and Posterior Corneal Surface Keratometry and Astigmatism as Measured in the 8-mm Diameter Zone Before and After Treatment

	Before Treatment				After Treatment			
Parameter	**Average (D)**	**SD (D)**	**Max (D)**	**Min (D)**	**Average (D)**	**SD (D)**	**Max (D)**	**Min (D)**
Anterior cornea								
Flat	47.06	±6.02	78.50	33.70	43.97	±5.81	73.2	30.1
Steep	51.24	±6.75	80.70	39.50	47.04	±6.86	81.3	33.9
Mean	49.03	±6.21	78.80	38.80	46.37	±6.73	80.9	31.9
Astigmatism	-1.97	±6.21	11.30	-12.40	-1.56	±3.80	12.4	-11.5
Posterior cornea								
Flat	-6.70	±0.99	-4.60	-9.90	-6.58	±1.05	-3.3	-10.4
Steep	-7.67	±1.15	-5.60	-11.00	-7.69	±1.22	-5.2	-13.2
Mean	-7.08	±1.40	8.50	-10.20	-7.08	±1.06	-4.2	-11.5
Astigmatism	+0.53	±1.02	+4.00	-2.60	+0.45	±1.29	+4.3	-5.3

SD = standard deviation; D = diopters; Max = maximum; Min = minimum

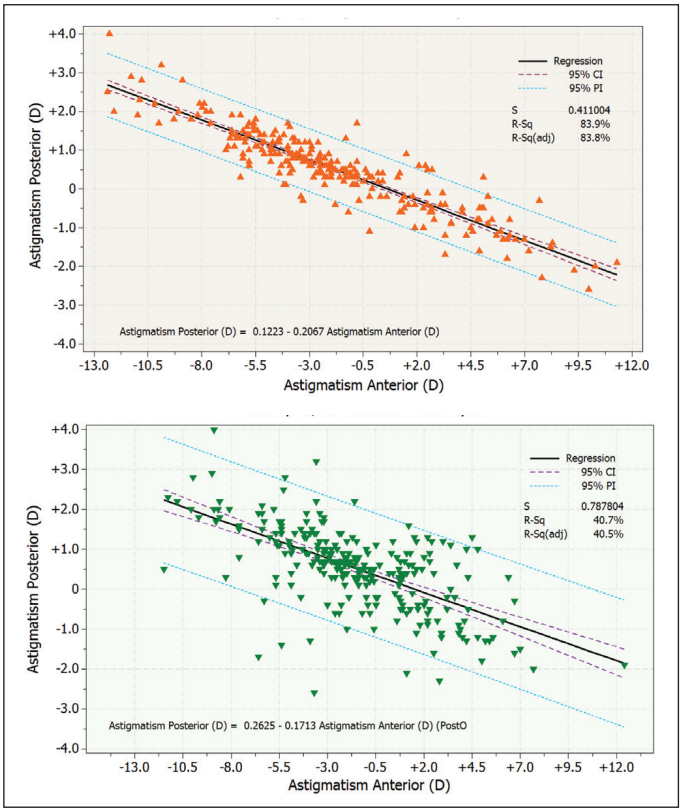

Figure 1. Scatter and fitted line plots of posterior astigmatism expressed in diopters (D) versus anterior astigmatism (also expressed in D) with 95% confidence intervals (CI) and 95% prediction intervals (PI). (Top) Before and (bottom) after treatment.

treatment, r^2 was 0.407 and P value less than .001 (**Table 2**).

Data analysis indicates that the mean of the paired differences regarding the flat anterior keratometric values was reduced (flattened) postoperatively by -3.09 ± 2.69 D, or -6.56%, and was statistically significant ($P < .05$) (**Table 2**). The uncertainty associated with estimating the difference from sample data indicated, with a 95% confidence interval, that the true difference was between -2.76 and -3.41 D. The steep anterior keratometric values showed a postoperative flattening by -4.19 ± 2.96 D, or -8.19%, again statistically significant ($P < .05$). The true 95% difference was between -3.84 and -4.55 D.

The mean of the paired differences regarding the flat posterior keratometric values showed an increase of +0.12 ± 0.61 D, or -1.76% (considering the negative sign of the posterior keratometric values). The 95% true difference was between -0.191 and -0.0449 D. The analysis for the steep posterior keratometric values showed a postoperative change of -0.02 ± 0.55 D or +0.04% (95% true difference between -0.0485 and +0.0829 D). These differences were not statistically significant (flat $P = .135$, steep $P = .606$).

DISCUSSION

In this study, a rotating Scheimpflug camera was employed to measure both the anterior and posterior corneal curvature in a large number (267) of keratoconic cases, before and after (1 year postoperatively) a combined CXL and anterior surface excimer laser normalization. In the case of keratoconus, highly irregular keratometric values were present. For example, the simultaneous investigation of anterior and posterior corneal keratometric values has indicated statistically significant differences between normal and keratoconus-suspect eyes.[16] In a study evaluating keratometric values in keratoconic compared to normal eyes, the

mean value was 43.28 ± 1.17 D (range: 41.53 to 45.40 D) for normal eyes and 49.29 ± 4.37 D (range: 42.97 to 60.33 D) for keratoconic eyes.[17]

In our study, the average keratometric values before treatment were 47.06 ± 6.02 D (range: 33.7 to 78.5 D) for flat and 51.24 ± 6.75 D (range: 39.5 to 80.7 D) for steep. As shown in the corresponding box plots in **Figures A-C** (available in the online version of this article), 95% of the sample population had a steep keratometric value greater than 46.025 D, consistent with the Collaborative Longitudinal Evaluation of Keratoconus group standards.[7]

In the current study, before treatment the results were characterized by a pattern of linear correlation between anterior and posterior astigmatism, as shown in the fitted line plot of **Figure 1**. The anterior astigmatism before treatment is generally with-the-rule and the posterior astigmatism is against-the-rule, with a linear fit coefficient ratio of -0.2067 and a robust coefficient of determination (r^2) of 0.839. Thus, posterior corneal keratometric values appeared in this large keratoconic population to be associated with the anterior keratometric values.

However, this pattern does not seem to be consistent after treatment (**Figure 1**). Although the ratio was similar (-0.26), the coefficient of determination was considered poor (r^2 = 0.405). Our results indicate that this was due to the induced changes in the anterior surface. Specifically, there was a statistically significant reduction in the anterior keratometric values after the Athens Protocol procedure demonstrated by a flattening of -3.09 D for the flat and -4.19 D for the steep meridians, in agreement with other studies of keratoconic cases receiving CXL treatment.[18] The observed changes in the posterior keratometric values were not statistically significant, and thus no measurable change in the posterior corneal surface could be established in our study.

The issue of posterior surface change following CXL,[19] surface ablation,[20] or a combination of both procedures has to be viewed with skepticism. We present these data with the reservation that measurements of the posterior surface might be influenced by the algorithm involving corneal thickness measurements, which, in the case of the densitometry principle-based imaging, might be influenced in the CXL-treated corneas.[21,22] Scheimpflug imaging in its current form can only provide data for the posterior surface on clear, normal corneas. Any significant cornea irregularity or light conduction interference may bias the findings. Also possible is that the denser CXL effect observed with application of the Athens Protocol may mask posterior surface changes. Therefore, although we observed some posterior surface changes, as expected, due to the dramatic alteration of the anterior surface and cornea stromal changes, these appear to be non-significant in comparison to the anterior surface changes.

TABLE 2

Anterior and Posterior Corneal Surface Keratometry Changes Before and After Treatment[a]

Parameter	K1 Anterior (D)	K2 Anterior (D)	K1 Posterior (D)	K2 Posterior (D)
Relative change (%)	-6.56	-8.19	-1.76	-0.04
Average change	-3.09	-4.19	0.12	-0.02
SD	2.67	2.96	0.61	0.55
Max	4.95	1.70	3.60	2.00
Min	-17.30	-17.30	-1.50	-2.90
P[b]	< .01	< .01	.135	.606

K = keratometry; K1 = flat; K2 = steep; D = diopters; SD = standard deviation; Max = maximum; Min = minimum

[a]*Average change is defined as the postoperative (after treatment) minus the preoperative value (before treatment), computed on each individual. Relative change is defined as the percent of the average change of the parameter with regard to the respective preoperative value.*

[b]*Two sample* t *test.*

There is an obvious clinical dilemma in deciding to ablate thin corneas with ectasia. Traditional clinical experience in the pro-CXL era may consider this dangerous for the ectasia progression. We investigated the principle of posterior curvature stability in these eyes because of a critical factor of establishing the safety of ablating these corneas. As expected, the posterior surface keratometric values did not show statistically significant postoperative change. Various data suggest that there is minimal change in the biomechanical behavior of the ectatic cornea after the Athens Protocol, despite the dramatic change in the anterior surface cone.

Before treatment the elevated anterior and posterior keratometric values were highly correlated. After treatment showed statistically significant anterior surface flattening, consistent with our previous studies. The posterior surface did not show a statistically significant change, validating the accomplished cornea stability despite the interventional thinning.

AUTHOR CONTRIBUTIONS

Conception and design (AJK); data collection (AJK); analysis and interpretation of data (AJK, GA); writing the manuscript (GA); critical revision of the manuscript (AJK, GA)

REFERENCES

1. Rabinowitz YS, Rasheed K. KISA% index: a quantitative videokeratography algorithm embodying minimal topographic criteria for diagnosing keratoconus. *J Cataract Refract Surg.* 1999;25:1327-1335.

2. Rabinowitz YS. Videokeratographic indices to aid in screening for keratoconus. *J Refract Surg.* 1995;11:371-379.
3. Wollensak G. Crosslinking treatment of progressive keratoconus: a new hope. *Curr Opin Ophthalmol.* 2006;17:356-360.
4. Raiskup-Wolf F, Hoyer A, Spoerl E, Pillunat LE. Collagen crosslinking with riboflavin and ultraviolet-A light in keratoconus: long-term results. *J Cataract Refract Surg.* 2008;34:796-801.
5. Kanellopoulos AJ, Binder PS. Management of corneal ectasia after LASIK with combined, same-day, topography-guided partial transepithelial PRK and collagen cross-linking: the Athens Protocol. *J Refract Surg.* 2011;27:323-331.
6. Kanellopoulos AJ, Asimellis G. Comparison of Placido disc and Scheimpflug image-derived topography-guided excimer laser surface normalization combined with higher fluence CXL: the Athens Protocol, in progressive keratoconus. *Clin Ophthalmol.* 2013;7:1385-1396.
7. Zadnik K, Barr JT, Edrington TB, et al. Baseline findings in the Collaborative Longitudinal Evaluation of Keratoconus (CLEK) Study. *Invest Ophthalmol Vis Sci.* 1998;39:2537-2546.
8. Kanellopoulos AJ. Long term results of a prospective randomized bilateral eye comparison trial of higher fluence, shorter duration ultraviolet A radiation, and riboflavin collagen cross linking for progressive keratoconus. *Clin Ophthalmol.* 2012;6:97-101.
9. Kanellopoulos AJ, Asimellis G. Correlation between central corneal thickness, anterior chamber depth, and corneal keratometric values as measured by Oculyzer II and WaveLight OB820 in preoperative cataract surgery patients. *J Refract Surg.* 2012;28:895-900.
10. McAlinden C, Khadka J, Pesudovs K. A comprehensive evaluation of the precision (repeatability and reproducibility) of the Oculus Pentacam HR. *Invest Ophthalmol Vis Sci.* 2011;52:7731-7737.
11. Kanellopoulos AJ, Asimellis G. Long-term bladeless LASIK outcomes with the FS200 femtosecond and EX500 Excimer Laser workstation: the Refractive Suite. *Clin Ophthalmol.* 2013;7:261-269.
12. Kanellopoulos AJ. Comparison of sequential vs same-day simultaneous collagen cross-linking and topography-guided PRK for treatment of keratoconus. *J Refract Surg.* 2009;25:S812-S818.
13. Kanellopoulos AJ. Long term results of a prospective randomized bilateral eye comparison trial of higher fluence, shorter duration ultraviolet A radiation, and riboflavin collagen cross linking for progressive keratoconus. *Clin Ophthalmol.* 2012;6:97-101.
14. Kanellopoulos AJ, Asimellis G. Introduction of quantitative and qualitative cornea optical coherence tomography findings induced by collagen cross-linking for keratoconus: a novel effect measurement benchmark. *Clin Ophthalmol.* 2013;7:329-335.
15. Gordon-Shaag A, Millodot M, Shneor E. The epidemiology and etiology of keratoconus. *Int J Keratoco Ectatic Corneal Dis.* 2012;1:7-15.
16. Schlegel Z, Hoang-Xuan T, Gatinel D. Comparison of and correlation between anterior and posterior corneal elevation maps in normal eyes and keratoconus-suspect eyes. *J Cataract Refract Surg.* 2008;34:789-795.
17. Alió JL, Shabayek MH. Corneal higher order aberrations: a method to grade keratoconus. *J Refract Surg.* 2006;22:539-545.
18. Mazzotta C, Caporossi T, Denaro R, et al. Morphological and functional correlations in riboflavin UV A corneal collagen cross-linking for keratoconus. *Acta Ophthalmol.* 2012;90:259-265.
19. Kránitz K, Kovács I, Miháltz K, et al. Corneal changes in progressive keratoconus after cross-linking assessed by Scheimpflug camera. *J Refract Surg.* 2012;28:645-649.
20. Sy ME, Ramirez-Miranda A, Zarei-Ghanavati S, Engle J, Danesh J, Hamilton DR. Comparison of posterior corneal imaging before and after LASIK using dual rotating scheimpflug and scanning slit-beam corneal tomography systems. *J Refract Surg.* 2013;29:96-101.
21. Kanellopoulos AJ, Asimellis G. Keratoconus management: long-term stability of topography-guided normalization combined with high-fluence CXL stabilization (The Athens Protocol). *J Refract Surg.* 2014;30:88-92.
22. Nakagawa T, Maeda N, Kosaki R, et al. Higher-order aberrations due to the posterior corneal surface in patients with keratoconus. *Invest Ophthalmol Vis Sci.* 2009;50:2660-2665.

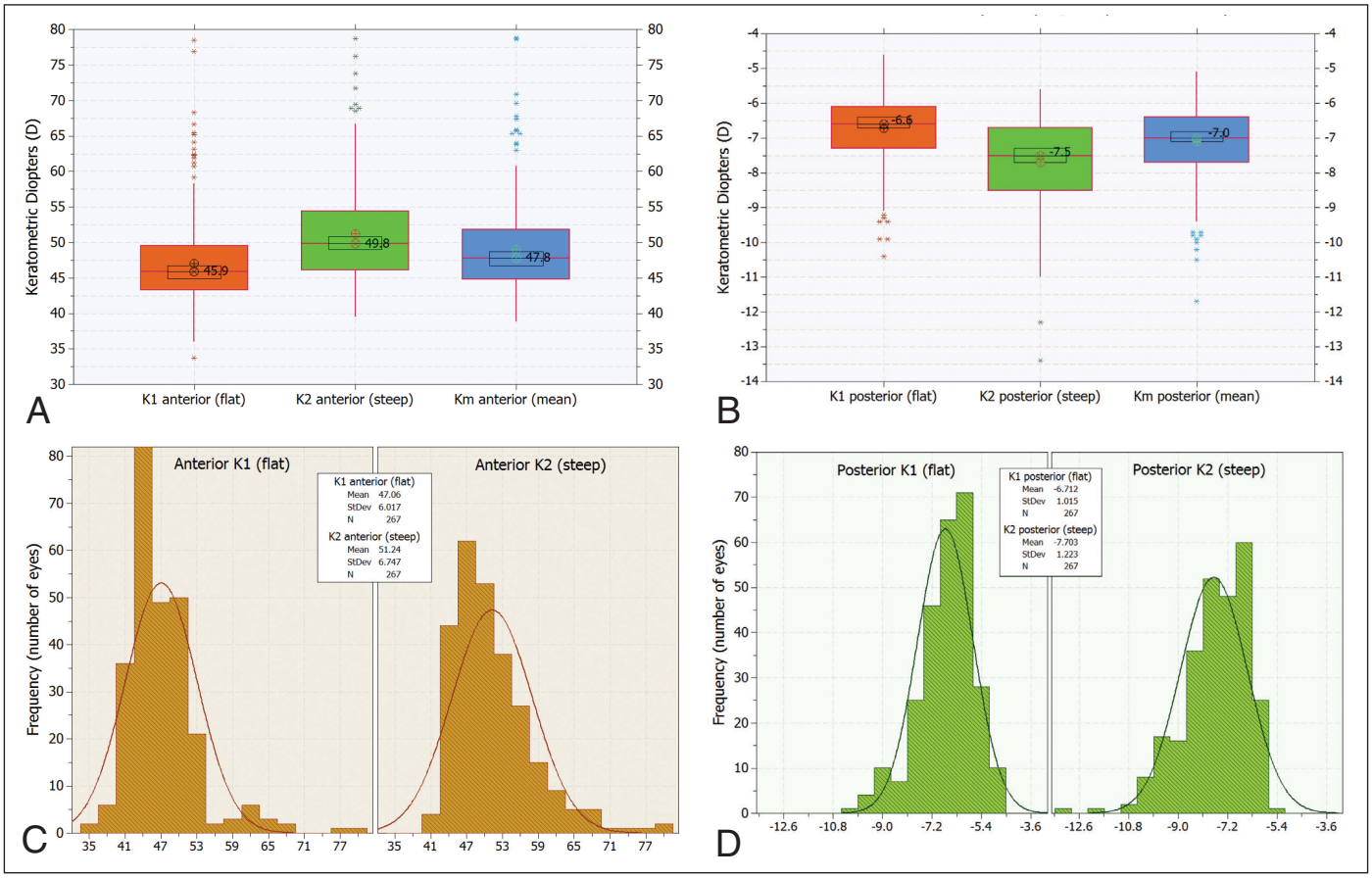

Figure A. Anterior and posterior surface keratometric values (K1 [flat], K2 [steep], and Km [mean]) before treatment. (A, B) Box plots showing median level (indicated by ⊗, average symbol ⊕), 95% median confidence range box (black line boxes), and interquartile intervals range box (red line boxes). (C, D) The corresponding histogram plots)for K1 and K2. All units in keratometric diopters (D).

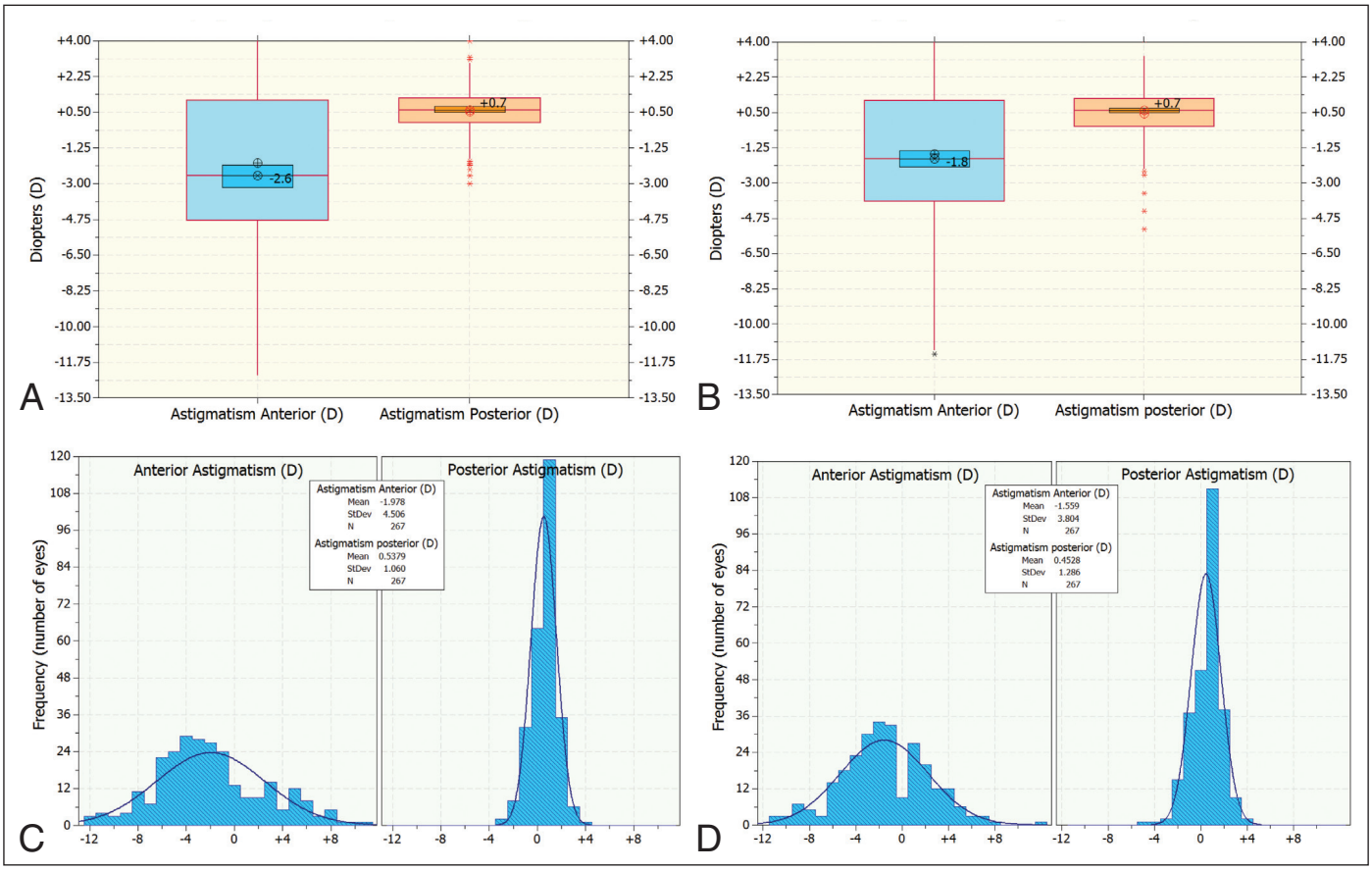

Figure B. Corneal astigmatism for the (left) before and (right) after treatment. (A, B) Box plots showing anterior and posterior astigmatism median level (indicated by ⊗, average symbol ⊕), 95% median confidence range box (black line boxes), and interquartile intervals range box (red line boxes). (C, D) The corresponding histogram plots for anterior and posterior astigmatism. All units in diopters (D).

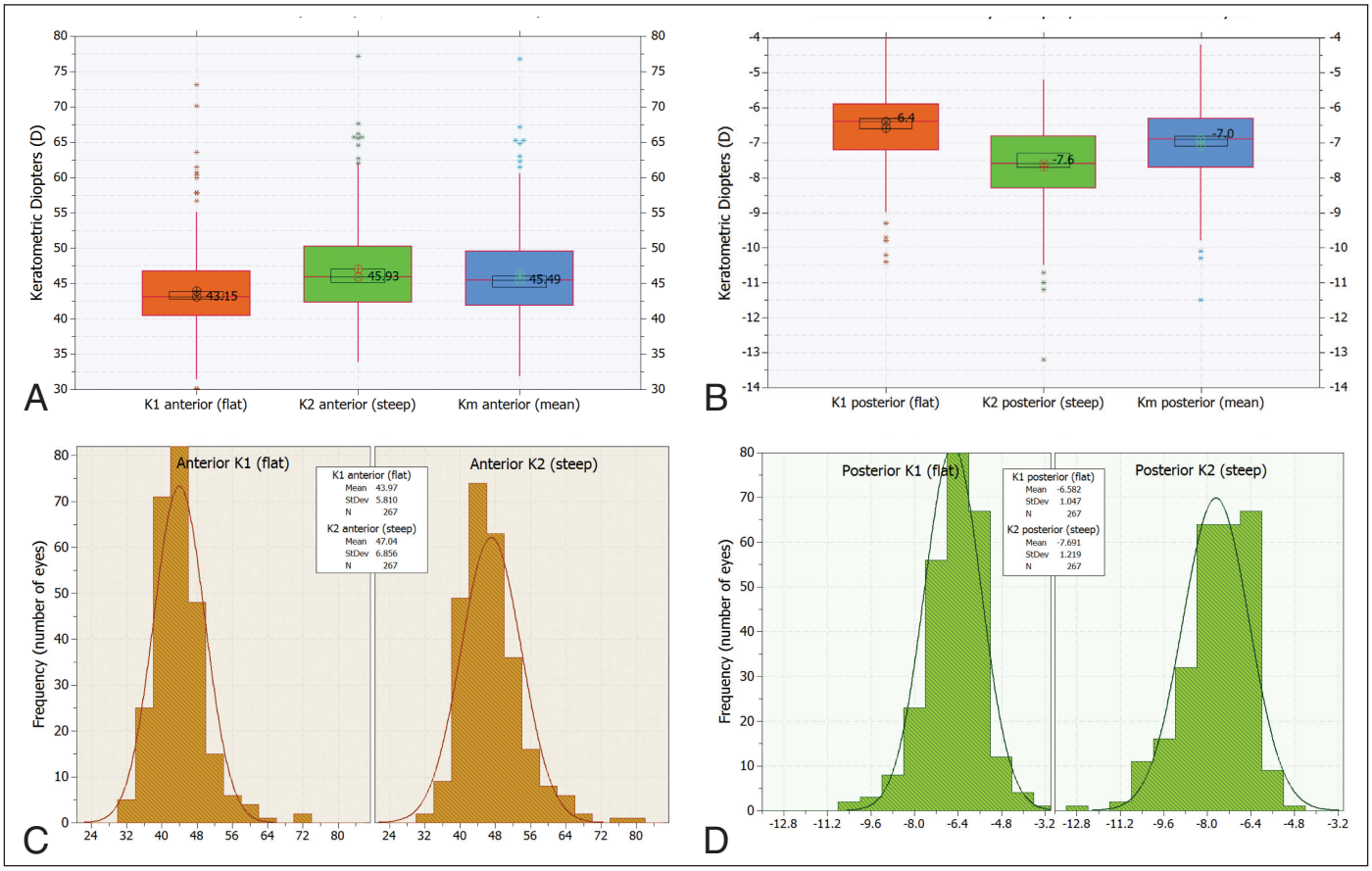

Figure C. Anterior and posterior surface keratometric values (K1 [flat], K2 [steep], and Km [mean]) after treatment. (A, B) Box plots showing median level (indicated by ⊗, average symbol ⊕), 95% median confidence range box (black line boxes), and interquartile intervals range box (red line boxes). (C, D) The corresponding histogram plots for K1 and K2. All units in keratometric diopters (D).

Epithelial remodeling after partial topography-guided normalization and high-fluence short-duration crosslinking (Athens protocol): Results up to 1 year

Anastasios John Kanellopoulos, MD, George Asimellis, PhD

PURPOSE: To compare epithelial remodeling in keratoconic eyes that had photorefractive keratectomy and corneal collagen crosslinking (Athens protocol) with that in untreated keratoconic eyes and healthy eyes.

SETTING: Private clinical practice, Athens, Greece.

DESIGN: Comparative case series.

METHODS: Fourier-domain anterior segment optical coherence tomography (AS-OCT) was used to obtain in vivo 3-dimensional epithelial thickness maps and center, superior, inferior, maximum, minimum, mean, midperipheral, and variability data.

RESULTS: Group A comprised 175 treated keratoconic eyes (Athens protocol); Group B, 193 untreated keratoconic eyes; and Group C, 160 healthy eyes. The 1-year mean center epithelial thickness in Group A was 47.78 μm ± 7.36 (SD) (range 33 to 64 μm). At the first clinical visit, it was 52.09 ± 6.80 μm (range 36 to 72 μm) in Group B and 52.54 ± 3.23 μm (range 45 to 59 μm) in Group C. The mean thickness range in Group A at 1 year was −19.94 ± 7.21 μm (range −6 to −34 μm). It was −21.83 ± 12.07 μm (range −4 to −66 μm) in Group B and −6.86 ± 3.33 μm (range −3 to −29 μm) in Group C. The mean topographic thickness variability in Group A at 1 year was 4.64 ± 1.63 μm (range 1.6 to 8.1 μm) ($P<.05$). It was 5.77 ± 3.39 μm (range 1.3 to 17.8 μm) in Group B and 1.59 ± 0.79 μm (range 0.6 to 5.6 μm) in Group C.

CONCLUSION: Anterior segment OCT indicated a thinner and more homogeneous remodeled epithelium in the keratoconic eyes treated using the Athens protocol.

Financial Disclosure: Dr. Kanellopoulos is a consultant to Alcon Surgical, Inc.; Wavelight Laser Technologie AG; Avedro, Inc.; and i-Optics Optikgeräte GmbH. Dr. Asimellis has no financial or proprietary interest in any material or method mentioned.

J Cataract Refract Surg 2014; 40:1597–1602 © 2014 ASCRS and ESCRS

We previously reported overall reduced corneal epithelial thickness in keratoconic eyes that were treated with (1) excimer laser debridement of the top 50 μm of the epithelium, (2) partial topography-guided excimer ablation, and (3) immediate high-fluence ultraviolet-A radiation (10 mW/cm^2) and short-duration (10 minutes) corneal collagen crosslinking (CXL) with riboflavin in a procedure known as the Athens protocol.[1–3] Our goal was to arrest the keratectasia progression[4] and provide a less irregular anterior corneal surface. In l study,[1] which was performed using high-frequency scanning ultrasound biomicroscopy (UBM), the epithelial thickness in a group of untreated keratoconic eyes was compared with that in a group of keratoconic eyes treated using the Athens protocol.

Epithelial thickness assessment has been facilitated by the development of anterior segment optical coherence tomography (AS-OCT).[5] Although there are studies of AS-OCT epithelium measurement in the peer-reviewed literature, until recently and to our knowledge, the methodology and instrumentation mainly used an on-screen caliper tool[6]; thus, only local point–thickness measurements were reported. The

http://dx.doi.org/10.1016/j.jcrs.2014.02.036

recent availability of in vivo, 3-dimensional (3-D) corneal epithelial mapping by AS-OCT in clinical practice[7] allows easy capture of optical images and high-speed measurements conferred by Fourier-domain signal processing.[8,9]

This study used this new clinical modality to evaluate the longitudinal postoperative changes in epithelial thickness distribution as well as the epithelial layer topographic variability in a large group of keratoconic cases treated using the Athens protocol. The results in these eyes were compared with those in untreated keratoconic eyes and in healthy control eyes.

PATIENTS AND METHODS

This observational comparative prospective study received approval by the Ethics Committee, LaserVision.gr Institute, and adhered to the tenets of the Declaration of Helsinki. All patients provided informed written consent at the time of the first clinical visit. Exclusion criteria were systemic disease, previous corneal surgery, history of chemical injury or delayed epithelial healing, and pregnancy or lactation.

Patient Enrollment and Surgical Technique

Group A In Group A, eyes were treated for keratoconus with the Athens protocol. All procedures were performed by the same surgeon (A.J.K.) using an EX500 excimer laser[10] (Alcon Surgical, Inc.) with topography-guided custom partial ablation. Figure 1 shows an example of treatment planning, the distribution of the ablation depth, a preoperative axial curvature map, a postoperative axial curvature map, and the difference in axial curvature map between preoperatively and postoperatively. Immediately after surface normalization, accelerated CXL was applied using the KXL System (Avedro, Inc.). The patients were followed for up to 1 year.

Group B Group B comprised eyes with keratoconus that had not received surgical treatment. Inclusion criteria were a clinical diagnosis of progressive keratoconus (confirmed by a complete ophthalmologic evaluation), minimum age 17 years, and corneal thickness of at least 300 µm. The keratoconus diagnosis was further confirmed using the Wavelight Oculyzer II (Alcon Surgical, Inc.) and the Pentacam high-resolution Scheimpflug imaging camera[11] (Oculus Optikgeräte GmbH).

Submitted: November 11, 2013.
Final revision submitted: February 4, 2014.
Accepted: February 5, 2014.

From Laservision.gr Eye Institute (Kanellopoulos), Athens, Greece, and the New York University Medical School (Kanellopoulos, Asimellis), New York, New York, USA.

Corresponding author: Anastasios John Kanellopoulos, MD, Laservision.gr Clinical and Research Institute, 17 Tsocha Street, Athens, Greece, Postal Code: 115 21. E-mail: ajk@brilliantvision.com.

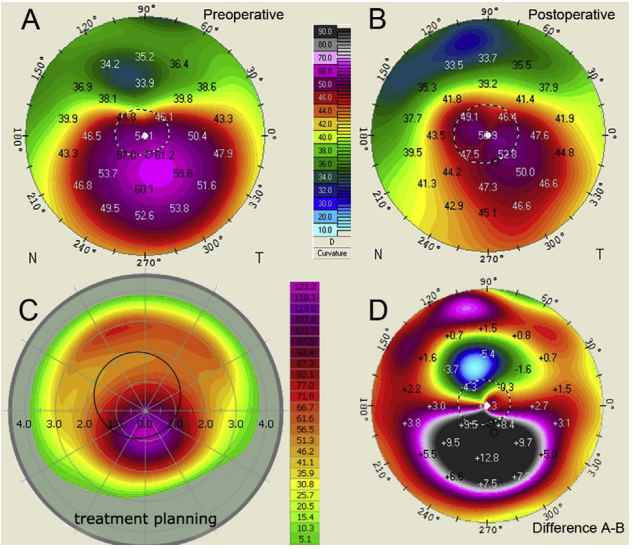

Figure 1. *A*: Preoperative tomographic (anterior corneal instantaneous [tangential]) map obtained via Scheimpflug imaging. Keratometric power reported in diopters. *B*: Corresponding postoperative map. *C*: Treatment planning showing ablation depth (in µm) and topographic distribution obtained via the refractive platform software. *D*: Difference between postoperative sagittal curvature map (*B*) and preoperative sagittal curvature map (*A*) (N = nasal; T = temporal).

Group C Group C, the control group, comprised unoperated normal eyes with no current or past ocular pathology other than refractive error and no present irritation or dry-eye disorder, all of which were confirmed during a complete ophthalmologic evaluation. Contact lens wearers were excluded from this group.

Imaging Instrumentation

The RTVue-100 Fourier-domain AS-OCT system (Optovue, Inc.), running on analysis and report software version A6 (9.0.27), was used in the study. Data output included total corneal and epithelial thickness maps corresponding to a 6.0 mm diameter area. In all cases, to avoid potential artifacts (eg, due to eyedrop instillation), OCT imaging preceded the ocular clinical examination and was performed by the same trained investigator. The settings were as follows: L-Cam lens and 8 radial meridional B-scans per acquisition consisting of 1024 A-scans each with a 5 µm axial resolution. These 8 radial meridional scans, all acquired in less than 0.5 second, were used by the system software to produce by interpolation 3-D thickness maps. Images with quality greater than 30, determined using the signal strength index parameter, were considered in the study. The signal strength index parameter measures the average signal strength across the scan. Two consecutive individual acquisitions were obtained in each case (eye) to ensure data validity; the mean value of 2 was used in this study.

Data Collection and Statistical Analysis

In Group A, the postoperative measurements were performed at 1 and 6 months as well as at 1 year. Imaging in

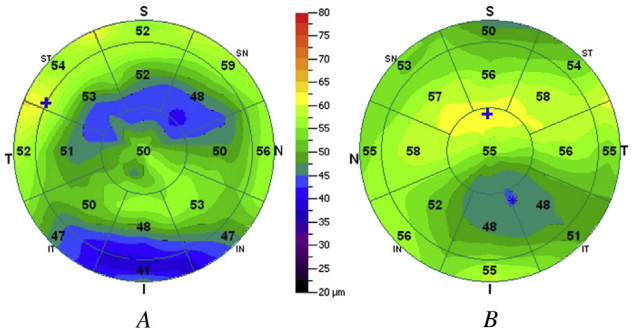

Figure 2. Comparative AS-OCT epithelial thickness (μm) 3-D maps shows an *i*mage from Group A taken 1 year postoperatively and an image from Group B (I = inferior; IN = inferior–nasal; IT = inferior–temporal; N = nasal; S = superior; SN = superior–nasal; ST = superior–temporal; T = temporal).

Group B and Group C was performed during the first clinical visit.

The main analysis report produced by the AS-OCT system displayed total corneal (reported as pachymetry) and epithelial 3-D thickness maps covering the 6.0 mm diameter area. Corneal pachymetry was assessed by the central corneal thickness (CCT) and minimum corneal thickness. Epithelial thickness assessment comprised the following measurements: pupil center, superior, inferior, minimum, maximum, mean, peripheral, topographic thickness variability, and epithelial thickness range. These data were collected as follows (Figure 2): Each thickness map was divided into 17 sections (2.0 mm diameter pupil center disk of 12.56 mm^2 area; 8 sectors [octants] within the annulus between the 2.0 mm and 5.0 mm zones, each of 8.24 mm^2 areas; and 8 sectors [octants] within the annulus of the 5.0 to 6.0 mm zones, each of 4.32 mm^2 areas). For each of these sections, the mean epithelial thickness was displayed numerically in integer form with a minimum difference of 1 μm over the corresponding area.

In this study, the reported center epithelium thickness was taken from the integer indication over the center 2.0 mm disk. The mean epithelial thickness was computed by the mean of all segments, and the peripheral epithelial thickness was computed by the mean of the thickness corresponding to 18 equispaced points along the 5.0 mm radius (data harvested by mouse-over indication over the epithelial thickness map). The superior, inferior, minimum, maximum, and topographic epithelial thickness variability (computed by the standard deviation [SD] of the 17 thickness values) were provided in tabular form by the software of the AS-OCT device (Figure 2). The thickness range was computed as follows: minimum epithelial thickness – maximum epithelial thickness.

Descriptive statistics, linear regression analysis to look for possible correlations, paired analysis *t* tests, and analysis of variance were performed using Minitab software (version 16.2.3, Minitab, Ltd.) and Origin Lab software (version 9, Originlab Corp.). Paired-analysis *P* values less than 0.05 were considered an indication of statistically significant results.

RESULTS

Table 1 shows the CCT, minimum corneal thickness, epithelial thicknesses, topographic thickness variability, and epithelial thickness range measured by AS-OCT in the 3 groups.

Group A (Athens protocol) comprised 175 eyes, 74 of women and 101 of men. The mean patient age at the time of surgery was 26.8 years ± 7.2 (SD) (range 18 to 48 years). There were 87 right eyes and 88 left eyes. The Athens protocol treatment was uneventful in all cases.

Group B (untreated keratoconic) comprised 193 eyes, 92 of women and 101 of men. The mean patient age at the time of examination was 31.1 ± 9.9 years (range 18.0 to 51.0 years). There were 91 right eyes and 102 left eyes.

Group C (control) comprised 160 eyes, 67 of women and 93 of men. The mean patient age at the time of examination was 35.45 ± 9.55 years (range 18.0 to 52.0 years). There were 74 right eyes and 86 left eyes.

Epithelial Thickness

In Group A, the difference in the center epithelial thickness between each postoperative timepoint was statistically significant (all $P<.05$). The difference in the mean center epithelial thickness (−4.31 μm; 95% confidence interval [CI], −6.31 to −2.30) between Group A 1 year after treatment and Group B at the time of examination was statistically significant ($P<.05$, 2-sample *t* test). The difference in the mean center epithelial thickness (−4.75 μm, 95% CI, −6.59 to −2.92) between Group A 1 year after treatment and Group C at the time of examination was also statistically significant ($P<.05$) (Figure 3).

In Group A, the difference in topographic thickness variability between each postoperative timepoint was statistically significant (all $P<.05$). Figure 4 shows the epithelial thickness variability and range by group.

DISCUSSIONS

Until recently, high-frequency UBM had been the gold standard for in vivo corneal epithelial 3-D imaging.[12] The recent, rapid development and current high-speed imaging capabilities of AS-OCT[13–15] have made acquisition of in vivo 3-D pachymetry corneal maps reliable and fast.[16–19] Software refinement also enables clinical assessment of corneal asymmetry and focal thinning parameters for keratoconus classification.[20] In addition, the higher axial resolution, increased accuracy, and finer image-processing capabilities of the current AS-OCT imaging systems have enabled, among other things, 3-D imaging of epithelial thickness.[7]

Epithelial thickness and irregularity indices (eg, center and mean epithelial thickness, epithelial thickness topographic irregularity, and thickness range)

Table 1. Central corneal thickness (CCT), minimum corneal thickness, epithelial thicknesses, topographic thickness variability, and epithelial thickness range measured by the AS-OCT in the 3 groups. All units are in microns.

			Epithelial Thickness								
Group	CCT	MinCT	Center	Superior	Inferior	Minimum	Maximum	Mean	Mid	Topographic Variability	Range
Group A (AP treated)											
1 month											
Mean	382.7	330.5	42.6	43.2	44.5	33.3	58.0	43.9	44.2	5.4	−24.7
SD	32.8	34.5	7.3	5.3	6.0	7.8	7.2	6.0	6.0	3.0	12.8
Max	444	432	52	51	53	45	74	52.1	52.1	13.5	−10.0
Min	336	248	36	36	39	18	49	38.7	38.9	2.7	−54.0
6 months											
Mean	397.7	341.8	46.38	47.3	47.9	36.7	58.5	47.4	47.6	5.1	−21.8
SD	36.9	42.2	6.80	7.0	5.7	5.9	10.0	5.6	5.4	1.9	8.5
Max	481	412	58	61	57	46	78	56.9	58.3	9.3	−9.0
Min	300	242	34	33	38	22	44	38.0	38.8	2.1	−39.0
1 year											
Mean	435.8	365.9	47.8	49.7	48.9	38.5	59.0	48.9	49.2	4.6	−19.9
SD	42.0	50.0	4.6	6.0	3.9	8.4	6.0	5.3	5.2	1.6	7.2
Max	550	500	64	61	62	55	75	60.6	59.9	8.1	−6.0
Min	351	252	33	36	38	18	44	37.3	38.2	1.6	−34.0
Group B (KCN)											
Mean	482.7	439.1	52.1	55.4	50.0	41.3	63.1	52.5	52.6	5.8	−21.8
SD	41.7	62.8	6.8	6.5	5.3	8.1	8.5	5.2	5.1	3.4	12.1
Max	570	548	72	76	69	60	94	70.3	70.0	17.8	−4.0
Min	356	193	36	42	33	19	49	43.5	43.6	1.3	−66.0
Group C (healthy)											
Mean	532.4	525.1	52.5	51.4	53.1	48.5	55.3	52.2	52.2	1.6	−6.9
SD	28.5	27.9	3.2	3.4	3.3	4.0	3.7	3.2	3.2	0.8	3.3
Max	592	580	59	60	59	57	64	59	60	5.6	−3.0
Min	462	455	45	44	45	28	46	45	45	0.6	−29.0

AT = Athens Protocol; CCT = central corneal thickness; KCN = keratoconus, no treatment; Mid = midperipheral; MinCT = minimum corneal thickness

measured quantitatively with AS-OCT can serve as possible indicators of cornea instability, including ectasia and keratoconus.[14] In this study, we evaluated these parameters with a Fourier-domain AS-OCT system in a large group of keratoconic patients who had combined treatment of excimer laser anterior surface normalization and simultaneous high-fluence accelerated CXL. This study adds new information based on its large group of treated keratoconic eyes and its comparison with untreated keratoconic eyes and healthy eyes. In addition, our study was performed with a commercially available AS-OCT system whose use may become more widespread in clinical settings.

Our findings confirm compensatory epithelial thickness changes previously described after various refractive corneal ablation procedures.[21,22,A]

The epithelial thickness and irregularity assessment in the Athens protocol–treated Group A suggests short-term variability in corneal thickness distribution between the third month and the sixth month.[3] Specifically, in our study, the corneal and epithelial thickness distributions were characterized by large deviations that gradually became less irregular. The mean SD at the center epithelial thickness of 7.36 μm at 1 month gradually decreased to 6.80 at 3 months and to 4.57 μm at 1 year. The SD in Group B (untreated keratoconic) and in Group C (control) was 6.79 μm and 3.23 μm, respectively. In addition to fluctuating less between different eyes, the epithelial thickness in Group A progressed toward a reduced mean topographic variability and mean thickness range (from 5.43 μm and −24.69 μm to 4.64 μm and −19.94 μm, respectively). Both metrics were more regular than in Group B (5.77 μm and −21.83 μm, respectively). These results indicate that the epithelial thickness distribution was more uniform in the Athens protocol–treated group than in the untreated group of keratoconic eyes and had less overall thickness, as suggested by the reduced mean and center thickness values.

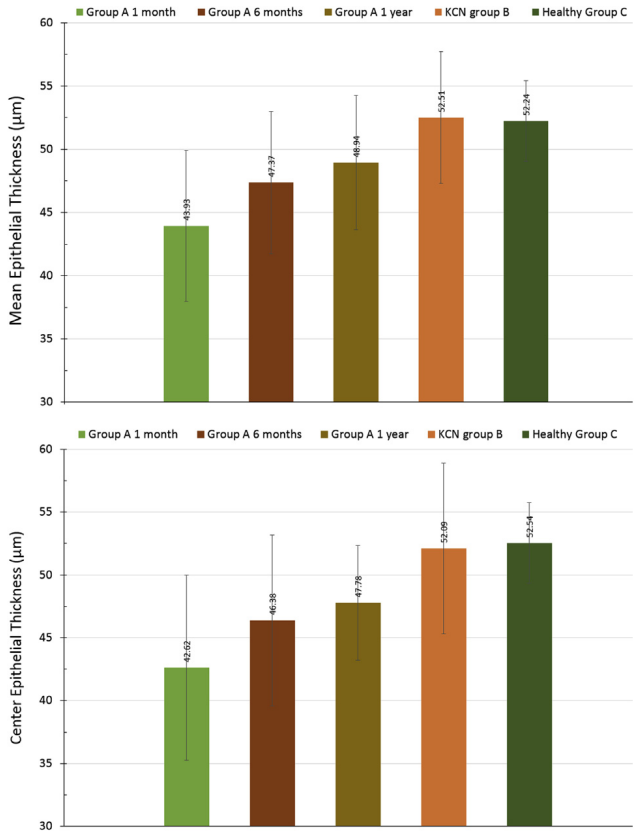

Figure 3. Mean and center epithelial thicknesses in the 3 groups. Error bars correspond to the SD (KCN = keratoconus, no treatment).

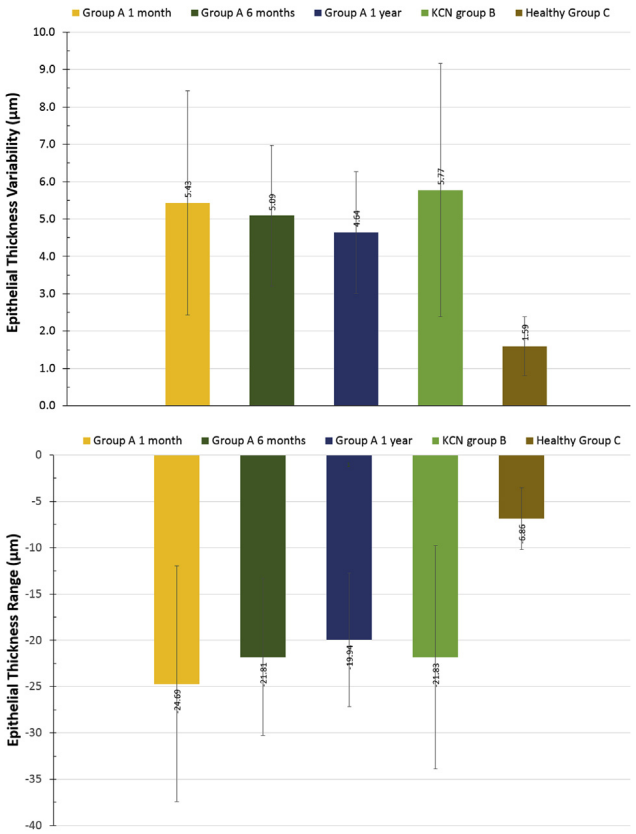

Figure 4. Epithelial thickness variability and range in the 3 groups. Error bars correspond to the SD (KCN = keratoconus, no treatment).

The findings in the current study agree with those in our previous study[1]; that is, although an overall thicker epithelium with large variations can be observed clinically and topographically in eyes with keratoconus, in eyes treated with CXL the variability in epithelium thickness and topographic thickness decreased by a statistically significant margin and was more uniform. We have theorized that epithelial hyperplasia in biomechanically unstable corneas (ie, increased epithelial regrowth activity) might be associated with a more elastic cornea.[1] The laboratory and clinical findings of increased corneal rigidity after CXL are widely accepted,[23–25] including in studies of accelerated high-fluence CXL.[26]

In conclusion, we present the results in a comprehensive study of the postoperative development of corneal epithelial thickness distribution after keratoconus management using combined anterior corneal normalization by topography-guided excimer ablation and accelerated CXL. The epithelial healing processes can be monitored by AS-OCT with ease in a clinical setting, expanding the clinical application of this technology. Our findings suggest less topographic variability and overall reduced epithelial thickness distribution in keratoconus eyes treated with CXL using the Athens protocol.

WHAT WAS KNOWN

- Postoperative epithelial remodeling after partial anterior surface normalization with an excimer laser and high-fluence CXL, assessed with high-frequency scanning UBM, results in reduced overall epithelial thickness and topographic variability.

WHAT THIS PAPER ADDS

- Detailed follow-up of Athens protocol–treated eyes up to 1 year confirmed previous ultrasound findings of the overall thinner and smoother epithelial thickness profiles compared with the profiles of untreated keratoconic eyes.

REFERENCES

1. Kanellopoulos AJ, Aslanides IM, Asimellis G. Correlation between epithelial thickness in normal corneas, untreated ectatic corneas, and ectatic corneas previously treated with CXL; is overall epithelial thickness a very early ectasia prognostic factor? Clin Ophthalmol 2012; 6:789–800. Available at: http://www.ncbi.nlm.nih.gov/pmc/articles/PMC3373227/pdf/opth-6-789.pdf. Accessed June 11, 2014
2. Kanellopoulos AJ. Long term results of a prospective randomized bilateral eye comparison trial of higher fluence, shorter duration ultraviolet A radiation, and riboflavin collagen cross

linking for progressive keratoconus. Clin Ophthalmol 2012; 6:97–101. Available at: http://www.ncbi.nlm.nih.gov/pmc/articles/PMC3261695/pdf/opth-6-097.pdf. Accessed June 11, 2014
3. Kanellopoulos AJ, Asimellis G. Keratoconus management: long-term stability of topography-guided normalization combined with high fluence CXL stabilization (the Athens Protocol). J Refract Surg 2014; 30:88–92
4. Kanellopoulos AJ, Asimellis G. Introduction of quantitative and qualitative cornea optical coherence tomography findings induced by collagen cross-linking for keratoconus: a novel effect measurement benchmark. Clin Ophthalmol 2013; 7:329–335. Available at: http://www.ncbi.nlm.nih.gov/pmc/articles/PMC3577010/pdf/opth-7-329.pdf. Accessed June 11, 2014
5. Kanellopoulos AJ, Asimellis G. In vivo three-dimensional corneal epithelium imaging in normal eyes by anterior-segment optical coherence tomography: a clinical reference study. Cornea 2013; 32:1493–1498
6. Francoz M, Karamoko I, Baudouin C, Labbé A. Ocular surface epithelial thickness evaluation with spectral-domain optical coherence tomography. Invest Ophthalmol Vis Sci 2011; 52:9116–9123. Available at: http://www.iovs.org/content/52/12/9116.full.pdf. Accessed June 11, 2014
7. Kanellopoulos AJ, Asimellis G. In vivo 3-dimensional corneal epithelial thickness mapping as an indicator of dry eye: preliminary clinical assessment. Am J Ophthalmol 2014; 157:63–68
8. Chen TC, Cense B, Pierce MC, Nassif N, Park BH, Yun SH, White BR, Bouma BE, Tearney GJ, de Boer JF. Spectral domain optical coherence tomography; ultra-high speed, ultra-high resolution ophthalmic imaging. Arch Ophthalmol 2005; 123:1715–1720
9. Oh W-Y, Vakoc BJ, Shishkov M, Tearney GJ, Bouma BE. >400 kHz repetition rate wavelength-swept laser and application to high-speed optical frequency domain imaging. Opt Lett 2010; 35:2919–2921. Available at: http://www.ncbi.nlm.nih.gov/pmc/articles/PMC3003227/pdf/nihms255350.pdf. Accessed June 11, 2014
10. Kanellopoulos AJ, Asimellis G. Long term bladeless LASIK outcomes with the FS200 femtosecond and EX500 excimer laser workstation: the Refractive Suite. Clin Ophthalmol 2013; 7:261–269. Available at: http://www.ncbi.nlm.nih.gov/pmc/articles/PMC3583408/pdf/opth-7-261.pdf. Accessed June 11, 2014
11. Kanellopoulos AJ, Asimellis G. Correlation between central corneal thickness, anterior chamber depth, and corneal keratometry as measured by Oculyzer II and WaveLight OB820 in preoperative cataract surgery patients. J Refract Surg 2012; 28:895–900
12. Reinstein DZ, Gobbe M, Archer TJ, Silverman RH, Coleman DJ. Epithelial, stromal, and total corneal thickness in keratoconus: three-dimensional display with Artemis very-high frequency digital ultrasound. J Refract Surg 2010; 26:259–271. Available at: http://www.ncbi.nlm.nih.gov/pmc/articles/PMC3655809/pdf/nihms211821.pdf. Accessed June 11, 2014
13. Potsaid B, Baumann B, Huang D, Barry S, Cable AE, Schuman JS, Duker JS, Fujimoto JG. Ultrahigh speed 1050nm swept source/Fourier domain OCT retinal and anterior segment imaging at 100,000 to 400,000 axial scans per second. Opt Exp 2010; 18:20029–20048. Available at: http://www.ncbi.nlm.nih.gov/pmc/articles/PMC3136869/pdf/nihms304233.pdf. Accessed June 11, 2014
14. Rocha KM, Perez-Straziota CE, Stulting RD, Randleman JB. SD-OCT analysis of regional epithelial thickness profiles in keratoconus, postoperative corneal ectasia, and normal eyes. J Refract Surg 2013; 29:173–179
15. Ge L, Yuan Y, Shen M, Tao A, Wang J, Lu F. The role of axial resolution of optical coherence tomography on the measurement of corneal and epithelial thicknesses. Invest Ophthalmol Vis Sci 2013; 54:746–755. Available at: http://www.iovs.org/content/54/1/746.full.pdf. Accessed June 11, 2014
16. Wojtkowski M, Kaluzny B, Zawadzki RJ. New directions in ophthalmic optical coherence tomography. Optom Vis Sci 2012; 89:524–542. Available at: http://journals.lww.com/optvissci/Fulltext/2012/05000/New_Directions_in_Ophthalmic_Optical_Coherence.4.aspx. Accessed June 11, 2014
17. Khurana RN, Li Y, Tang M, Lai MM, Huang D. High-speed optical coherence tomography of corneal opacities. Ophthalmology 2007; 114:1278–1485
18. Li Y, Shekhar R, Huang D. Corneal pachymetry mapping with high-speed optical coherence tomography. Ophthalmology 2006; 113:792–799.e2
19. Dutta D, Rao HL, Addepalli UK, Vaddavalli PK. Corneal thickness in keratoconus; comparing optical, ultrasound, and optical coherence tomography pachymetry. Ophthalmology 2013; 120:457–463
20. Kanellopoulos AJ, Chiridou M, Asimellis G. Optical coherence tomography-derived corneal thickness asymmetry indices: clinical reference study in 561 normal eyes. In press, J Cataract Refract Surg 2014
21. Gauthier CA, Holden BA, Epstein D, Tengroth B, Fagerholm P, Hamberg-Nyström H. Role of epithelial hyperplasia in regression following photorefractive keratectomy. Br J Ophthalmol 1996; 80:545–548. Available at: http://bjo.bmj.com/content/80/6/545.full.pdf. Accessed June 11, 2014
22. Erie JC, Patel SV, McLaren JW, Ramirez M, Hodge DO, Maguire LJ, Bourne WM. Effect of myopic laser in situ keratomileusis on epithelial and stromal thickness; a confocal microscopy study. Ophthalmology 2002; 109:1447–1452
23. Raiskup-Wolf F, Hoyer A, Spoerl E, Pillunat LE. Collagen cross-linking with riboflavin and ultraviolet-A light in keratoconus: long-term results. J Cataract Refract Surg 2008; 34:796–801
24. Vinciguerra P, Albè E, Trazza S, Rosetta P, Vinciguerra R, Seiler T, Epstein D. Refractive, topographic, tomographic, and aberrometric analysis of keratoconic eyes undergoing corneal cross-linking. Ophthalmology 2009; 116:369–378
25. O'Brart DPS, Kwong TQ, Patel P, McDonald RJ, O'Brart NA. Long-term follow-up of riboflavin/ultraviolet A (370 nm) corneal collagen cross-linking to halt the progression of keratoconus. Br J Ophthalmol 2013; 97:433–437. Available at: http://bjo.bmj.com/content/97/4/433.full.pdf. Accessed June 11, 2014
26. Schumacher S, Oeftiger L, Mrochen M. Equivalence of biomechanical changes induced by rapid and standard corneal cross-linking, using riboflavin and ultraviolet radiation. Invest Ophthalmol Vis Sci 2011; 52:9048–9052. Available at: http://www.iovs.org/content/52/12/9048.full.pdf. Accessed June 11, 2014

OTHER CITED MATERIAL

A. Reinstein DZ, Aslanides IM, Patel S, Silverman RH, Coleman DJ, "Epithelial Lenticular Types of Human Cornea: Classification and Analysis of Influence on PRK," poster presented at the annual meeting of the American Academy of Ophthalmology, Atlanta, Georgia, USA, October 1995. Abstract available in: Ophthalmology 1995; 102(suppl):S156

First author:
Anastasios John Kanellopoulos, MD

Laservision.gr Clinical and Research Institute, Athens, Greece

Novel Placido-derived Topography-guided Excimer Corneal Normalization With Cyclorotation Adjustment: Enhanced Athens Protocol for Keratoconus

Anastasios John Kanellopoulos, MD; George Asimellis, PhD

ABSTRACT

PURPOSE: To comparatively investigate the efficacy of the enhanced Athens Protocol procedure guided by novel Placido-derived topography with cyclorotation compensation (the cyclorotation adjusted group) to similar cases guided by Scheimpflug-derived tomography without cyclorotation compensation (the non-cyclorotation adjusted group).

METHODS: Two groups were evaluated: the cyclorotation adjusted group (n = 110 eyes) and the non-cyclorotation adjusted group (n = 110 eyes). Analysis was based on digital processing of Scheimpflug imaging derived curvature difference maps preoperatively and 3 months postoperatively. The vector (r, ϑ) corresponding to the steepest corneal point (cone) on the preoperative surgical planning map (r_p, ϑ_p) and on the curvature difference map (r_d, ϑ_d) were computed. The differences between the peak topographic angular data ($\Delta\vartheta = |\vartheta_p - \vartheta_d|$) and weighted angular difference ($W\Delta\vartheta = \Delta\vartheta \times \Delta r$) were calculated.

RESULTS: For the cyclorotation adjusted group, $\Delta\vartheta$ was 7.18° ± 7.53° (range: 0° to 34) and $W\Delta\vartheta$ was 3.43 ± 4.76 mm (range: 0.00 to 21.41 mm). For the non-cyclorotation adjusted group, $\Delta\vartheta$ was 14.50° ± 12.65° (range: 0° to 49°) and $W\Delta\vartheta$ was 10.23 ± 15.15 mm (range: 0.00 to 80.56 mm). The cyclorotation adjusted group appeared superior to the non-cyclorotation adjusted group, in both the smaller average angular difference between attempted to achieved irregular curvature normalization and in weighted angular difference, by a statistically significant margin ($\Delta\vartheta$: $P = .0058$; $W\Delta\vartheta$: $P = .015$).

CONCLUSIONS: This study suggests that employment of the novel Placido-derived topographic data of highly irregular corneas, such as in keratoconus, treated with topography-guided profile with cyclorotation compensation leads to markedly improved cornea normalization.

[*J Refract Surg.* 2015;31(11):768-773.]

Corneal cross-linking (CXL) is considered a valid option for progressive keratoconus/corneal ectasia treatment.[1] By increasing corneal biomechanical strength, CXL results in keratectasia arrest.[2] In addition, CXL has also been shown to improve corneal irregularity and reduce central anterior corneal steepening.[3]

Combined with CXL, partial anterior surface normalization via topography-guided customized partial excimer laser ablation may offer, in addition to keratectasia arrest, improved topographic and refractive outcomes.[3,4] The Athens Protocol comprises phototherapeutic keratectomy (PTK) of 50 µm, a partial photorefractive keratectomy (PRK) for the topography-guided customized anterior surface normalization, and high-fluence CXL for corneal stabilization.[5] Long-term results[6] and anterior segment optical coherence tomography quantitative findings[7] have demonstrated the stability of the procedure in large cohorts of patients. Variations of this technique have been applied and reported globally.[8-14]

Because the topography-guided ablation step of the procedure bears a high degree of customization, the impact of effective alignment between treatment planning based on the topography-derived data and surgically applied ablation pattern is pivotal for a successful outcome. Critical parameters affecting alignment are horizontal and vertical eye movements, eye pupil centroid shift, and possible cyclorotation. The significance of these principles has been reported preoperatively and intraoperatively in refractive procedures.[15] High-speed active eye tracking along with cyclorotational topographic adjustment (CTA) has been introduced during the past 2 years in refractive lasers such as the EX500 excimer laser (Alcon Laboratories, Inc., Fort Worth, TX), which

From Laservision.gr Clinical and Research Eye Institute, Athens, Greece (AJK); and NYU Medical School, Department of Ophthalmology, New York, New York (GA).

Submitted: April 28, 2015; Accepted: August 11, 2015

Dr. Kanellopoulos is a consultant for Alcon/WaveLight, Allegran, Avedro, and i-Optics. Dr. Asimellis has no financial or proprietary interest in the materials presented herein.

Correspondence: Anastasios John Kanellopoulos, MD, Laservision.gr Clinical and Research Eye Institute, 17 Tsocha Street, Athens, 115 21 Greece. E-mail: ajk@brilliantvision.com

doi: 10.3928/1081597X-20151021-06

is employed for the excimer ablation step of the Athens Protocol studied herein.

The enhanced Athens Protocol incorporates the above surgical device improvements and also introduces surgical procedure changes, specifically the choice of the Placido-derived topography data produced by a novel topographic device (Vario instead of the Oculyzer II Scheimpflug-derived tomography [Alcon Laboratories, Inc./WaveLight AG, Erlangen, Germany]) and the reversal of the two excimer laser ablation steps: PRK now precedes PTK.

The purpose of this study is to comparatively investigate the correlation between achieved and intended corneal topography changes when employing the novel CTA procedure in comparison to the previously developed technique (based on the available technology at that time) in which no cyclorotational adjustment was available.

PATIENTS AND METHODS

This retrospective comparative study received approval by the ethics committee of Laservision.gr Clinical and Research Eye Institute, Athens, Greece, and adhered to the tenets of the Declaration of Helsinki. Signed informed consent was obtained from the patients at the time of the first clinical visit.

Two hundred twenty consecutive eyes of 220 different patients who had the Athens Protocol were retrospectively investigated. Inclusion criteria were clinical diagnosis of progressive keratoconus, minimum age of 17 years, and a minimum corneal thickness of approximately 300 µm measured by anterior segment optical coherence tomography. All patients had completed an uneventful Athens Protocol and were observed for approximately 1 year. Exclusion criteria for the procedure were systemic disease, previous eye surgery, ocular chemical injury, a history of delayed epithelial healing, and pregnancy or lactation (female patients).

Two groups were evaluated: patients who had CTA (the cyclorotation adjusted group [n = 110 eyes]) and patients who did not have CTA (the non-cyclorotation adjusted group [n = 110 eyes]).

Common to both groups, the design of the ablation pattern (profile) was performed via the Aqua software of the Alcon Refractive Suite, which is part of the EX500 excimer laser. The imported topography-derived data (approximately four acquisitions usually selected from 10 to 30 actual individual acquisitions) were selected to improve the default statistical data provided by the planning software. Specifically, we tried to match images with consistent keratometries and cylinder axes, as well as reproducibility that would minimize the maximum deviation index to a value less than 0.1. This methodology aimed to select a group of topography images that were consistent and reproducible. In all cases, the neuro-tracking option was on. No manual marking was used in either group.

In both groups, the excimer laser ablation steps (employing the EX500 excimer laser) were applied with the following sequence (**Figure A**, available in the online version of this article):

1. Partial excimer laser PRK performed with the EX500 laser's topography-guided custom ablation treatment mode. A typical optical zone was 5 to 5.50 mm with a limit of 50 µm to be removed over the steepest/thinnest cornea point.
2. Excimer laser ablation (uniform 50 µm over a 7-mm zone) employing the PTK mode.

The enhanced Athens Protocol presented herein also stems from recently reported[16] optimized ablation profiles. Previously, the procedure employed the sequence as follows: the PTK step was performed first, followed by the PRK step.[6]

Following ablation, the cross-linking step of the procedure involved ultraviolet-A irradiance of 6 mW/cm^2, applied for 15 minutes employing the KXL system (Avedro Inc., Waltham, MA).

The differences between the two groups were the following. In the cyclorotation adjusted group, the surgical planning corneal topography data were derived from the novel Allegro Topolyzer Vario (Alcon Laboratories, Inc.), a wide-cone Placido corneal topographer.[17] CTA was based on infrared iris imaging data comparison between the Vario device and the EX500 imaging. On the EX500 excimer laser, the previously imported iris information data is compared to the live infrared image of the eye tracking system, and any detected cyclotortional change (detection threshold 0.5°) was statically compensated. The angle sign is positive for clockwise and negative for counter-clockwise rotation. The notation in this system was common for both eye lateralities (ie, does not follow the positive for excyclotorsion, corresponding to the upper pole of the eye rotating to the temporal side, and negative for incyclotorsion).

In the non-cyclorotation adjusted group, the surgical planning corneal imaging topography data were derived from the Oculyzer II, a Scheimpflug imaging device based on the Pentacam (Oculus Optikgeräte GmbH, Wetzlar, Germany). Cyclorotational topographic adjustment is not available with this system.

Data Collection and Analysis

The public domain, Java-based image processing software ImageJ (version 1.49; National Institutes of

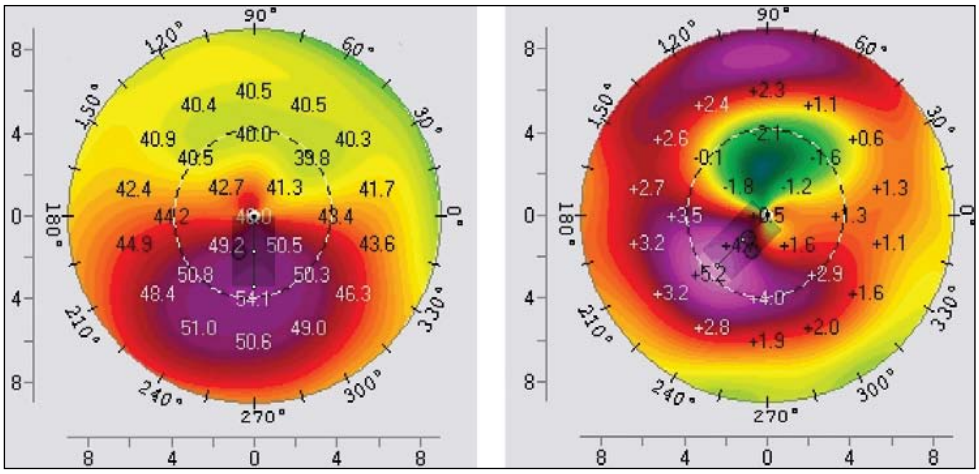

Figure 1. Measurement of axial and radial coordinates of the steepest corneal point with the ImageJ software (National Institutes of Health, Bethesda, MD) corresponding to (left) the preoperative map and (right) difference map. The preoperative map vector had the coordinates r_p = 1.69 mm, ϑ_p = 270°. The difference map vector had the coordinates, r_d = 1.69 mm, ϑ_d = 225°. There is evident difference between the two maps, which may be attributed to non-compensation of cyclorotation: the difference between the peak topographic angular data ($\Delta\vartheta$) and weighted angular difference ($W\Delta\vartheta$) corresponding to these data were 45° and 58.30 mm, respectively.

Health, Bethesda, MD)[18] was used to digitally process Scheimpflug-imaging data derived from the Pentacam HR. Specifically, the 'compare 2 exams' output from the Scheimpflug imaging device was analyzed. The output consists of three sagittal curvature images (**Figure B**, available in the online version of this article) consisting of the preoperative map, the postoperative map, and the difference (change) of the two maps. The first map corresponds to the planned ablation pattern, whereas the third map corresponds to the achieved ablation pattern.

Scheimpflug screening, an integral step of the Athens Protocol, was chosen to analyze both groups for the simple reason that the available software offers more data output options. Standardizing on one analysis device also helps eliminate potential bias in data evaluation.

Employing the straight line tool offered by ImageJ, we computed the vector (expressed in polar coordinates radius r, reported in pixels; and angle ϑ, reported in degrees) corresponding to the steepest (peak topographic) corneal point (cone) on the preoperative map (r_p, ϑ_p) and the difference map (r_d, ϑ_d) (**Figure 1**). The origin of each vector (r = 0, ϑ = 0) was the center of the curvature map. Pixels were converted to millimeters, based on the measured correspondence of the 9-mm diameter of the curvature maps to 254 pixels. Thus, the pixel data were converted to millimeters using the 1 pixel to 0.035 mm ratio. Due to the terminology in ImageJ, the lower hemicycle angles were reported as negative (range: 0° to -180°); to adjust for the Scheimpflug imaging terminology, the value of 360° was added to all negative angle data (lower hemicycle). Subsequently, we computed and subjected to analysis the following metrics:

1. $\Delta\vartheta$ is defined as the absolute angular difference between the peak topographic angular data: $\Delta\vartheta = |\vartheta_p - \vartheta_d|$. $\Delta\vartheta$ is expressed in degrees.
2. $W\Delta\vartheta = \Delta\vartheta \times \Delta r$ is defined as the weighted angular difference between the peak topographic data, where ϑr is the modulus of the difference between the two vectors: $\Delta r = |r_d - r_p|$. $W\Delta\vartheta$ is expressed in millimeters.

By virtue of their definition, an ideal treatment on an eye with zero cyclorotation corresponds to a zero $\Delta\vartheta$ and a zero $W\Delta\vartheta$. Realistically, however, there are always some deviations. In addition, due to the nature of the treatment, the postoperative cone location changes not only angularly, but also radially. This is why we also introduced the weighted angular difference, which accounts for both deviations.

Additional data employed in the study include visual acuity, thinnest corneal thickness, and topographic keratoconus classification, both Scheimpflug-imaging derived. Descriptive statistics and analysis were performed by Minitab (version 16.2.3; MiniTab Ltd., Coventry, United Kingdom). A *P* value less than .05 was considered statistically significant. Data are presented by mean ± standard deviation (minimum to maximum).

RESULTS

The 110 eyes (37 women and 73 men) included in the cyclorotation adjusted group included 53 right eyes and 57 left eyes. Mean patient age at the time of the operation was 25.7 ± 6.9 years (range: 18 to 44 years). Follow-up was 15.7 ± 10.5 months (range: 12 to 24 months). Preoperative uncorrected distance visual acuity was 0.19 ± 0.22 decimal (range: 0.001 to 0.7 decimal) and corrected distance visual acuity was 0.62 ± 0.24 decimal (range: 0.10 to 1.00 decimal). Preoperative thinnest corneal thickness was 441.87 ± 45.29 µm (range: 325 to 541 µm). One year postoperatively, uncorrected distance visual acuity was 0.53 ± 0.28 (range: 0.01 to 1.0), corrected distance visual acuity was 0.78 ± 0.25 (range: 0.25 to 1.00), and thinnest corneal thickness was 375.98 ± 63.12 µm (range: 302 to 498 µm).

The 110 eyes (41 females and 69 males) in the non-cyclorotation adjusted group included 60 right eyes and

50 left eyes. Mean patient age at the time of the operation was 25.2 ± 6.5 years (range: 18 to 38 years). Follow-up was 19.9 ± 12.1 months (range: 12 to 36 months). Preoperative uncorrected distance visual acuity was 0.18 ± 0.23 (range: 0.001 to 1.0) and corrected distance visual acuity was 0.63 ± 0.33 (range: 0.10 to 1.00). Preoperative thinnest corneal thickness was 448.11 ± 48.65 µm (range: 315 to 539 µm). One year postoperatively, uncorrected distance visual acuity was 0.59 ± 0.28 (range: 0.01 to 1.20), corrected distance visual acuity was 0.82 ± 0.19 (range: 0.20 to 1.25), and thinnest corneal thickness was 363.13 ± 55.43 µm (range: 298 to 487 µm).

Both groups were matched for age, gender laterality, follow-up time, visual acuity, and corneal thickness (in all cases $P > .05$). In addition, both groups had preoperative average topographic keratoconus classification (KC) between KC2 and KC2-3.

Digital Analysis Data

The distributions of the vectors corresponding to the steepest (peak topographic) corneal point on the preoperative map (r_p, ϑ_p) and the change map (r_d, ϑ_d) are illustrated in **Figure 2**. In the majority of the cases (more than 90%) the location of the steepest corneal point was inferior in either group.

Average radial displacement of the cone location in the cyclorotation adjusted group was 1.60 ± 0.69 mm (range: 0.57 to 3.12 mm) preoperatively; the difference maps corresponded to an average cone location at 1.39 ± 0.56 mm (range: 0.50 to 2.91 mm). The difference between preoperative and achieved change was not statistically significant ($P = .074$).

The cyclorotation adjusted group had an average value of 0.89° ± 3.28° (range: -7.5° to 9.0°); considering the absolute value of cyclorotation, the average was 2.42° ± 2.36° (range: 0.0° to 9.0)°. We were able to engage CTA in 100% of the Vario-driven cases studied. It has to be underscored that in some cases more than 30 images with the Vario were necessary to obtain reliable and feasible CTA data, a laborious process. Of the 110 eyes, 35 (32%) eyes had 0° cyclorotation (ie, below the detection limit of 0.5°), 33 (30%) eyes had between 0° and 2°, and only 8 (8%) had greater than 8°.

Average radial displacement of the cone location in the non-cyclorotation adjusted group was 1.47 ± 0.49 mm (range: 0.76 to 2.83 mm) preoperatively; the difference maps corresponded to an average cone location of 1.28 ± 0.51 mm (range: 0.46 to 2.88 mm). The difference between preoperative and achieved change in the non-cyclorotation adjusted group was also not statistically significant ($P = .067$). In addition, the preoperative cone location radial displacement between the two groups was not statistically significant ($P = .097$).

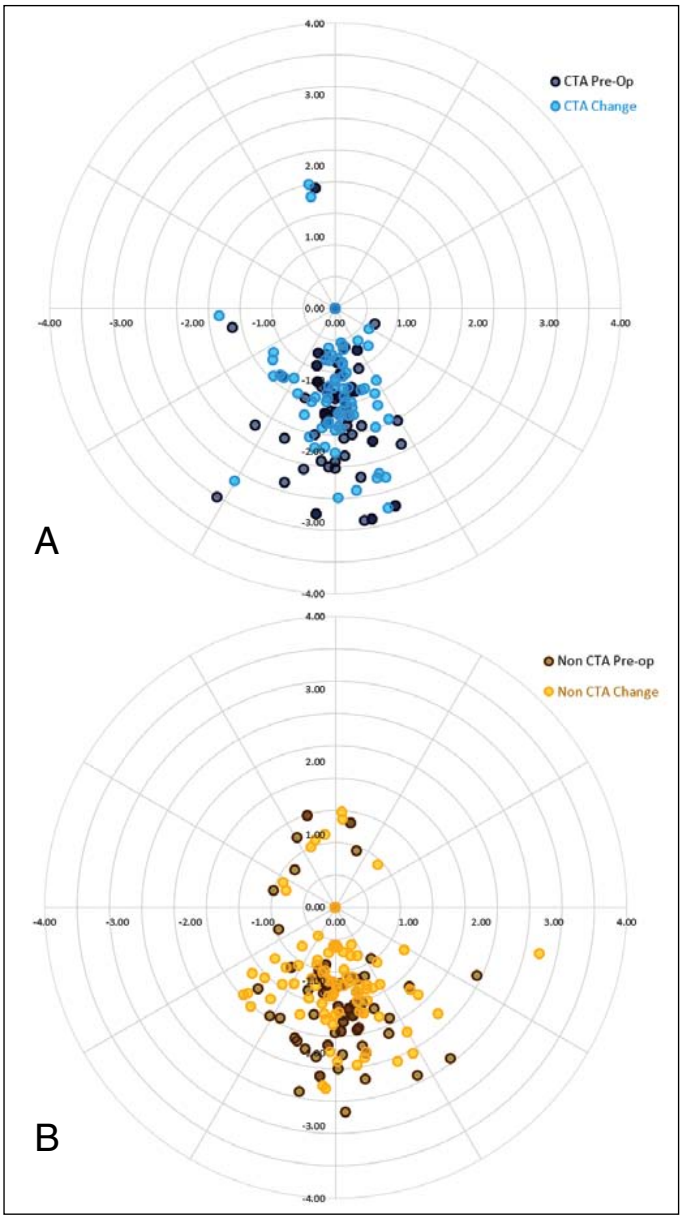

Figure 2. The distribution of the vectors corresponding to the steepest (peak topographic) corneal point on the preoperative map (r_p, ϑ_p) and the change (achieved difference) map (r_d, ϑ_d). (A) Cyclorotation adjusted and (B) non-cyclorotation adjusted groups. CTA = cyclorotational topographic adjustment

Table 1 summarizes the statistical analysis results for $\Delta\vartheta = |\vartheta_p - \vartheta_d|$, the absolute angular difference between the peak topographic angular data, and $W\Delta\vartheta = \Delta\vartheta \times \Delta r$, the weighted angular difference between the peak topographic data. The cyclorotation adjusted group had on average smaller angular difference and weighted angular difference by a statistically significant margin ($\Delta\vartheta$: $P = .0058$; $W\Delta\vartheta$: $P = .015$) compared to the non-cyclorotation adjusted group.

DISCUSSION

This study provides additional evidence for the potential of incorporating cyclorotation compensation in

TABLE 1

Statistical Analysis of Absolute Angular Difference Between the Peak Topographic Angular Data $\Delta\vartheta$ and Weighted Angular Difference W$\Delta\vartheta$

	Cyclorotation Adjusted Group			Non-cyclorotation Adjusted Group		
Parameter	$\Delta\vartheta$ (°)	W$\Delta\vartheta$ (mm)	***P***	$\Delta\vartheta$ (°)	W$\Delta\vartheta$ (mm)	***P***
Average	7.18	3.43	.0058	14.50	10.23	.0015
Standard deviation	±7.53	±4.76		±12.65	±15.15	
Minimum	0	0.00		0	0.00	
Maximum	34	21.41		49	80.56	
Confidence intervals						
0.95	±1.77	±1.12		±2.64	±3.21	
0.99	±2.35	±1.49		±3.49	±4.25	

such highly customized topography-guided treatments. We studied two large groups, which were matched preoperatively in all aspects of vision, corneal thickness, keratoconus stage, and cone location (displacement).

The Athens Protocol screening protocol involves preoperative imaging by both the Scheimpflug topometry and Placido topography devices. Either device can be synced to the operational laser planning computer on the EX500 excimer laser via a closed ethernet circuit to provide the necessary topography data. Surgeons may choose data from either device based on their own criteria. We have made it standard to review both topographies as a potential treatment and compare the treatment patterns that invariably are similar. The main difference, as far as the implementation of either treatment, is that only the Placido topography-guided treatment can employ adjunct cyclorotation adjustment, whereas the Scheimpflug-derived treatment cannot. Prior to the availability of the cyclotortional compensation option with the new Placido-imaging device (Vario), the majority of the procedures by our team adopted the Scheimpflug option, due to the improved sensitivity at the center section, when compared to the older version of Placido-produced topography employed by a predecessor device to the current Vario topographer (the Topolyzer). We have previously studied the efficacy of the Placido-derived treatments to Scheimpflug-derived treatments and with that older technology on both the topography devices (Oculyzer I vs Topolyzer) evaluated both with the 400-Hz EyeQ WaveLight excimer laser (Alcon Laboratories, Inc.) and found that the Scheimpflug-driven treatments were superior.[19]

Herein, we introduce a digital analysis technique to objectively evaluate the possible cyclotorsion effect, which may be applicable to analysis of outcomes in topography-guided treatments.

In addition to adopting cyclotortional compensation, the enhanced Athens Protocol incorporates a change in the ablation pattern sequences, by the partial PRK step preceding the PTK step. The rationale for this has been that the topography-guided ablation pattern bears the customized part, for which the active eye tracking should be performing with minimal interference. Thus, the partial-PRK step is performed first to interfere with less ablated debris and with intact epithelium for the most part providing a better image for the EX500 active tracker camera, and therefore providing the best possible pupil, iris architecture, centroid shift, and limbal anatomy imaging. The PTK step, which was initially designed to debride a uniform 50-µm thickness of epithelium over a 7-mm zone, may be performed subsequently. This rotationally symmetric PTK step does not necessitate cyclorotation compensation and is not dependent on saccadic motions to the extent of the partial PRK step.

In addition to ocular movement, there is also variable ocular rotation, known as cyclorotation or cyclotorsion. Cyclorotation affects ocular imaging and toric corrections. Cyclorotation may vary from +7.7° (excyclotorsion) to -11.0° (incyclotorsion), with a mean absolute value of 2.74° ± 2.30°.[20] Our data for cyclotorsion had an average absolute value of 2.42° ± 2.36°.

Because the majority of laser vision correction platforms incorporate custom ablation patterns, such as topography-guided or corneal wavefront ablation profiles,[21,22] accurate compensation for both movement and rotation has a major part in achieving optimal results. It would be interesting to evaluate some of these platforms with the novel methodology described herein to objectively assess perhaps equivalent, superior, or inferior accuracy.

Until recently, eye tracking with the topography-guided profile by the EX500 platform only addressed horizontal (x), vertical (y), and depth (z) movements,[23]

with limited cyclorotation compensation.[24] Even in the current configuration employed in the EX500 excimer laser, the cyclorotation compensation is static, meaning that one initial value is recorded. Thus, active cyclorotation compensation perhaps remains the last piece of the puzzle that had not been addressed until recently.[25,26]

This study indicates that incorporation of novel topography imaging technology coupled with novel excimer laser tracking technology (to include cyclorotation compensation) leads to markedly improved correlation between targeted and achieved topographic changes in the management of severely irregular corneas such as in progressive clinical keratoconus.

AUTHOR CONTRIBUTIONS

Study concept and design (AJK); data collection (AJK, GA); analysis and interpretation of data (AJK, GA); writing the manuscript (GA); critical revision of the manuscript (AJK, GA); statistical expertise (GA); administrative, technical, or material support (AJK); supervision (AJK)

REFERENCES

1. Raiskup F, Spoerl E. Corneal crosslinking with riboflavin and ultraviolet A: I. Principles. *Ocul Surf*. 2013;11:65-74.
2. Sinha Roy A, Rocha KM, Randleman JB, Stulting RD, Dupps WJ Jr. Inverse computational analysis of in vivo corneal elastic modulus change after collagen crosslinking for keratoconus. *Exp Eye Res*. 2013;113:92-104.
3. Kanellopoulos AJ. Comparison of sequential vs same-day simultaneous collagen cross-linking and topography-guided PRK for treatment of keratoconus. *J Refract Surg*. 2009;25:S812-S818.
4. Labiris G, Giarmoukakis A, Sideroudi H, Gkika M, Fanariotis M, Kozobolis V. Impact of keratoconus, cross-linking and cross-linking combined with photorefractive keratectomy on self-reported quality of life. *Cornea*. 2012;31:734-739.
5. Kanellopoulos AJ. Long term results of a prospective randomized bilateral eye comparison trial of higher fluence, shorter duration ultraviolet A radiation, and riboflavin collagen cross linking for progressive keratoconus. *Clin Ophthalmol*. 2012;6:97-101.
6. Kanellopoulos AJ, Asimellis G. Keratoconus management: long term stability of topography-guided normalization combined with high fluence CXL stabilization (the Athens Protocol). *J Refract Surg*. 2014;30:88-93.
7. Kanellopoulos AJ, Asimellis G. Introduction of quantitative and qualitative cornea optical coherence tomography findings, induced by collagen cross-linking for keratoconus; a novel effect measurement benchmark. *Clin Ophthalmol*. 2013;7:329-335.
8. Kymionis GD, Portaliou DM, Kounis GA, Limnopoulou AN, Kontadakis GA, Grentzelos MA. Simultaneous topography-guided photorefractive keratectomy followed by corneal collagen cross-linking for keratoconus. *Am J Ophthalmol*. 2011;152:748-755.
9. Stojanovic A, Zhang J, Chen X, Nitter TA, Chen S, Wang Q. Topography-guided transepithelial surface ablation followed by corneal collagen cross-linking performed in a single combined procedure for the treatment of keratoconus and pellucid marginal degeneration. *J Refract Surg*. 2010;26:145-152.
10. Kymionis GD, Grentzelos MA, Portaliou DM, Kankariya VP, Randleman JB. Corneal collagen cross-linking (CXL) combined with refractive procedures for the treatment of corneal ectatic disorders: CXL plus. *J Refract Surg*. 2014;30:566-576.
11. Tuwairqi WS, Sinjab MM. Safety and efficacy of simultaneous corneal collagen cross-linking with topography-guided PRK in managing low-grade keratoconus: 1-year follow-up. *J Refract Surg*. 2012;28:341-345.
12. Lin DT, Holland S, Tan JC, Moloney G. Clinical results of topography-based customized ablations in highly aberrated eyes and keratoconus/ectasia with cross-linking. *J Refract Surg*. 2012;28:S841-S848.
13. Siqueira JA, Dias LC, Siqueira R, et al. Longterm improvement after the Athens Protocol for advanced keratoconus with significant ectasia progression in the fellow eye. *International Journal of Keratoconus and Ectatic Corneal Diseases*. 2013;2:143-146.
14. Alessio G, L'abbate M, Sborgia C, La Tegola MG. Photorefractive keratectomy followed by cross-linking versus cross-linking alone for management of progressive keratoconus: two years follow up. *Am J Ophthalmol*. 2013;155:54-65.
15. Narváez J, Brucks M, Zimmerman G, Bekendam P, Bacon G, Schmid K. Intraoperative cyclorotation and pupil centroid shift during LASIK and PRK. *J Refract Surg*. 2012;28:353-357.
16. Tomita M, Waring GO 4th, Magnago T, Watabe M. Clinical results of using a high-repetition-rate excimer laser with an optimized ablation profile for myopic correction in 10,235 eyes. *J Cataract Refract Surg*. 2013;39:1543-1549.
17. Kanellopoulos AJ, Asimellis G. Long term bladeless LASIK outcomes with the FS200 femtosecond and EX500 excimer laser workstation: the Refractive Suite. *Clin Ophthalmol*. 2013;7:261-269.
18. Schneider CA, Rasband WS, Eliceiri KW. NIH Image to ImageJ: 25 years of image analysis. *Nat Methods*. 2012;9:671-675.
19. Kanellopoulos AJ, Asimellis G. Comparison of Placido disc and Scheimpflug image-derived topography-guided excimer laser surface normalization combined with higher fluence CXL: the Athens Protocol, in progressive keratoconus. *Clin Ophthalmol*. 2013;7:1385-1396.
20. Lucena AR, Mota JA, Lucena DR, Ferreira Sde L, Andrade NL. Cyclotorsion measurement in laser refractive surgery. *Arq Bras Oftalmol*. 2013;76:339-340.
21. Alió JL, Piñero DP, Plaza Puche AB. Corneal wavefront-guided photorefractive keratectomy in patients with irregular corneas after corneal refractive surgery. *J Cataract Refract Surg*. 2008;34:1727-1735.
22. Shaheen MS, El-Kateb M, Hafez TA, Piñero DP, Khalifa MA. Wavefront-guided laser treatment using a high-resolution aberrometer to measure irregular corneas: a pilot study. *J Refract Surg*. 2015;31:411-418.
23. Prakash G, Ashok Kumar D, Agarwal A, Jacob S, Sarvanan Y, Agarwal A. Predictive factor analysis for successful performance of iris recognition-assisted dynamic rotational eye tracking during laser in situ keratomileusis. *Am J Ophthalmol*. 2010;149:229-237.
24. Kohnen T, Kühne C, Cichocki M, Strenger A. Cyclorotation of the eye in wavefront-guided LASIK using a static eyetracker with iris recognition [article in German]. *Ophthalmologe*. 2007;104:60-65.
25. Arba-Mosquera S, Merayo-Lloves J, de Ortueta D. Clinical effects of pure cyclotorsional errors during refractive surgery. *Invest Ophthalmol Vis Sci*. 2008;49:4828-4836.
26. Wang L, Koch DD. Residual higher-order aberrations caused by clinically measured cyclotorsional misalignment or decentration during wavefront-guided excimer laser corneal ablation. *J Cataract Refract Surg*. 2008;34:2057-2062.

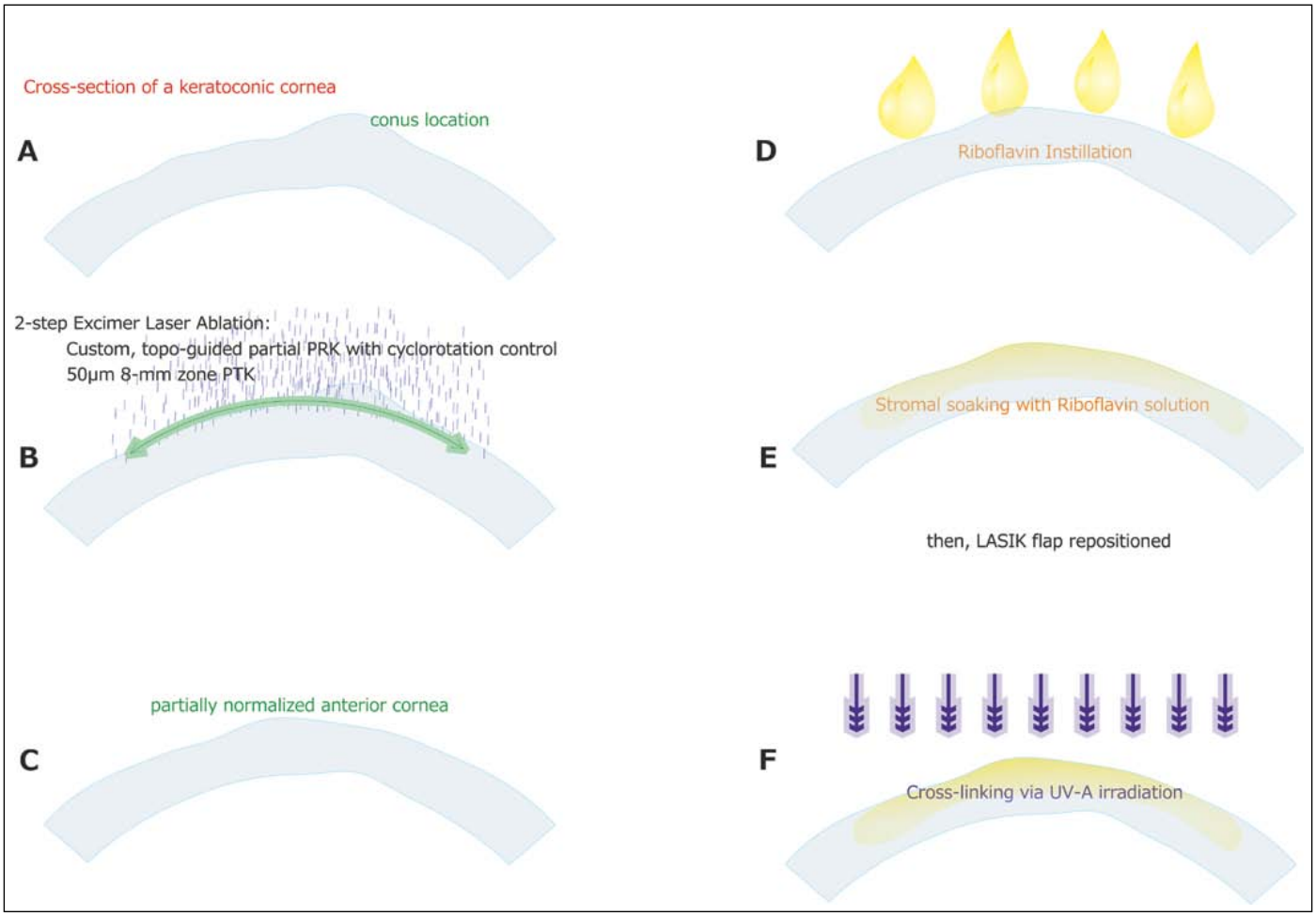

Figure A. Basic steps of the enhanced Athens Protocol procedure. (A) Import of topography-guided data to the surgical platform, (B) a two-step excimer laser ablation comprising custom topography-guided partial photorefractive keratectomy (PRK) with cyclorotation control, followed by a 50-μm deep, 8-mm optical zone diameter phototherapeutic keratectomy (PTK), (C) application of mytomicin C, (D) instillation of riboflavin, (E) stromal soaking for 80 seconds, and (F) ultraviolet-A (UV-A) irradiance of 6 mW/cm^2 applied for 15 minutes.

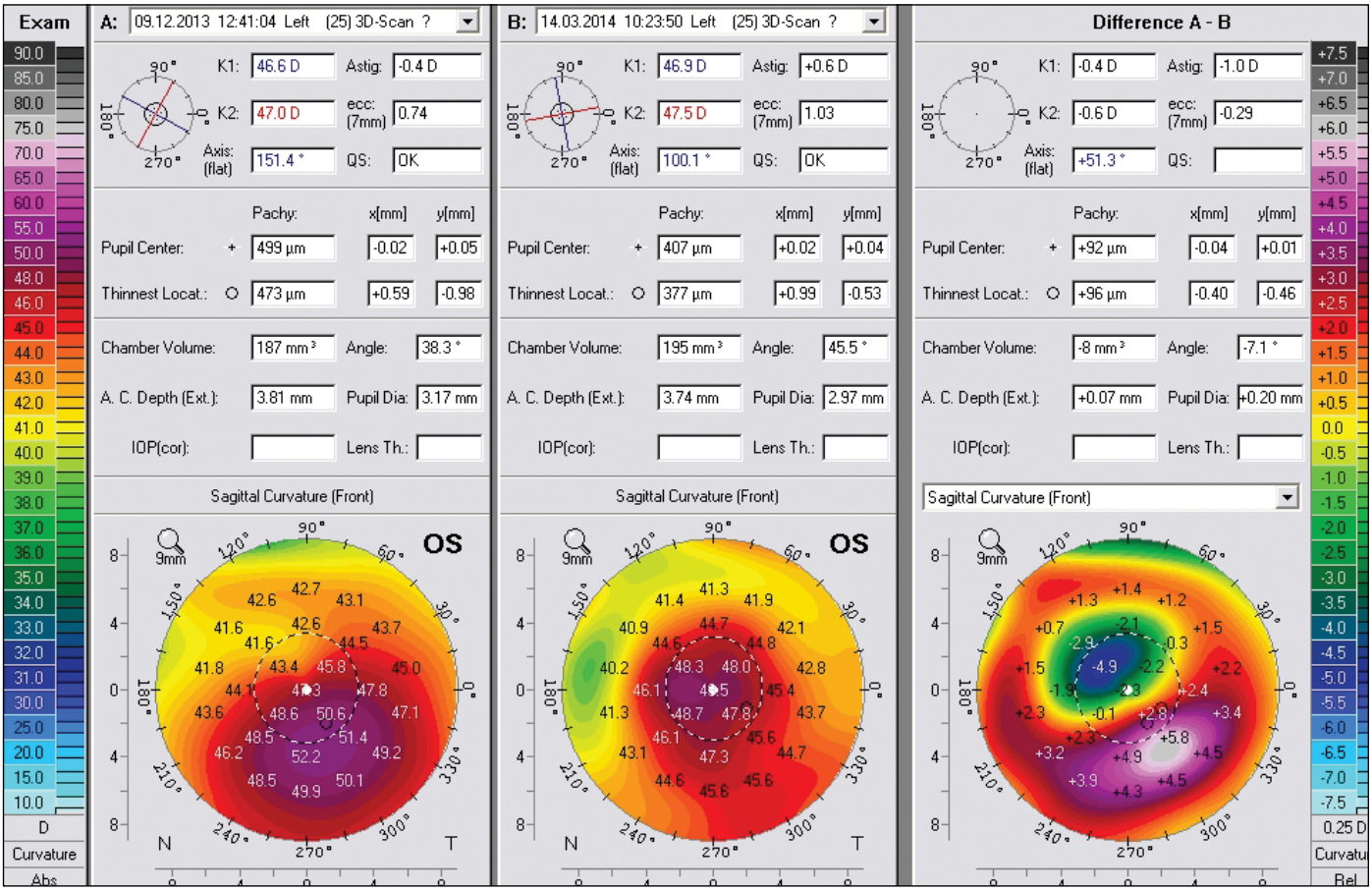

Figure B. The 'compare 2 exams' output from the Scheimpflug imaging device. (Left) The preoperative sagittal curvature map, (middle) the postoperative map, and (right) the difference of the two maps.

Clinical Ophthalmology

Dovepress
open access to scientific and medical research

Open Access Full Text Article

ORIGINAL RESEARCH

Topography-modified refraction (TMR): adjustment of treated cylinder amount and axis to the topography versus standard clinical refraction in myopic topography-guided LASIK

Anastasios John Kanellopoulos[1,2]

[1]LaserVision Clinical and Research Institute, Athens, Greece; [2]Department of Ophthalmology, NYU Medical School, New York, NY, USA

Purpose: To evaluate the safety, efficacy, and contralateral eye comparison of topography-guided myopic LASIK with two different refraction treatment strategies.

Setting: Private clinical ophthalmology practice.

Patients and methods: A total of 100 eyes (50 patients) in consecutive cases of myopic topography-guided LASIK procedures with the same refractive platform (FS200 femtosecond and EX500 excimer lasers) were randomized for treatment as follows: one eye with the standard clinical refraction (group A) and the contralateral eye with the topographic astigmatic power and axis (topography-modified treatment refraction; group B). All cases were evaluated pre- and post-operatively for the following parameters: refractive error, best corrected distance visual acuity (CDVA), uncorrected distance visual acuity (UDVA), topography (Placido-disk based) and tomography (Scheimpflug-image based), wavefront analysis, pupillometry, and contrast sensitivity. Follow-up visits were conducted for at least 12 months.

Results: Mean refractive error was −5.5 D of myopia and −1.75 D of astigmatism. In group A versus group B, respectively, the average UDVA improved from 20/200 to 20/20 versus 20/16; post-operative CDVA was 20/20 and 20/13.5; 1 line of vision gained was 27.8% and 55.6%; and 2 lines of vision gained was 5.6% and 11.1%. In group A, 27.8% of eyes had over −0.50 diopters of residual refractive astigmatism, in comparison to 11.7% in group B ($P<0.01$). The residual percentages in both groups were measured with refractive astigmatism of more than –0.5 diopters.

Conclusion: Topography-modified refraction (TMR): topographic adjustment of the amount and axis of astigmatism treated, when different from the clinical refraction, may offer superior outcomes in topography-guided myopic LASIK. These findings may change the current clinical paradigm of the optimal subjective refraction utilized in laser vision correction.

Keywords: TMR, topography-modified refraction, myopic LASIK, femtosecond laser, FS200, EX500 excimer laser, long-term stability, regression, astigmatism correction, post-LASIK refraction

Introduction

Laser vision correction has been established over the last 2 decades as a safe and effective intervention, with Laser-assisted in situ keratomileusis (LASIK) being one of the main techniques practiced globally.[1,2]

Femtosecond laser-assisted LASIK has become a popularized modification over the last decade and over the standard LASIK technique utilizing mechanical microkeratomes.[3,4]

Correspondence: Anastasios John Kanellopoulos
LaserVision Clinical and Research Institute, 17 Tsocha Street, Athens 11521, Greece
Tel +30 210 747 2777
Fax +30 210 747 2789
Email ajk@brilliantvision.com

submit your manuscript | www.dovepress.com
Dovepress
http://dx.doi.org/10.2147/OPTH.S122345

Excimer lasers, used in the second step of a LASIK procedure to correct refractive error (RE), have been evolving as well, with most platforms currently utilizing flying spot technology of very high repetition rates and advanced tracking mechanisms to track intra-operatively the pupillary aperture and some even to provide cyclorotation adjustment.[5–7] Aspherical ablation profiles have been employed to reduce spherical aberration associated with myopic corrections, so most LASIK procedures are performed currently as "wavefront optimized".[8] Further customization of the ablation pattern has been practiced by pairing wavefront eye data to the refractive data chosen to be corrected, as wavefront-guided treatments in pursue of improving visual function in aberrated eyes, or pre-empting wavefront aberrations created by the standard procedures.[9,10] Since most inherent and acquired eye aberrations lie in the cornea – the premiere refractive medium of the eye – topography-guided treatments have been additionally employed as a means of ablation customization in pursue of additionally correcting corneal irregularities affecting visual function and/or for angle kappa.[11,12]

LASIK outcomes appear to have improved in safety and efficacy with the evolutions described earlier[1,13] in both refractive outcomes and induced high-order aberrations.[5,14,15]

Further customization of the ablation pattern by utilizing topography data has been reported to provide excellent refractive data with regard to uncorrected distance visual acuity (UDVA) and corrected distance visual acuity (CDVA; WaveLight Allegretto Wave® Eye-Q Excimer Laser[16]).

The clinical refraction utilized in most laser vision correction treatments has been based on the subjective interaction of clinician and patient and ranging from the dry manifest to the wet manifest or a clinician-preferred medium of the two.

The author has had extensive experience in treating very irregular corneas, learning that refractive data sometimes are different from topographic data with regard to the amount and axis of the astigmatism. Thus, the adjustment of the clinical refraction with topographic data: topography-modified refraction (TMR) was introduced. The purpose of this study was to validate this novel measurement by comparing the visual outcomes when the TMR was used in myopic LASIK to using the standard clinical refraction.

Patients and methods

This prospective, randomized, interventional study received approval from the ethics committee of the LaserVision Clinical and Research Institute, adherent to the tenets of the Declaration of Helsinki. Written informed consent was obtained from each subject at the time of the intervention. The study was conducted in the author's clinical practice on patients during scheduled pre- and post-operative procedure visits.

The 50 consecutive patients enrolled in the study underwent uncomplicated primary bilateral topography-guided LASIK by the same surgeon (AJK) on the same refractive surgery platform (FS200 femtosecond and EX500 excimer lasers).

Pre-operative spherical equivalent was between 0.00 and −8.00 D and up to 6 D of cylinder RE (expressed in minus value).

Exclusion criteria for the LASIK operation were systemic or ocular diseases, eyes with a history of corneal dystrophy or herpetic eye disease, topographic evidence of keratoconus (as evidenced by Placido topography) or warpage from contact lenses, corneal scaring, glaucoma, severe dry eye, and collagen vascular diseases. Programmed planned flap thickness was 110 μm and diameter was 8 mm.

All eyes were evaluated pre-operatively for distance best CDVA and post-operatively for UDVA. Pre-operative evaluations included wavefront analysis, pupillometry, and contrast sensitivity utilizing the functional vision analyzer (Stereo Optical, Chicago, IL, USA). Post-operative examination included manifest and dilated refraction, slit-lamp microscopy, tonometry, and keratometry, by means of corneal topography utilizing the Vario (WaveLight, Erlagen, Germany) and Scheimpflug tomography assessment utilizing a Pentacam-based device, the Oculyzer II (WaveLight).

The treatment used for the eyes randomized in group A was the subjective clinical refraction, entered into the topography-guided software as the surgeon override data, and is the standard operation in these treatments.

The clinical refraction data are the first line of data on the treatment planning software window shown in Figure 1, both top and bottom. The specific patient example shows the clinical refraction on the top, of −6.50 D of sphere and −0.50 D of cylinder at 45°. The middle line of refraction in both top and bottom windows of Figure 1 shows the topography software-recommended cylindrical refraction. In this particular case, the sphere is −0.45 D (the topography software has no axial length data and cannot calculate myopia), and the cylinder that derives from several consistent Vario, topolyzer (Alcon, Fort Worth, TX, USA) topographies shows −1.11 D at 0°. The lower third refraction in both top and bottom images in Figure 1 is modified by the surgeon. In the top, all refraction data are set on purpose to 0°. In this way, the topography-guided software reveals the correction it will attempt in order to normalize this cornea with regard to the corneal vertex. Thus, the trefoil-like ablation image on

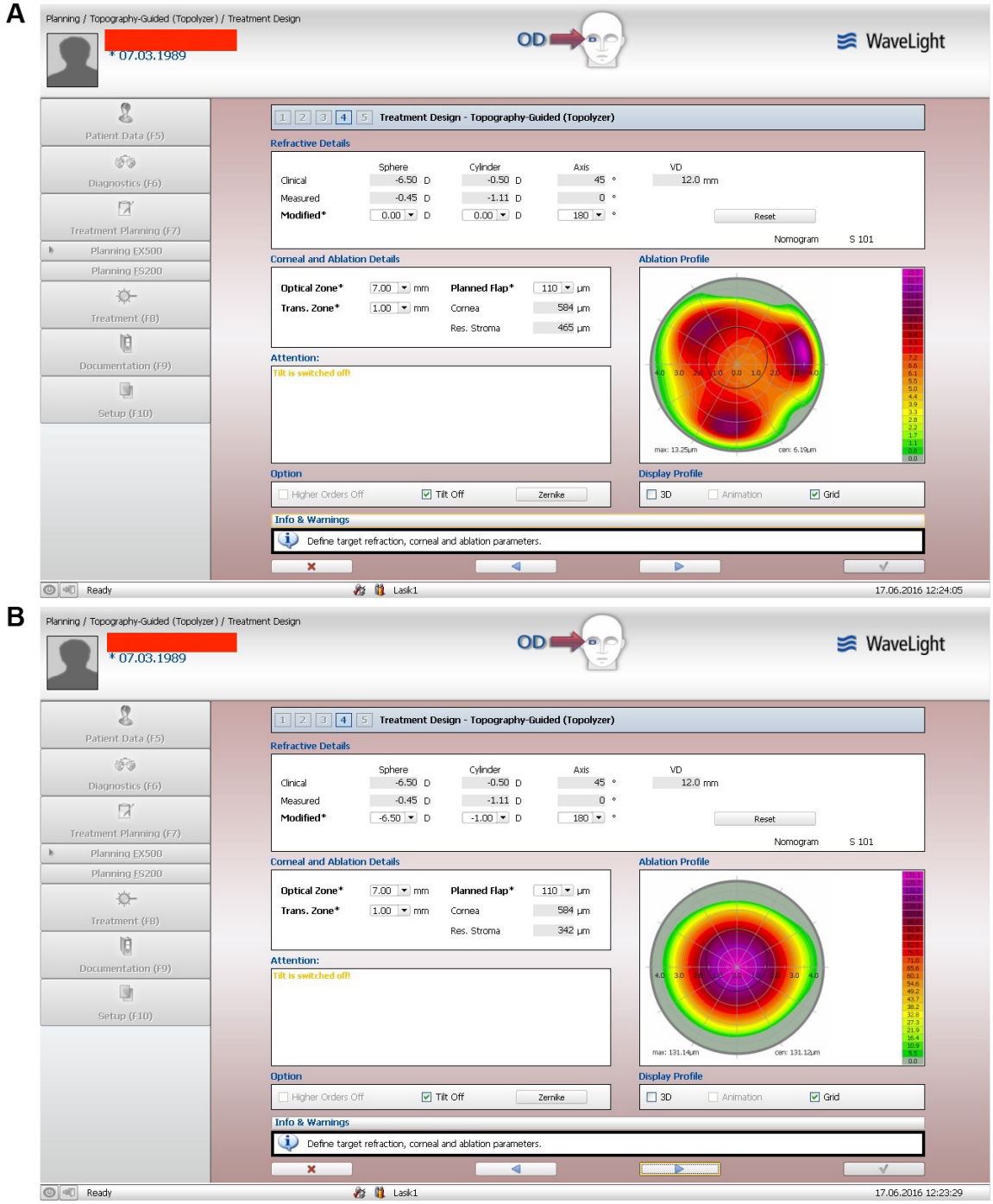

Figure 1 Image **A** shows the topography-guided treatment when refractive error is adjusted by the user to zero sphere and zero cylinder. This image allows the user to visualize the corrections made by the software and added to the excimer correction in order to normalize the anterior cornea curvature to the cornea vertex. Image **B** illustrates the topography treatment pattern after the refraction has been adjusted by the user to the desired sphere and cylinder and includes the changes noted in image **A**.
Notes: "Clinical" is the clinical refraction dialed by the user into the system; the "measured" refraction is the cylindrical amount and axis calculated by the topography software, to be corrected so the anterior cornea can me maximally normalized in regard to the cornea vertex; "modified" represents the surgeon/user adjusted data.
Abbreviations: 3D, three-dimensional; max, maximum, cen, center; trans, transition zone; res, residual; VD, vertex distance.

the right of the top image in Figure 1. The trefoil-like image is also presented here in correlation with the pupillary aperture, also captured by the Vario topographer, and in this top window it shows clearly decentration to the trefoil-like normalization ablation, revealing angle-kappa compensation by the topography software. This ablation pattern will induce some myopia and it was calculated that in order to keep it neutral there is a need to add −0.25 D of myopia to the clinical

refraction sphere, so the total sphere should be −6.75 D. The cylinder suggested by the software (middle refraction) is much higher than the clinical by 0.5 D and of different axis: 0° instead of 45°. The topography suggested cylinder is then entered into the third lower "modified" refraction to read −1.0 D at 0° or 180° in the bottom version of Figure 1. This would further increase the spherical equivalent by −0.25 D of sphere; hence the final adjustment made to the modified refraction on the bottom window of this same treatment image is to reduce the sphere from −6.75 D, as noted earlier, to −6.50 D so as to keep the same spherical equivalent. Therefore, the TMR in this case is −6.50 D to 1.00 D at 180°, instead of the −6.50 D to 0.50 D at 45° of the standard clinical refraction.

The treatment used in the contralateral eyes of group B was modified, as noted earlier, to reflect the topography-guided suggested cylinder power and axis calculated by the software based on the Vario topographies uploaded, as seen in the middle "measured" refraction of both top and bottom images of Figure 1. In most cases, the cylinder was increased and the sphere decreased accordingly, but there were some cases that the actual clinical refraction cylinder was reduced and the sphere increased accordingly. In the TMR cases of group B, the cylinder axis was always that suggested by the topography processing as noted in the middle measured refraction line.

Post-operative follow-up examinations were conducted at 1 week, 1, 3, and 6 months, and at 1 year. Data processed in this study represent the 3-, 6-, and 12-month visits.

Data were loaded in and processed by the web-based ophthalmic outcome analysis software application known as "Internet-based refractive analysis" (IBRA; Zubisoft GmbH, Oberhasli, Switzerland).[17]

Results

Of the 50 patients, 32 were female and 18 were male. Mean age at the time of the operation was 29.6±7.8 years, range 18–52 years.

The mean pre-operative UDVA for group A eyes were: UDVA mean in decimal scale and standard deviation (SD): 0.04±0.007, UDVA range: 0.001–0.8; spherical equivalent (SE) mean and SD: −5.19±2.15 D, SE range −8.00 D to −0.50 D; cylinder mean: −1.15±1.15 D and cylinder range: −4.25 D to 0 D.

The respective pre-operative data for the randomized group B contralateral eyes were: UDVA: 0.04±0.05, UDVA range: 0.002–0.8, SE mean: −4.75±2.49 D, SE range: −7.50 D to −0.75 D, cylinder mean: −1.12 D±0.95 D, and cylinder range: −3.75 D to −0.50 D. These data are also shown in Table 1.

Table 1 Pre-operative parameters

Pre-operative parameters	Group A	Group B
UDVA mean/SD	0.04±0.07	0.04±0.05
UDVA range	0.001–0.8	0.002–0.8
SE mean/SD	−5.19±2.15	−4.75±2.49
SE range	−8.00 to −0.50	−7.50 to −0.75
Cyl mean/SD	−1.15±1.15	−1.12±0.95
Cyl range	−4.25 to 0	−3.75 to −0.50

Notes: Group A: one eye with the standard clinical refraction; Group B: the contralateral eye with the topographic astigmatic power and axis (topography-modified treatment refraction). Units of measure: SE units = diopters; UDVA units = decimal scale; Cyl = cylinder in diopter units.
Abbreviations: UDVA, uncorrected distance visual acuity; SD, standard deviation; SE, spherical equivalent; Cyl, cylinder.

Post-operative average RE for the standard group A was −0.27±0.39 D and for the topography adjusted group B was +0.15±0.19 D at 3 months. At the 12-month visit, the residual refractive error for group A was −0.47±0.55 D and for group B (the topography modified refraction group) −0.19±0.08 D. These data were statistically significantly different by $P<0.02$. This compares to the pre-operative average RE of −5.29±2.39 D (range −8.00 D to −0.50 D) for all eyes.

Post-operative refractive astigmatism was −0.54±0.24 D for the standard group A and −0.15±0.14 for the topography adjusted group B at 3 months and −0.76±0.44 and −0.18±0.24 for the 1-year visit, respectively. This compares to the pre-operative refractive astigmatism of −1.07±0.91 D (range −4.25 D to 0 D) as an average for all eyes.

Corrected and uncorrected visual acuity outcome and stability

The corrected visual acuity (distance monocular; CDVA) outcome at 3 months (Figure 2) shows that 88.9% of the eyes in group A had post-operatively CDVA better than 1.0 (decimal) after 3 months, which was maintained at the 1 year visit. Figure 2 also depicts the best-corrected pre-operative distance visual acuity (CDVA) for group B: 94.4%. CDVA of 20/16 or better was measured for 33.3% of group A eyes, compared to 61.1% of group B eyes (statistically significant at $P<0.001$).

UDVA of 20/20 or better was measured at 3 months (Figure 3) in 61.1% of eyes in group A and 83.3% of eyes in group B ($P<0.002$). UDVA of 20/16 or better was measured in 22.2% of eyes in group A and 50% of eyes in group B, a difference that was also statistically significant ($P<0.001$).

Safety of corrected visual acuity

As shown in Figure 4, the safety distance visual acuity graph at 3-month visit comparison of pre-operative best CDVA and post-operative UDVA indicates that 66.7% of

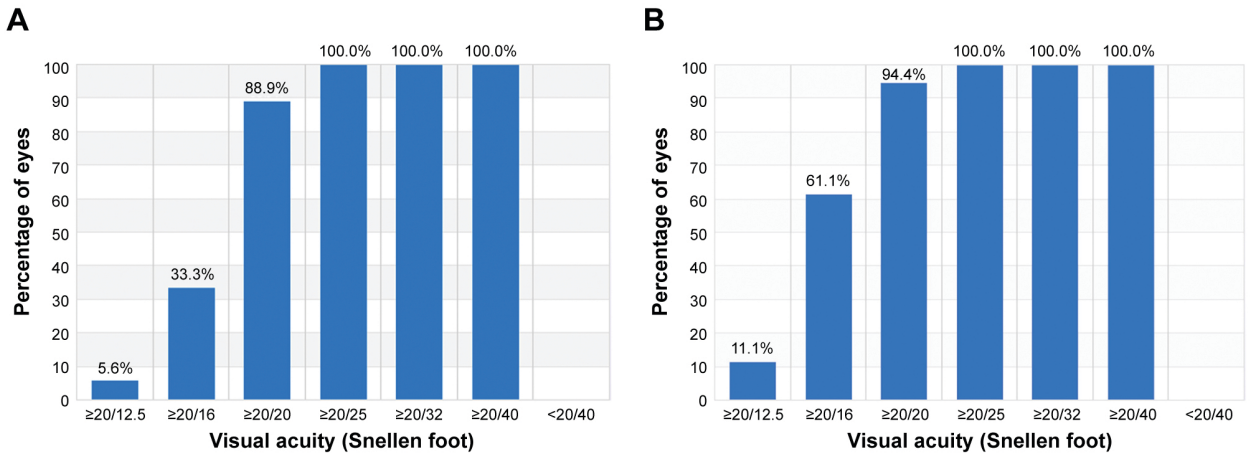

Figure 2 Corrected distance visual acuity at 3 months: (**A**) group A and (**B**) group B.
Notes: Group A: one eye with the standard clinical refraction; Group B: the contralateral eye with the topographic astigmatic power and axis (topography-modified treatment refraction).

the eyes were unchanged, while 27.8% of the eyes gained one Snellen line and 5.6% gained two or more Snellen lines in group A. In group B, 33.3% of the eyes were unchanged, while 55.6% of the eyes gained one Snellen line and 11.1% gained two or more Snellen lines. All differences were statistically significant at $P<0.2$. Residual RE grouped in 3 categories of +0.01 to +0.5 D, −0.5 to 0 D, and −1 to −0.5 D, at the 3 month visit for groups A and B is illustrated in Figure 5.

Refractive predictability

Predictability is demonstrated in Figure 6, where the achieved SE versus attempted SE (in D) is plotted, for gate =0.5 D for group A and group B.

Post-operative RE data for the two groups are noted in Figure 5. Refractive astigmatism is noted in Figure 7 with again statistically significant differences with group B presenting less refractive astigmatism.

Contrast sensitivity

Figure 8 illustrates the contrast sensitivity results in special frequencies of 1.5–18 cycles per degree for all pre-operative, group A, and group B.

High-order aberrations and coma, as measured with the Allegro Wavefront analyzer (WaveLight): at 3 months average high order aberrations (RMSH) were for group A: 0.85 µm and for group B: 0.025 µm; coma measurements were 0.65 µm and 0.45 µm, respectively.

Discussion

The combined Alcon/WaveLight refractive surgery laser platform comprising the FS200 femtosecond laser,[18] the EX500

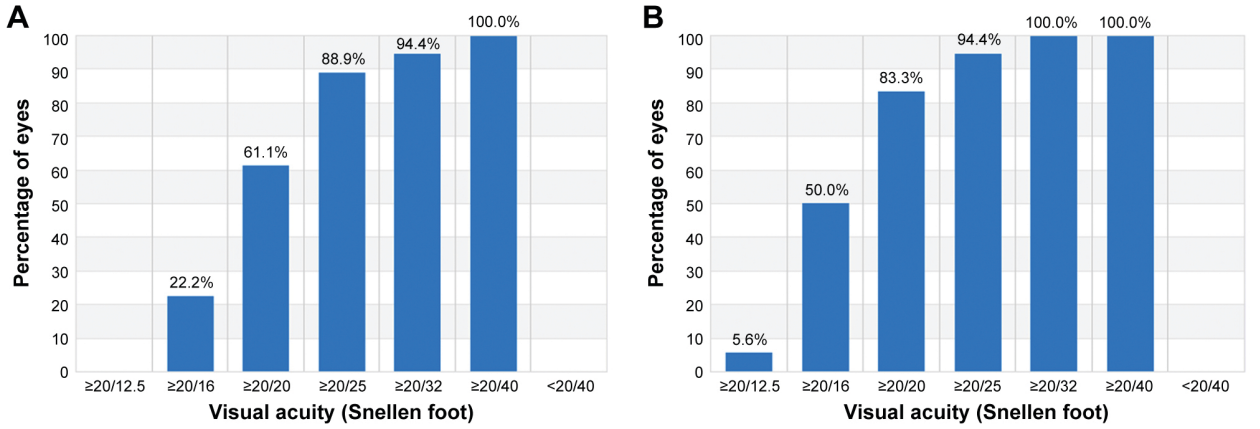

Figure 3 Post-operative uncorrected distance visual acuity at 3-month visit: (**A**) group A and (**B**) group B.
Notes: Group A: one eye with the standard clinical refraction; Group B: the contralateral eye with the topographic astigmatic power and axis (topography-modified treatment refraction).

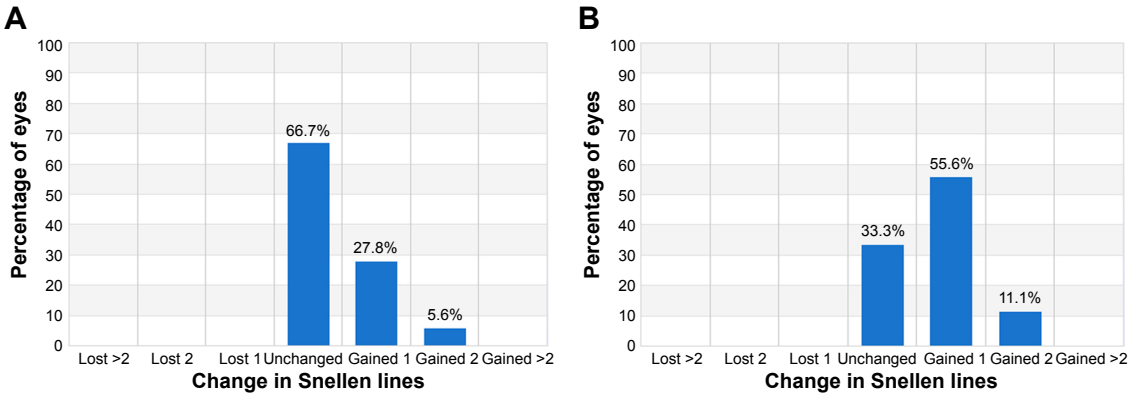

Figure 4 Safety distance visual acuity graph (percentage of eyes with gain/loss in Snellen lines), at 3-month visit: (**A**) group A and (**B**) group B.
Notes: Group A: one eye with the standard clinical refraction; Group B: the contralateral eye with the topographic astigmatic power and axis (topography-modified treatment refraction).

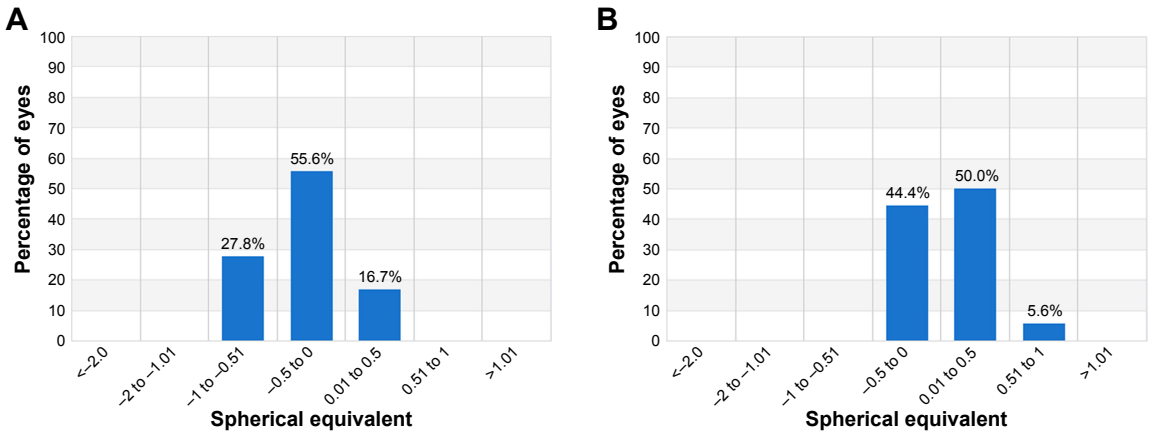

Figure 5 Defocus equivalent results at 3-month visit: (**A**) group A and (**B**) group B.
Notes: Group A: one eye with the standard clinical refraction; Group B: the contralateral eye with the topographic astigmatic power and axis (topography-modified treatment refraction).

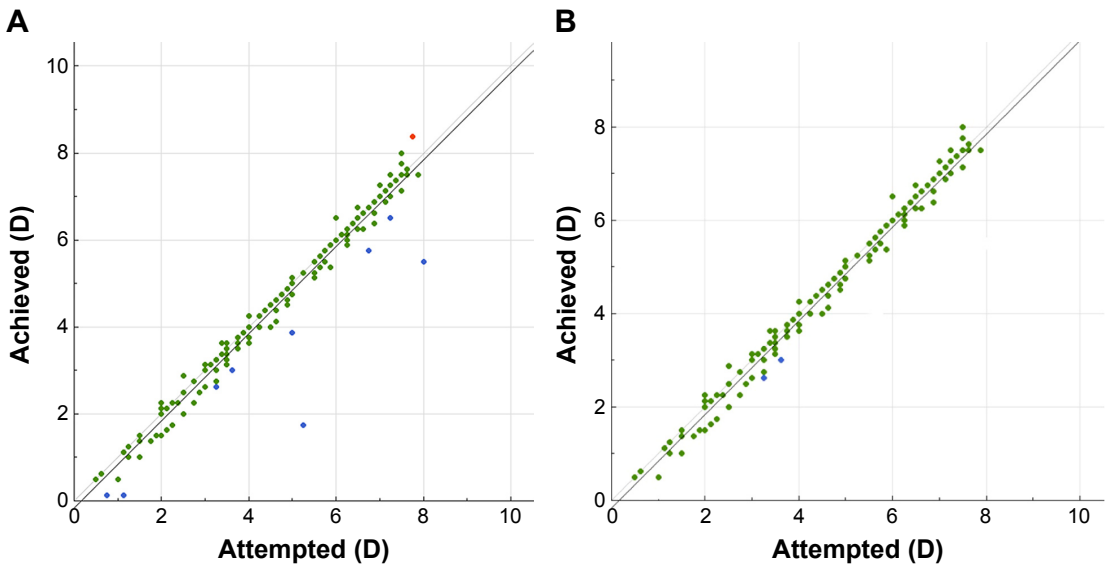

Figure 6 Predictability of spherical equivalent (SE) correction, showing achieved SE versus attempted SE: (**A**) group A and (**B**) group B.
Notes: Group A: one eye with the standard clinical refraction; Group B: the contralateral eye with the topographic astigmatic power and axis (topography-modified treatment refraction). Green marks show outcomes within 0.25 diopters of attempted vs achieved; blue marks show attempted vs achieved of under 0.25 diopters (under-corrections); red marks show attempted vs achieved of over 0.25 diopters (over-corrections).

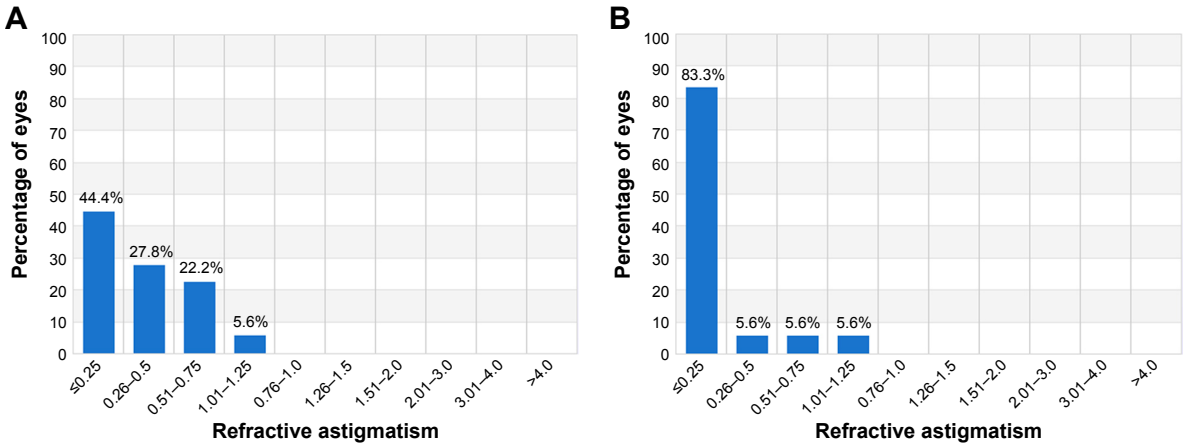

Figure 7 Refractive astigmatism, pre-operatively and at 3-month post-operative visits.
Notes: Percentage of eyes (vertical axis) versus refractive astigmatism (D), horizontal axis: (**A**) group A and (**B**) group B. Group A: one eye with the standard clinical refraction; Group B: the contralateral eye with the topographic astigmatic power and axis (topography-modified treatment refraction).

excimer laser, and a series of diagnostic networked devices that constitute the Refractive Suite® (including Vario Placido topography, Oculyzer II Scheimpflug topometry imaging, and Tscherning Wavefront system) were used clinically.[19]

Clinical results and features of the previous generations of the WaveLight excimer series (200 Hz Allegretto and 400 Hz Eye Q) have been reported by the author's team.[12,20]

The EX500 laser, the latest evolution of the aforementioned excimer lasers, employs a 1,050 Hz multidimensional active tracker with estimated response time (latency) of 2 ms, able to track pupil size from 1.5 mm to 8 mm.[21]

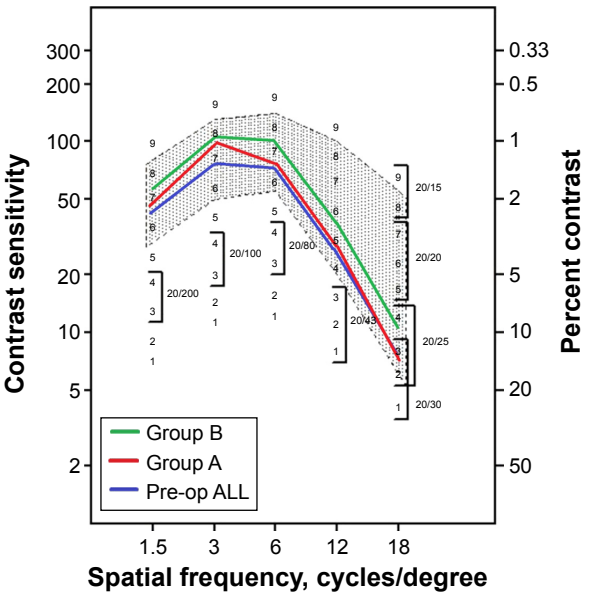

Figure 8 Contrast sensitivity comparison at 3-month visit.
Notes: As pre-operative data were not statistically significant in groups A and B, they are noted together as "Pre-op ALL". The average contrast sensitivity data is indicated with the green, red, and blue lines. Group A: one eye with the standard clinical refraction; Group B: the contralateral eye with the topographic astigmatic power and axis (topography-modified treatment refraction).

The Refractive Suite operates on its own ethernet network and allows the import of diagnostic data from networked screening devices into the planning software tools of both lasers. The platform offers the ability to import into the laser treatment planning mode the topographic data from the Placido-disk topographer (Vario, WaveLight) and topometry data from a Scheimpflug-based device (Oculyzer II-WaveLight), and accordingly customize the excimer treatment to the cornea (eg, for topography-guided treatment).[12] This study and previous studies have reported extensively the applications of topography-guided treatments with these platforms in irregular and normal eyes.[22–29]

The long-term clinical results with the systems described in the "Patients and methods" section show impressive refractive outcome, predictability, and stability with both refraction treatments. The modification of the clinical refraction with topography-guided data with regard to the amount and axis of astigmatism appears to offer superior visual function with regard to UDVA, CDVA, residual RE in terms of spherical equivalent and residual astigmatism, total high-order aberrations, coma, and functional contrast sensitivity. Specifically, the percentage of eyes achieving a post-operative spherical equivalent refraction within 0.5 D of the target and the total range of RE, which are considered the best markers of the quality of a refractive procedure. The better refractive results obtained in terms of spherical equivalent refraction were also confirmed by the defocus equivalent results achieved from the first 3 months with the refraction adjusted with topography data (group B). This parameter gives a better understanding of the accuracy of a procedure for correcting the entire RE.

It was theorized that this treatment adjustment preemptively bypasses the bias of lenticular astigmatism that

is probably active in young myopic eyes in their physiological state and may compensate for some amount of cornea astigmatism and cornea coma generated by angle kappa. This theoretical lenticular astigmatism appears to be the factor that distorts the objective cylindrical refractive data, resulting in wavefront refractive data similar to the subjective refraction, which appears to subside within months following the refractive surgery intervention. The author has adopted this concept in modern refractive cataract surgery, assuming that the post-operative cylindrical refraction will depend mainly on the cornea astigmatism, but have not adopted this concept yet in laser vision correction techniques applied on the cornea. The data in this contralateral eye study are compelling in studying further this novel principle that may increase accuracy in refractions used for laser vision correction.

Conclusion

Topographic adjustment of the amount and axis of astigmatism treated: TMR when different from the clinical refraction may offer superior outcomes in topography-guided myopic LASIK. These findings may change the current clinical paradigm of the optimal subjective refraction utilized in laser vision correction. Further studies by additional investigators may further validate this data.

Disclosure

The author reports no conflicts of interest in this work.

References

1. Kugler LJ, Wang MX. Lasers in refractive surgery: history, present, and future. *Appl Opt*. 2010;49(25):F1–F9.
2. Lukenda A, Martinović ZK, Kalauz M. Excimer laser correction of hyperopia, hyperopic and mixed astigmatism: past, present, and future. *Acta Clin Croat*. 2012;51(2):299–304.
3. Reggiani-Mello G, Krueger RR. Comparison of commercially available femtosecond lasers in refractive surgery. *Expert Rev Opthalmol*. 2011; 6(1):55–56.
4. Salomão MQ, Wilson SE. Femtosecond laser in laser in situ keratomileusis. *J Cataract Refract Surg*. 2010;36(6):1024–1032.
5. Vega-Estrada A, Alió JL, Arba Mosquera S, Moreno LJ. Corneal higher order aberrations after LASIK for high myopia with a fast repetition rate excimer laser, optimized ablation profile, and femtosecond laser-assisted flap. *J Refract Surg*. 2012;28(10):689–696.
6. Winkler von Mohrenfels C, Khoramnia R, Lohmann CP. Comparison of different excimer laser ablation frequencies (50, 200, and 500 Hz). *Graefes Arch Clin Exp Ophthalmol*. 2009;247(11):1539–1545.
7. Iseli HP, Mrochen M, Hafezi F, Seller T. Clinical photoablation with a 500-Hz scanning spot excimer laser. *J Refract Surg*. 2004;20(6):831–834.
8. de Ortueta D, Magnago T, Triefenbach N, Arba Mosquera S, Sauer U, Brunsmann U. In vivo measurements of thermal load during ablation in high-speed laser corneal refractive surgery. *J Refract Surg*. 2012;28(1): 53–58.
9. Aslanides IM, Kolli S, Padron S, Arba Mosquera S. Stability of therapeutic retreatment of corneal wavefront customized ablation with the SCHWIND CAM: 4-year data. *J Refract Surg*. 2012;28(5): 347–352.
10. Smadja D, Reggiani-Mello G, Santhiago MR, Krueger RR. Wavefront ablation profiles in refractive surgery: description, results, and limitations. *J Refract Surg*. 2012;28(3):224–232.
11. Kanellopoulos AJ. Topography-guided custom retreatments in 27 symptomatic eyes. *J Refract Surg*. 2005;21(5):S513–S518.
12. Kanellopoulos AJ. Topography-guided hyperopic and hyperopic astigmatism femtosecond laser-assisted LASIK: long-term experience with the 400 Hz eye-Q excimer platform. *Clin Ophthalmol*. 2012;6:895–901.
13. Zheng H, Song LW. Visual quality of Q-value-guided LASIK in the treatment of high myopia. *Yan Ke Xue Bao*. 2011;26(4):208–210.
14. Alio JL, Vega-Estrada A, Piñero DP. Laser-assisted in situ keratomileusis in high levels of myopia with the amaris excimer laser using optimized aspherical profiles. *Am J Ophthalmol*. 2011;152(6):954–963.
15. El Awady HE, Ghanem AA, Saleh SM. Wavefront-optimized ablation versus topography-guided customized ablation in myopic LASIK: comparative study of higher order aberrations. *Ophthalmic Surg Lasers Imaging*. 2011;42(4):314–320.
16. WaveLight Allegretto Wave® Eye-Q Excimer Laser – P020050/S012. *Summary of Safety and Effectiveness Data [SSED]*. Available from: http://www.accessdata.fda.gov/cdrh_docs/pdf2/P020050S012b.pdf. Accessed August 27, 2016.
17. Zuberbühler B, Galloway P, Reddy A, Saldana M, Gale R. A web-based information system for management and analysis of patient data after refractive eye surgery. *Comput Methods Programs Biomed*. 2007;88(3):210–216.
18. Mrochen M, Wüllner C, Krause J, Klafke M, Donitzky C, Seiler T. Technical aspects of the WaveLight FS200 femtosecond laser. *J Refract Surg*. 2010;26(10):S833–S840.
19. Kanellopoulos AJ, Asimellis G. Correlation between central corneal thickness, anterior chamber depth, and corneal keratometry as measured by oculyzer II and WaveLight OB820 in preoperative cataract surgery patients. *J Refract Surg*. 2012;22:1–6.
20. Kanellopoulos AJ. Long term results of a prospective randomized bilateral eye comparison trial of higher fluence, shorter duration ultraviolet A radiation, and riboflavin collagen cross linking for progressive keratoconus. *Clin Ophthalmol*. 2012;6:97–101.
21. Matsuura T, Ikeda H, Idota N, Motokawa R, Hara Y, Annaka M. Anisotropic swelling behavior of the cornea. *J Phys Chem B*. 2009; 113(51):16314–16322.
22. Han DC, Chen J, Htoon HM, Tan DT, Mehta JS. Comparison of outcomes of conventional WaveLight(®) Allegretto Wave(®) and Technolas(®) excimer lasers in myopic laser in situ keratomileusis. *Clin Ophthalmol*. 2012;6:1159–1168.
23. Celik HU, Alagöz N, Yildirim Y, et al. Accelerated corneal crosslinking concurrent with laser in situ keratomileusis. *J Cataract Refract Surg*. 2012;38(8):1424–1431.
24. Kanellopoulos AJ. Long-term safety and efficacy follow-up of prophylactic higher fluence collagen cross-linking in high myopic laser-assisted in situ keratomileusis. *Clin Ophthalmol*. 2012;6:1125–1130.
25. Kanellopoulos AJ, Asimellis G. Refractive and keratometric stability in high myopia LASIK with high-frequency femtosecond and excimer lasers. *J Refract Surg*. 2013;29(12):832–837.
26. Kanellopoulos AJ, Asimellis G. Keratoconus management: long-term stability of topography-guided normalization combined with high-fluence CXL stabilization (the Athens Protocol). *J Refract Surg*. 2014;30(2): 88–92.
27. Kanellopoulos AJ, Asimellis G. Corneal refractive power and symmetry changes following normalization of ectasias treated with partial topography-guided PTK combined with higher-fluence CXL (the Athens Protocol). *J Refract Surg*. 2014;30(5):342–346.
28. Kanellopoulos AJ, Asimellis G. LASIK ablation centration: an objective digitized assessment and comparison between two generations of an excimer laser. *J Refract Surg*. 2015;31(3):164–169.
29. Kanellopoulos AJ, Asimellis G. Novel placido-derived topography-guided excimer corneal normalization with cyclorotation adjustment: enhanced athens protocol for keratoconus. *J Refract Surg*. 2015;31(11): 768–773.

Topography-Guided LASIK Versus Small Incision Lenticule Extraction (SMILE) for Myopia and Myopic Astigmatism: A Randomized, Prospective, Contralateral Eye Study

Anastasios John Kanellopoulos, MD

ABSTRACT

PURPOSE: To compare safety and efficacy of topography-guided LASIK and contralateral eye SMILE for myopia and myopic astigmatism correction.

METHODS: This prospective, randomized contralateral eye study included 44 eyes of 22 patients with bilateral myopia or myopic astigmatism. Treated eyes were divided into two groups: 22 eyes were treated with topography-guided LASIK and the fellow eye of each patient was treated with SMILE. The following parameters were evaluated preoperatively and up to 3 months postoperatively: uncorrected distance vision acuity (UDVA), corrected distance vision acuity (CDVA), refractive error, corneal keratometry, contrast sensitivity, and Objective Scatter Index.

RESULTS: At 3 months, 86.4% of the LASIK group and 68.2% of the SMILE group had UDVA of 20/20 ($P < .002$) and 59.1% and 31.8%, respectively, had UDVA of 20/16 ($P < .002$). Spherical equivalent refraction (± 0.50 D) was 95.5% for the LASIK group and 77.3% for the SMILE group ($P < .002$). Residual refraction cylinder (≤ 0.25 D) was 81.8% for the LASIK group and 50% for the SMILE group ($P < .001$). Contrast sensitivity (6 cycles/degree) was 7.2 ± 1.01 in the LASIK group and 6.20 ± 1.52 in the SMILE group. Objective Scatter Index measurements at 3 months were 1.35 in the LASIK group and 1.42 in the SMILE group.

CONCLUSIONS: Topography-guided LASIK was superior in all visual performance parameters studied, both subjective and objective. The main difference between the two techniques likely derives from the eye tracking, cyclorotation compensation, and active centration control in the LASIK technology studied in contrast to the current technology available with SMILE-like procedures. This difference appears to affect refractive and visual aberration performance outcomes.

[*J Refract Surg.* 2017;33(5):306-312.]

LASIK is a widely accepted method for correcting the refractive error, as evidenced by the number of publications in the peer-reviewed literature.[1,2] We previously reported, in agreement with many others, on the safety and accuracy of flap making with mechanical keratomes for correction of myopia and myopic astigmatism[3] and hyperopia.[4]

In recent years, bladeless LASIK using a femtosecond laser for lamellar flap creation as an alternative option to the mechanical microkeratome has been studied.[5,6] Greater predictability of flap depth and higher precision in planar flap thickness creation in long-term follow-up have already been reported.[7-13] Meanwhile, current excimer laser platforms for LASIK have evolved to offer significantly more accurate centration, eye tracking, and cornea customization, which seems to increase the overall safety and efficacy of the procedure.[14-17]

Small incision lenticule extraction (SMILE) is a new method of intrastromal keratomileusis that involves the creation of an intrastromal lenticule between two photodisruption planes that is mechanically removed through a small corneal incision tunnel without the use of an excimer laser. It was clinically introduced in 2006,[18-24] and has recently received approval from the U.S. Food and Drug Administration for refractive correction of myopia and myopic astigmatism.

This single laser "flapless" refractive procedure seems to be a viable alternative for refractive correction because numerous recent studies validate its safety and efficacy, even when compared to LASIK. This prospective, randomized study was designed to compare the safety and efficacy of topography-guided femtosecond laser–assisted LASIK to SMILE in the contralateral eyes.

From The Laservision.gr Clinical & Research Eye Institute, Athens, Greece; and the Department of Ophthalmology, New York University Medical School, New York, New York.

Submitted: November 2, 2016; Accepted: February 3, 2017

Dr. Kanellopoulos is a consultant for Alcon, Avedro, Allergan, i-Optics, Keramed, Zeiss, and ISP Surgical.

Correspondence: Anastasios John Kanellopoulos, MD, The Laservision.gr Research & Clinical Eye Institute, 17 Tsocha Street, Athens 11521, Greece. E-mail: ajkmd@mac.com

doi:10.3928/1081597X-20170221-01

PATIENTS AND METHODS

This prospective, randomized clinical study received approval from the Ethics Committee of our institution and adhered to the tenets of the Declaration of Helsinki. Informed consent was provided and documented in writing from each patient prior to the time of the intervention. The study was conducted on patients in our clinical practice, during scheduled preoperative and postoperative procedure visits and unscheduled visits when necessary. The inclusion criteria were: age between 18 and 65 years, no previous ocular surgery, documented refractive stability for at least 3 years, and discontinuation of contact lens use for at least 2 weeks. Prior to intervention, a complete preoperative ophthalmologic evaluation ensured there was no current or past ocular pathology other than refractive error. Preoperative myopia was between -3.00 and -10.00 diopters (D), and up to -6.00 D of cylinder refractive error. According to the available and recommended treatment range of the SMILE technique, at that time within the European Union the sum of myopic plus astigmatic absolute numbers was up to -10.00 D. Finally, preoperative CDVA was least 20/30 in 22 patients studied. Exclusion criteria comprised history of corneal dystrophy and/or herpetic eye disease, topographic evidence of keratoconus as evidenced by Placido topography or Scheimpflug-based tomography, epithelial warpage from contact lens use, corneal scarring, glaucoma, severe dry eye, and collagen vascular disease.

Twenty-two patients with bilateral myopia or myopic astigmatism were enrolled in this study. One eye of each patient was randomly assigned (coin flip) to the topography-guided femtosecond laser–assisted LASIK group (LASIK group) and the fellow eye was then assigned to the SMILE group. Each patient was not aware which eye received LASIK or SMILE until the completion of the study. All surgeries were performed by the same surgeon (AJK).

The Alcon WaveLight Refractive Suite, specifically the FS200 femtosecond and EX500 excimer lasers (Alcon Laboratories, Inc., Fort Worth, TX), was employed for all femtosecond laser-assisted LASIK procedures. All cases had planned flap thickness of 110 µm and planned flap diameter of 8.5 mm. The 110-µm flap thickness was chosen in all LASIK cases because this has been optimal in our practice and has been used as the clinical standard during the past 10 years. Topographic data were imported by the Vario topolyzer (WaveLight, Erlagen, Germany) and corneal pachymetric data were imported by the Oculyzer II (WaveLight), a Scheimpflug-based tomography device associated with the Refractive Suite, a diagnostic device that is essentially based on the Pentacam HD (Oculus Optikgeräte GmbH, Wetzlar, Germany). The cylindrical refraction was adjusted by the surgeon to match the amount and axis of the topographically measured cylinder and appropriate sphere adjustments were made to keep the same spherical equivalent (topography modified refraction).[25]

All SMILE procedures were performed prior to the topography-guided LASIK procedure on a same-day basis using the VisuMax femtosecond laser (Carl Zeiss Meditec, Jena, Germany). The reason for this was the potential need for an excimer ablation in case the SMILE procedure ran into intraoperative complications that allowed conversion to LASIK (by converting the actual SMILE cap into a LASIK flap, and using an excimer laser to correct the refractive error). The intended thickness of the cap tissue was 130 µm because this was the optimal recommended by the Zeiss surgical application consultant and planned lenticule diameter was 6.5 mm.

All eyes were evaluated preoperatively and on each postoperative visit for corrected distance visual acuity (CDVA), uncorrected distance visual acuity (UDVA), and manifest spherical equivalent before and after cycloplegia with two drops of 1% tropicamide topical solution, autorefraction/keratometry with the Speedy-i-K model (Righton, Tokyo, Japan), slit-lamp biomicroscopy, dilated fundus examination including retinal periphery, and applanation tonometry.

Additionally, several tests were completed at each preoperative and postoperative visit: Vario Placido-based topography, described above; Scheimpflug corneal tomography with the Oculyzer II, noted above; anterior segment optical coherence tomography (Avanti; Optovue, Fremont, CA); Objective Scatter Index using the HD analyzer model OQAS-HDA (Visiometrics, Barcelona, Spain); contrast sensitivity using the Functional Vision Analyzer (Stereo Optical Company, Inc., Chicago, IL) with the Eye View functional vision analysis software (Vision Sciences Research Corporation, Walnut Creek, CA); photopic, mesopic, and scotopic binocular pupillometry with the Pupillometer P3000 SA (Procyon Instruments limited, London, United Kingdom); and wavefront analysis with the Allegro II Tserning-type Wavefront analyzer (WaveLight), a device also part of the Refractive Suite operative network. Preoperative evaluations included wavefront analysis, pupillometry, keratometry and contrast sensitivity (Stereo Vision, Chicago, IL), and Objective Scatter Index (HD analyzer device; Visiometrics). Postoperative examination included manifest and dilated refraction, slit-lamp microscopy, tonometry, and keratometry by means of corneal topography and tomography assessment.

Postoperative follow-up examinations were conducted at 1 day, 1 week, 1 month, and 3 months. All patients were postoperatively treated with moxifloxacin (Vigamox; Alcon Laboratories, Inc.) and 0.1%

TABLE 1
Preoperative Data

	LASIK		SMILE		
Variable	**Mean ± SD**	**Range**	**Mean ± SD**	**Range**	***P***
UDVA (logMAR)	0.04 ± 0.09	-0.2 to 0.2	-0.02 ± 0.1	-0.3 to 0.1	.0592
CDVA (logMAR)	0.07 ± 0.07	-0.1 to 0.2	0.03 ± 0.07	-0.1 to 0.2	.1047
MRSE (D)	-5.02 ± 1.74	-1.25 to -8	-5.17 ± 2.30	-0.75 to -9.5	.9127
Corneal thickness (μm)	541.72 ± 28.90	502 to 610	541.81 ± 28.82	500 to 605	.9919
Objective Scatter Index	1.57 ± 2.20	0.2 to 9	1.58 ± 2.07	0.2 to 8.6	.9870
Low contrast sensitivity (6 cpd)	6.50 ± 1.78	2 to 9	6.35 ± 2.06	1 to 9	.8460

SMILE = small incision lenticule extraction; SD = standard deviation; UDVA = uncorrected distance visual acuity; CDVA = corrected distance visual acuity; MRSE = manifest refraction spherical equivalent; D = diopters; cpd = cycles per degree

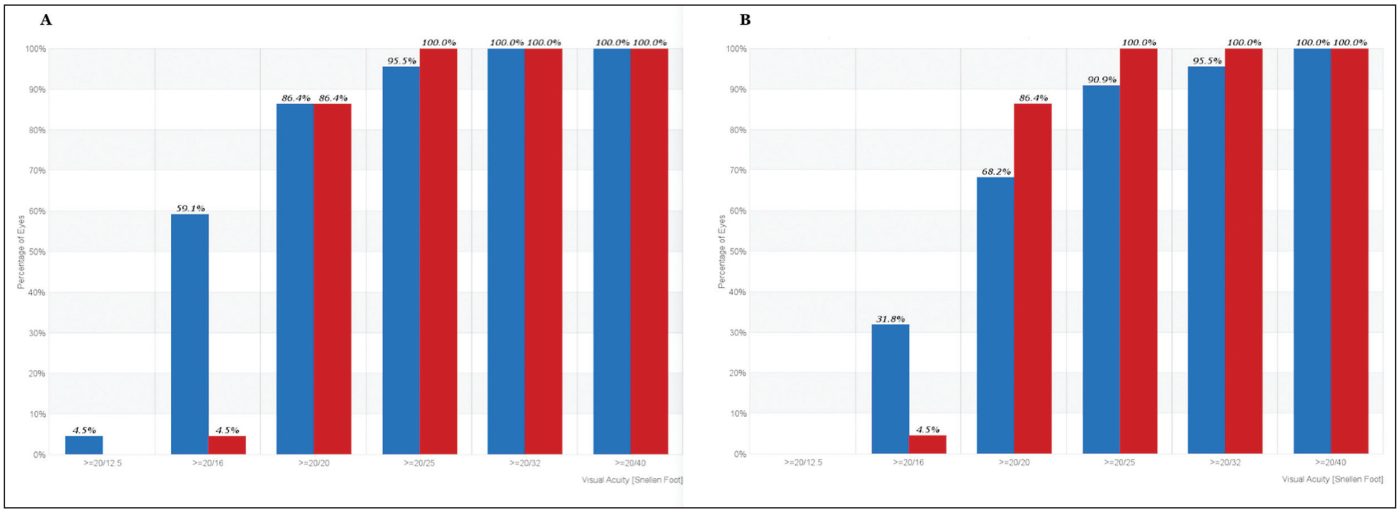

Figure 1. Visual outcomes for the (A) topography-guided LASIK and (B) small incision lenticule extraction (SMILE) groups at the end of 3 months, showing the change in postoperative uncorrected distance visual acuity (blue) preoperative corrected distance visual acuity (red).

dexamethasone/chloramphenicol solution (Dispersadron C; Alcon Laboratories, Inc.) four times a day for both eye drops for 1 week in each eye and preservative-free artificial tears as needed. The frequency of artificial tear use was not monitored in this study, nor was corneal sensitivity.

All possible adverse effects or patient complaints were closely monitored. Preoperative refractive measurements were masked by default because eye allocation had not been held at the time. At each follow-up visit, the outcome assessors (eg, optometrists and research assistants) and the patients themselves remained masked to the assigned treatment to improve objectivity and minimize potential bias.

RESULTS

Of the 22 patients enrolled in this study, 13 were women and 9 men. The patient ages at the time of surgery ranged from 21 to 45 years (average: 29.5 years). Preoperative patient demographics are listed in **Table 1**.

Most patients responded that they found SMILE (95.4%; 21 of 22) more comfortable than LASIK (4.6%, 1 of 22). Preoperatively, UDVA was 0.02 ± 0.07 (range: 0.01 to 0.25) (there was no statistical difference between the preoperative UDVA for the LASIK group compared to the SMILE group), manifest spherical equivalent range was -3.125 to -10.00 D, and mean cylinder was -1.12 ± 0.99 D (range: 0.00 to -4.25 D).

UDVA Outcomes and Stability

At 3 months of follow-up, 86.4% of the LASIK group had UDVA of 20/20 (1.0 decimal) and 59.1% had UDVA of 20/16. In the SMILE group, 68.2% of the eyes had UDVA of 20/20 and 31.8% had UDVA of 20/16. The differences between the two groups at the 20/20 and the 20/16 levels were statistically significant ($P < .002$ for both comparisons) (**Figure 1**).

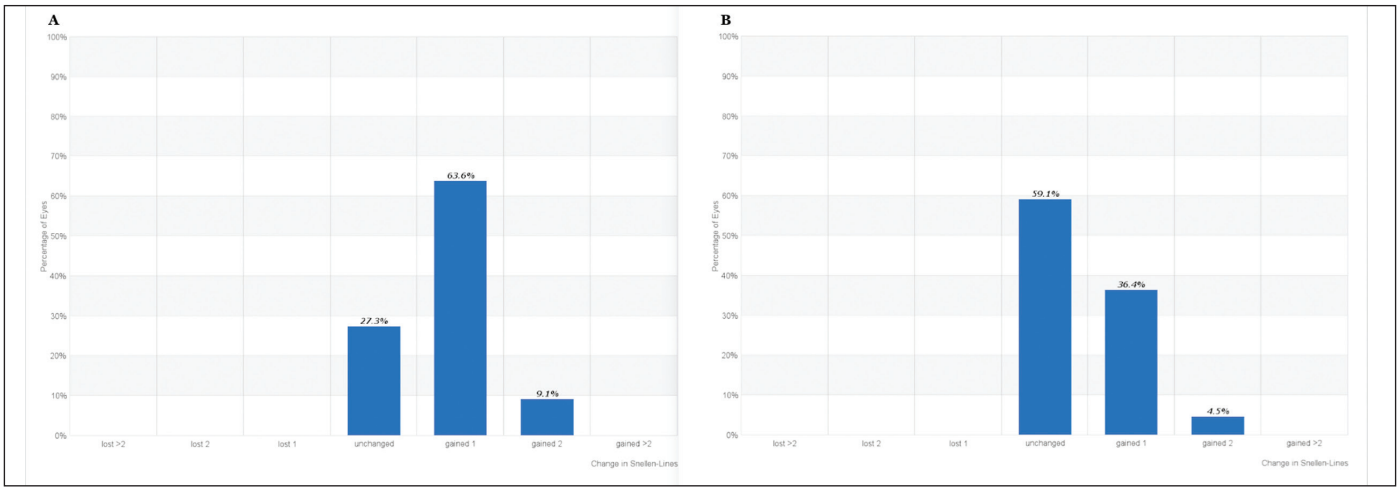

Figure 2. Percentage of eyes with unchanged/gain in Snellen lines of corrected distance visual acuity (CDVA) at 3 months for the (A) topography-guided LASIK and (B) small incision lenticule extraction (SMILE) groups.

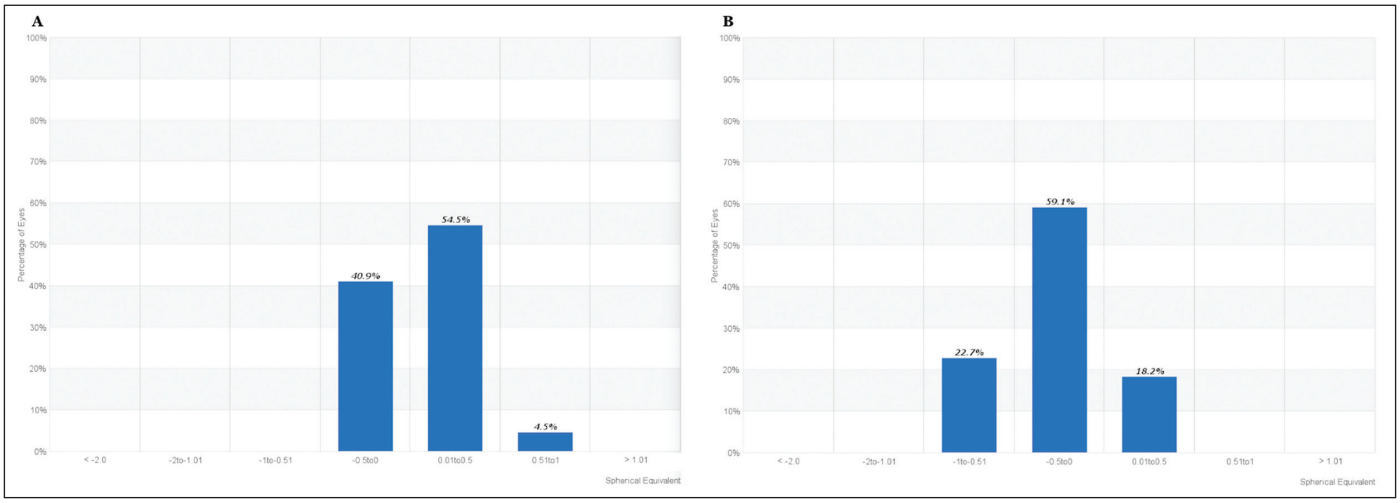

Figure 3. Spherical equivalent refraction (SEQ) correction in diopters for the (A) topography-guided LASIK and (B) small incision lenticule extraction (SMILE) groups.

Efficacy of CDVA

The gain–loss data (preoperative CDVA versus postoperative UDVA, **Figure 2**) indicated that 9.1% of the eyes in the LASIK group and 4.5% of the eyes in the SMILE group gained two lines. These data were also statistically significant in comparison ($P < .02$).

Refractive Predictability and Accuracy

The residual manifest spherical equivalent between 0.00 and +0.50 D was achieved in 95.5% of the eyes in the LASIK group compared to 77.3% in the SMILE group ($P < .002$). Residual manifest refraction cylinder of less than 0.25 D representing the accuracy of cylinder correction was achieved in 81.8% of the eyes in the LASIK group and 50% of the eyes in the SMILE group ($P < .001$) (**Figures 4-5** and **Figure A**, available in the online version of this article).

Objective Scatter Index and Low Contrast Sensitivity Measurements

The average postoperative Objective Scatter Index (**Figure B**, available in the online version of this article) was 1.35 in the LASIK group (statistically better than preoperative mean value) and 1.42 in the SMILE group (not statistically different to preoperative values, but also not worse).

The average low contrast sensitivity at 6 cycles/degree postoperatively was in 7.2 ± 1.01 in the LASIK group, which constitutes an improvement in comparison to the preoperative measurements, and 6.20 ± 1.52 in the SMILE group (not statistically significantly different to preoperative measurements, but also not reduced at all). **Figure C** (available in the online version of this article) demonstrates the 1-month and 3-month data.

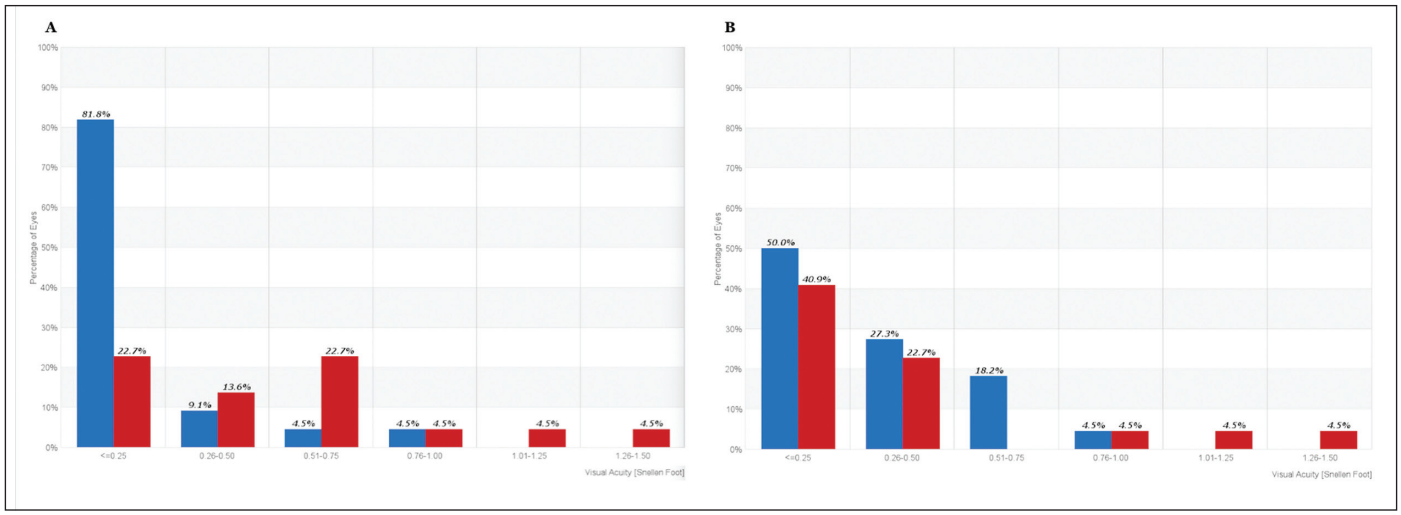

Figure 4. Preoperatively (red) and 3 months postoperatively (blue) cylinder distribution for the (A) topography-guided LASIK and (B) small incision lenticule extraction (SMILE) groups

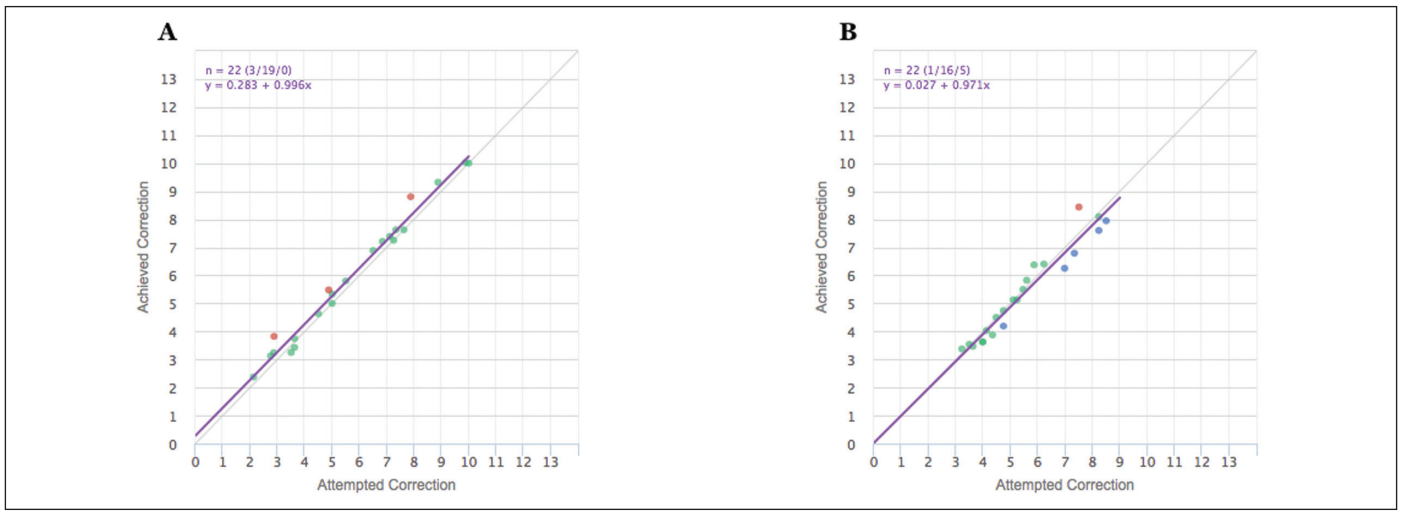

Figure 5. Predictability graph with red dots showing overcorrection and blue dots showing undercorrection, with green dots within ±0.50 diopters for (A) topography-guided LASIK and (B) small incision lenticule extraction (SMILE) groups.

DISCUSSION

Both topography-guided LASIK and SMILE performed in contralateral eyes exhibited adequate stability and efficacy in terms of myopia and myopic astigmatic correction evaluated through the 3-month postoperative period. However, virtually all parameters studied rendered a statistical significance in favor of the topography-guided LASIK group.

The reason for this statistical difference of the topography-guided LASIK procedure's efficacy should probably be attributed to its topography customization with additional centration and cyclorotation intraoperative compensation by the excimer laser. When comparing this well-established technique to an evolving procedure such as the current form of SMILE, in which centration is manually held by the surgeon, and where no tracking and/or cyclorotation adjustment is currently offered by the only femtosecond laser platform currently able to offer this procedure, these data should probably be anticipated. Admittedly initial studies report SMILE efficacy comparable to standard (wavefront-optimized) LASIK showing essentially "equal" postoperative results.[15-22] Investigators recently reported comparable visual outcomes when comparing wavefront-optimized to topography-guided profiles in a contralateral eye study.[26] However, this study did did not use topography-guided modification (TMR) of the clinical refraction in the respective treatments, something that was the backbone of the refractions used in our study herein and may explain the difference in outcomes.[25]

To limit possible intersubject bias such as different healing properties, environmental, psychological, and compliance issues, we decided to use a contralateral eye study protocol.

We theorize that this treatment adjustment preemptively bypasses the bias of lenticular astigmatism, which is probably an issue in young myopic eyes and may compensate for some amount of corneal astigmatism and corneal coma generated by angle kappa. This theoretical lenticular astigmatism appears to be the factor that distorts the objective cylindrical refractive data, resulting in wavefront refractive data similar to the subjective refraction, and which seems to subside within days or months at the latest following the refractive surgery intervention.[27] This concept has been adopted in modern refractive cataract surgery, with experience that the postoperative cylindrical refraction will depend mainly on the corneal astigmatism, but it is yet to be established in laser vision correction techniques applied on the cornea. The data provided by this contralateral eye study are compelling enough to encourage further study of this novel principle, which may ultimately increase our accuracy in refractions used for laser vision correction.

SMILE has undoubtedly constituted a promising method in our early clinical experience and possible future technological evolution enabling cyclorotation tracking and adjustment may offer improvement in refractive and quality of vision results. Additionally, possible future topographic data customization of SMILE-like procedures may also improve visual outcomes.

CONCLUSIONS

Topography-guided LASIK appears to offer improved outcomes in all parameters studied herein compared to the early clinical practice of SMILE for myopia and myopic astigmatism correction. The difference noted between the two techniques is likely to derive from the customization topography-guided excimer platform, offering automatic eye tracking with active centration control and cyclorotation compensation, aspects that may decisively affect refractive and visual performance outcomes.

AUTHOR CONTRIBUTIONS

Study concept and design (AJK); data collection (AJK); analysis and interpretation of data (AJK); writing the manuscript (AJK); critical revision of the manuscript (AJK); statistical expertise (AJK); administrative, technical, or material support (AJK); supervision (AJK)

REFERENCES

1. Solomon KD, Fernández de Castro LE, Sandoval HP, et al; Joint LASIK Study Task Force. LASIK world literature review: quality of life and patient satisfaction. *Ophthalmology.* 2009;116:691-701.
2. Shortt AJ, Allan BD, Evans JR. Laser-assisted in-situ keratomileusis (LASIK) versus photorefractive keratectomy (PRK) for myopia. *Cochrane Database Syst Rev.* 2013;1:CD005135.
3. Kanellopoulos AJ, Pe LH, Kleiman L. Moria M2 single use microkeratome head in 100 consecutive LASIK procedures. *J Refract Surg.* 2005;21:476-479.
4. Kanellopoulos AJ, Conway J, Pe LH. LASIK for hyperopia with the WaveLight excimer laser. *J Refract Surg.* 2006;22:43-47.
5. Reggiani-Mello G, Krueger RR. Comparison of commercially available femtosecond lasers in refractive surgery. *Expert Rev Ophthalmol.* 2011;6:55-65.
6. Salomão MQ, Wilson SE. Femtosecond laser in laser in situ keratomileusis. *J Cataract Refract Surg.* 2010;36:1024-1032.
7. Kanellopoulos AJ, Asimellis G. LASIK ablation centration: an objective digitized assessment and comparison between two generations of an excimer laser. *J Refract Surg.* 2015;31:164-169.
8. Kanellopoulos AJ, Asimellis G. Refractive and keratometric stability in high myopic LASIK with high-frequency femtosecond and excimer lasers. *J Refract Surg.* 2013;29:832-837.
9. Kanellopoulos AJ, Asimellis G. FS200 femtosecond laser LASIK flap digital analysis parameter evaluation: comparing two different types of patient interface applanation cones. *Clin Ophthalmol.* 2013;7:1103-1108.
10. Kanellopoulos AJ, Asimellis G. Long-term bladeless LASIK outcomes with the FS200 femtosecond and EX500 excimer laser workstation: the refractive suite. *Clin Ophthalmol.* 2013;7:261-269.
11. Kanellopoulos AJ, Kahn J. Topography-guided hyperopic LASIK with and without high irradiance collagen cross-linking: initial comparative clinical findings in a contralateral eye study of 34 consecutive patients. *J Refract Surg.* 2012;28(suppl 11):S837-S840.
12. Kanellopoulos AJ, Asimellis G. Digital analysis of flap parameter accuracy and objective assessment of opaque bubble layer in femtosecond laser-assisted LASIK: a novel technique. *Clin Ophthalmol.* 2013;7:343-351.
13. Kanellopoulos AJ, Asimellis G. Three-dimensional LASIK flap thickness variability: topographic central, paracentral and peripheral assessment, in flaps created by a mechanical microkeratome (M2) and two different femtosecond lasers (FS60 and FS200). *Clin Ophthalmol.* 2013;7:675-683.
14. Ang M, Tan D, Mehta JS. Small incision lenticule extraction (SMILE) versus laser in-situ keratomileusis (LASIK): study protocol for a randomized, non-inferiority trial. *Trials.* 2012;13:75.
15. Agca A, Ozgurhan EB, Demirok A, et al. Comparison of corneal hysteresis and corneal resistance factor after small incision lenticule extraction and femtosecond laser-assisted LASIK: a prospective fellow eye study. *Cont Lens Anterior Eye.* 2014;37:77-80.
16. Shen Z, Shi K, Yu Y, Yu X, Lin Y, Yao K. Small incision lenticule extraction (SMILE) versus femtosecond laser-assisted in situ keratomileusis (FS-LASIK) for myopia: a systematic review and meta-analysis. *PLoS One.* 2016;11:e0158176.
17. Zhang J, Wang Y, Chen X. Comparison of moderate- to high-astigmatism corrections using wavefront-guided laser in situ keratomileusis and small-incision lenticule extraction. *Cornea.* 2016;35:523-530.
18. Reinstein DZ, Archer TJ, Gobbe M. Small incision lenticule extraction (SMILE) history, fundamentals of a new refractive surgery technique and clinical outcomes. *Eye Vis.* 2014;1:3..
19. Sekundo W, Kunert KS, Blum M. Small incision corneal refractive surgery using the small incision lenticule extraction (SMILE) procedure for the correction of myopia and myopic

astigmatism: results of a 6 month prospective study. *Br J Ophthalmol.* 2011;95:335-339.

20. Sekundo W, Gertnere J, Bertelmann T, Solomatin I. One-year refractive results, contrast sensitivity, high-order aberrations and complications after myopic small-incision lenticule extraction (ReLEx SMILE). *Graefes Arch Clin Exp Ophthalmol.* 2014;252:837-843.
21. Han T, Zheng K, Chen Y, Gao Y, He L, Zhou X. Four-year observation of predictability and stability of small incision lenticule extraction. *BMC Ophthalmol.* 2016;16:149.
22. Pedersen IB, Ivarsen A, Hjortdal J. Three-year results of small incision lenticule extraction for high myopia: refractive outcomes and aberrations. *J Refract Surg.* 2015;31:719-724.
23. Vestergaard AH. Past and present of corneal refractive surgery: a retrospective study of long-term results after photorefractive keratectomy and a prospective study of refractive lenticule extraction. *Acta Ophthalmol.* 2014;92:1-21.
24. Luft N, Ring MH, Dirisamer M, et al. Corneal epithelial remodeling induced by small incision lenticule extraction (SMILE). *Invest Ophthalmol Vis Sci.* 2016;57:176-183.
25. Kanellopoulos AJ. Topography-modified refraction (TMR) adjustment of treated cylinder amount and axis to the topography versus standard clinical refraction in myopic topography-guided LASIK. *Clin Ophthalmol.* 2016;10:2213-2221.
26. Shetty R, Shroff R, Deshpande K, Gowda R, Lahane S, Jayadev C. A prospective study to compare visual outcomes between wavefront-optimized and topography-guided ablation profiles in contralateral eyes with myopia. *J Refract Surg.* 2017;33:6-10.
27. Miruna N, Andrei F, Vasile FM, Rotaru E. Smile--the next generation of laser vision correction. *Rom J Ophthalmol.* 2016;60:6-8.

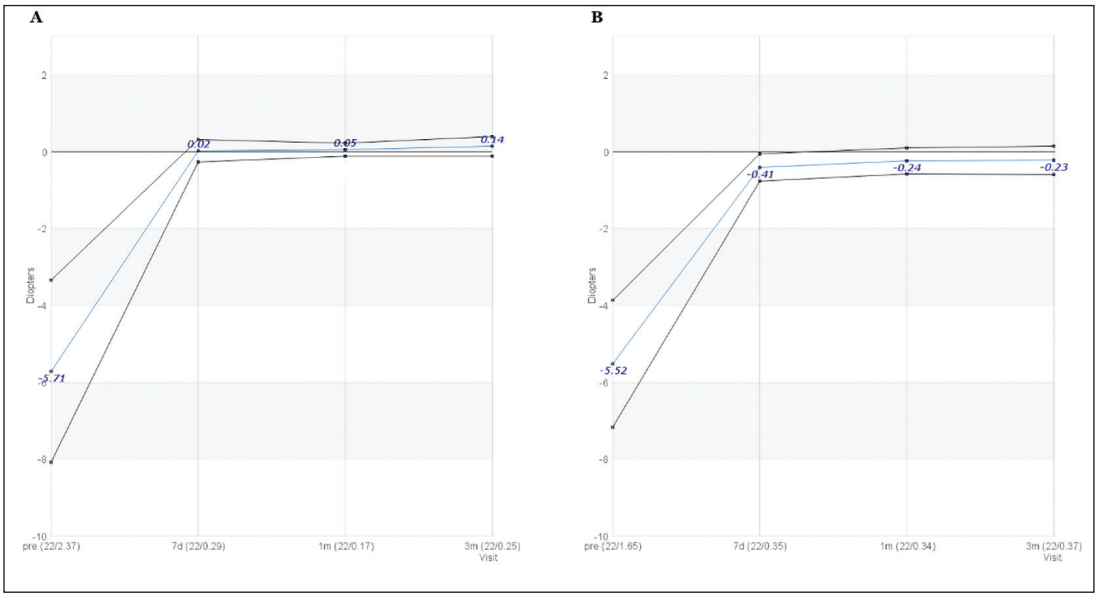

Figure A. Time course of manifest spherical equivalent refraction (SEQ) after (A) topography-guided LASIK and (B) small incision lenticule extraction (SMILE).

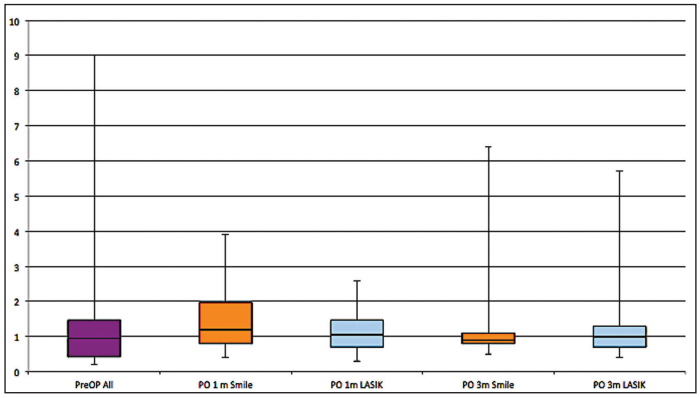

Figure B. Objective Scatter index (OSI) boxplots showing topography-guided LASIK versus small incision lenticule extraction (SMILE): the first boxplot represents the average for all, the second represents SMILE at 1 month, the third represents the LASIK at 1 month, the fourth the SMILE at 3 months and the fifth the LASIK at 3 months, respectively.

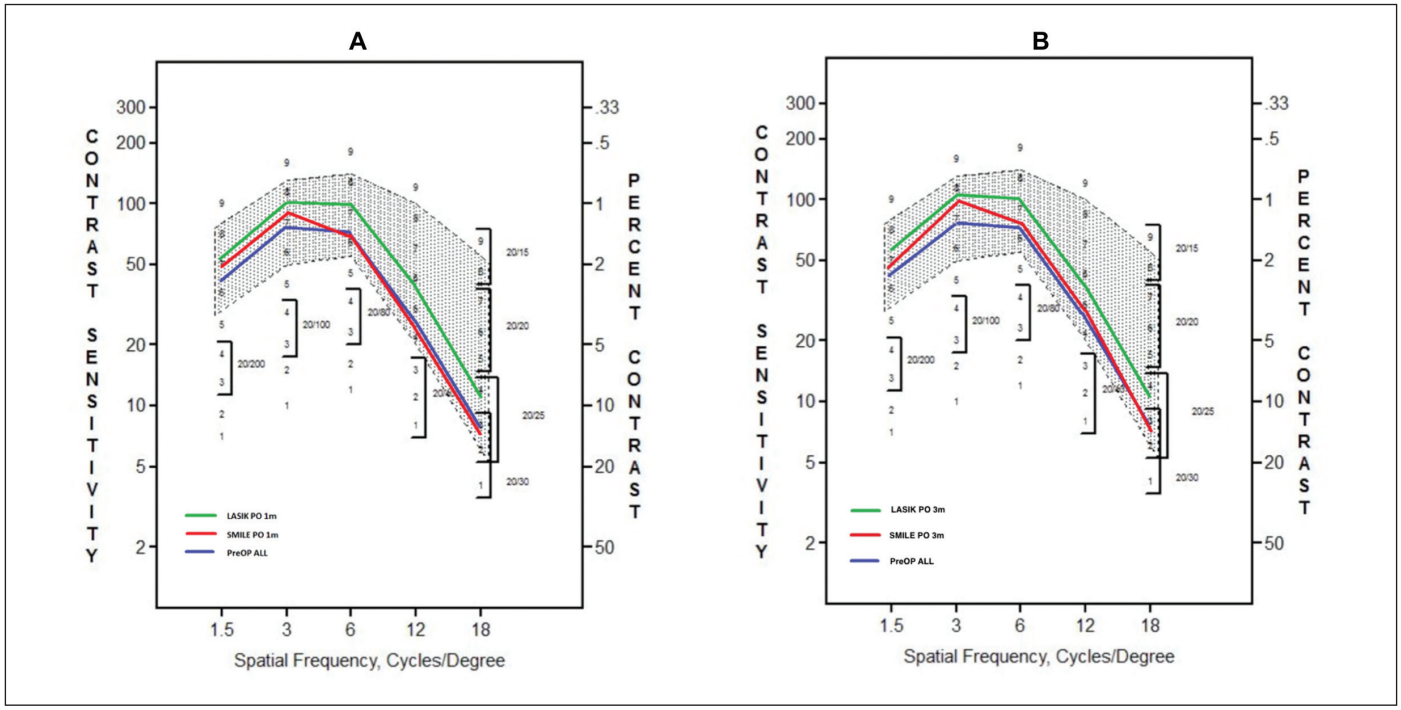

Figure C. Contrast sensitivity for postoperative month 1. The blue line represents the preoperative average for all, the red line the average small incision lenticule extraction (SMILE) data at 1 month, in all special frequencies, and the green line the respective topography-guided LASIK data at 1 month.